Ulm University

Institute of Pathology

Director: Prof. Dr. med. Peter Möller

The role of GSK3β for the pathogenesis of activated-B-cell type of diffuse large B cell lymphoma

Dissertation submitted in partial fulfilment of the requirements for the degree of "Doctor of Medicine" (Dr. med.) of the Faculty of Medicine, Ulm University.

By

Ali Mohamed Sayed Abd-Ellah

Born in Sohag, Egypt.

2018

Current Dean: Prof. Dr. T. Wirth

First reviewer: Prof. Dr. R. Marienfeld

Second reviewer: Prof. Dr. C. Brunner

Day of award: 23.05.2019

Dedication

This part was removed due to data protection.

A part of this dissertation was published in the journal: Scientific Reports.

Abd-Ellah A, Voogdt C, Krappmann D, Möller P and Marienfeld R (2018): "GSK3β modulates NF-kappaB activation and RelB degradation through site-specific phosphorylation of BCL10." Sci Rep **8**: 1352.

Index

List of abbreviations ……	VII
1- Introduction ……..…	1
1.1 Diffuse large B cell lymphoma …….	1
1.2 The NF-κB signalling system ……	5
1.3 The biology of the Glycogen synthase kinase 3β …….…….	12
1.4 Objective ……	15
2- Materials and methods ……	17
2.1 Materials ……...…….	17
2.1.1. Chemicals and reagents …….	17
2.1.2. Inducers and inhibitors ……..	18
2.1.3. Devices ……..	18
2.1.4. Disposables ……	19
2.1.5. Kits ……	20
2.1.6. Cell lines ……...	20
2.1.7. Buffers and solutions ……	20
2.1.8. Protein molecular weight standards …….	25
2.1.9. Antibodies ……	25
2.1.10. Oligonucleotides ……..	26
2.1.11. Plasmids ……..……..	27
2.1.12. Enzymes ……..…….	27
2.1.13. Software ……	27
2.2 Methods ……	28
2.2.1. Cell culture techniques …….	28
2.2.2. Bacterial culture techniques …….	29
2.2.3. Protein extraction from cells ……	30
2.2.4. Immunoblot analysis ……	31
2.2.5. Electrophoretic mobility shift assay …….……	33
2.2.6. Immunoprecipitation ……	35
2.2.7. Phosphorylation studies techniques …….	36
2.2.8. Luciferase reporter assay …….	37
2.2.9. Cell proliferation assay …….	37
2.2.10. Quantitative real time PCR ……..	38

2.2.11. Cloning methods ……..…….. 40
2.2.12. Immunohistochemical staining of FFPE slides …… 42
3- Results …….. 44
3.1 GSK3β is required for signal induced MALT1 endoprotease activity 44
3.2 GSK3β modulates the canonical NF-κB signalling pathway …….. 50
3.3 GSK3β modulates CBM complex formation …….. 54
3.4 GSK3β is a BCL10 kinase …….. 57
3.5 GSK3β modulate IKK complex activity ……. 61
3.6 GSK3β inhibition depresses ABC-DLBCL survival and proliferation 63
3.7 GSK3β inhibition attenuates MALT1 endoprotease activity in ABC-DLBCL …… 65
3.8 GSK3β modulates CBM complex formation and NF-κB signalling in ABC-DLBCL …….. 66
3.9 GSK3β modulate Wnt/β-catenin pathway in DLBCL …… 68
3.10 Immunohistochemistry expression of GSK3β and other related proteins in DLBCL …… 69
4- Discussion …… 75
5- Summary ……..…… 82
6- References …… 84

List of abbreviations:

ABC-DLBCL	Activated B-cell-like diffuse large B cell lymphoma
ANK	Ankyrin
APC	Adenomatous polyposis coli
ATM	Ataxia telangiectasia mutated kinase
BAFF-R	B-cell activation factor
BCL10	B-cell lymphoma/leukaemia 10
BCR	B-cell receptor
BSA	Bovine serum albumin
BTK	Bruton tyrosine kinase
CC	Coiled-coil domain
CHX	Cycloheximide
CKIα	Casein kinase Iα
CYLD1	Cylindromatosis-1
DD	Death domain
DHIT	Double hit lymphoma
DKK1	Dickkopf-1
DLBCL	Diffuse large B cell lymphoma
Dvl	Dishevelled
eIF2B	Initiation factor 2B
EMSA	Electrophoretic Mobility Shift Assay
FFBE	Formalin–fixed and paraffin embedded material
GC-DLBCL	germinal center B-cell-like diffuse large B cell lymphoma
GRG	Groucho-related gene
GS	Glycogen synthase enzyme
GSK3β	Glycogen synthase kinase 3β
HLH	Helix-loop-helix domain
HOIL1	Heme-oxidized IRP2 ubiquitin ligase 1
IHC	Immunohistochemistry
IKK	Inhibitors of NF-κB kinase
IL-1	Interleukin-1
IL-1R	Interleukin-1 receptor
IκB	Inhibitors of NF-κB
LEF	Lymphocyte-enhancer-binding factor
LGS	Legless homologue
LPS	Lipopolysaccharides
LRP	Lipoprotein-related receptor
LTβR	Lymphotoxin β-receptor
LUBAC	Linear ubiquitin chain assembly complex

LZ	Leucin-zipper-like motif
MALT1	Mucosa associated lymphoid tissue lymphoma translocation protein
NBD	NEMO-binding domain
NFAT	Nuclear factor of activated T cells
NF-κB	Nuclear factor-κB
NIK	NF-κB inducing kinase
P/I	PMA+Ionomycin
PEST	PEST domain
PI3K	Phosphatidylinositol-3-kinase
PKC	Protein kinase C
PKCβ	Protein kinase C beta
PYGO	Pygopus homologue
RANK	Receptor activator of NF-κB
RHD	Rel homology domain
SAP	Shrimp alkaline phosphatase
SB21	SB216763
SB41	SB415286
shRNA	Short hairpin RNA
siRNA	Small interfering RNA
SRC	SRC-kinase
SYK	Spleen tyrosine kinase
TAB	TAK1 binding protein
TAK1	Transforming growth factor beta-activated kinase 1
T-ALL	T-cell acute lymphoblastic leukaemia
Tas	Transactivation domain
TCF	T-cell factor
TCR	T-cell receptor
TLRs	Toll like receptors
TNFR	Tumor necrosis factor receptor
TNFα	Tumor necrosis factor α
WHO	World Health Organization
ZF	Zinc-finger domain
β-TRCP	β-transducin-repeat-containing protein
ΔCYLD1	cleavage product of CYLD1

1- Introduction:

1.1 Diffuse large B cell lymphoma

Diffuse large B cell lymphoma (DLBCL) is the most common lymphoma in adults, representing about 35-40% of cases (Rodriguez-Abreu et al. 2007). It is a typically aggressive lymphoma and is fatal without treatment. The median age of DLBCL falls between the sixth and seventh decade, but the age range is wide, and it may also occur in children. DLBCL corresponds to a heterogeneous group of lymphoid malignancies composed of large B cells with vesicular nuclei, prominent nucleoli, basophilic cytoplasm and usually a high proliferation rate (Martelli et al. 2013).

1.1.1. Sites of involvement:

Typically, DLBCL patients present with a rapidly enlarging mass at a single nodal or extranodal site. Extranodal DLBCL represent up to 40% of cases (Harris et al. 1994). The gastrointestinal tract (stomach or ileocecal region) is the most common extranodal site, although DLBCL can originate virtually from any extranodal location including skin, central nervous system, liver, spleen, salivary gland, bone, testis and female genital tract (Swerdlow et al. 2008).

1.1.2. Classification and subgroups:

The World Health Organization (WHO) classification of DLBCL of 2008 shows several variants displayed in table-1 (Swerdlow et al. 2008). Gene expression profiling studies on DLBCL identified two main, prognostically different subgroups termed germinal center B-cell-like (GC-DLBCL) and activated B-cell-like (ABC-DLBCL), which are believed to originate from different stages of B cell differentiation. Both were characterized by a distinct gene expression profile either characteristic of normal germinal center B-cells in case of GC-DLBCL or of activated blood memory B-cells in case of ABC-DLBCL (Alizadeh et al. 2000; Rosenwald et al. 2002). ABC-DLBCL patients show worse prognosis in comparison to GC-DLBCL patients even with treatment. Conventionally, it is treated with an anthracycline-based chemotherapy regimen composed of a combination of cyclophosphamide, doxorubicin, vincristine, and prednisone (CHOP) with the addition of the antagonistic anti-CD20 antibody rituximab (R-CHOP) (Lenz et al. 2008). Microarray analysis in daily diagnostic work is not yet feasible. For that reason, the usefulness of immunohistochemistry in the identification of GC and ABC subgroups of DLBCL has been investigated, but this usefulness is still

debated. Moreover, a gene expression study of DLBCL failed to demonstrate any statistically significant correlation between molecular defined ABC-like and GC-like DLBCL and the morphological variants defined by the WHO classification (De Paepe and De Wolf-Peeters 2007).

Table (1): Diffuse large B cell lymphoma variants, subgroups and subtypes (Swerdlow et al. 2008).

DLBCL variants
Common morphologic variants
Centroblastic
Immunoblastic
Anaplastic
Molecular subgroups
Germinal center B-cell-like (GCB)
Activated B-cell-like (ABC)
Immunohistochemical subgroups
CD5-positive DLBCL
GCB
Non-GCB
DLBCL subtypes
T-cell/histiocyte-rich large B-cell lymphoma
Primary DLBCL of the central nervous system
Primary cutaneous DLBCL, leg type
Epstein–Barr virus-positive DLBCL of the elderly
Other lymphomas of large B cells
Primary mediastinal (thymic) large B-cell lymphoma
Intravascular large B-cell lymphoma
DLBCL associated with chronic inflammation
Lymphomatoid granulomatosis
Anaplastic lymphoma kinase-positive DLBCL
Plasmablastic lymphoma
Large B-cell lymphoma arising in human herpesvirus-8-associated multicentric Castleman disease
Primary effusion lymphoma
Borderline cases
B-cell lymphoma, unclassifiable, with features intermediate between DLBCL and Burkitt lymphoma
B-cell lymphoma, unclassifiable, with features intermediate between DLBCL and classic Hodgkin lymphoma

Several studies tried to establish a practical algorithm to differentiate between the DLBCL subgroups using cost effective immunohistochemical stainings. The Hans' algorithm, using three immunohistochemistry (IHC) antibodies, CD10, BCL6 and

MUM1, was the first algorithm to typify DLBCL into GC- and Non-GC-DLBCL (Figure-1) with high similarity to gene expression profiling (Hans et al. 2004). This algorithm was later modified by the same group and two additional antibodies (FOXP1 and GCET1) were added to improve accuracy (Choi algorithm) (Choi et al. 2009). However, differences between using IHC and gene expression profiling regarding the clinical outcome still remain (Gutierrez-Garcia et al. 2011).

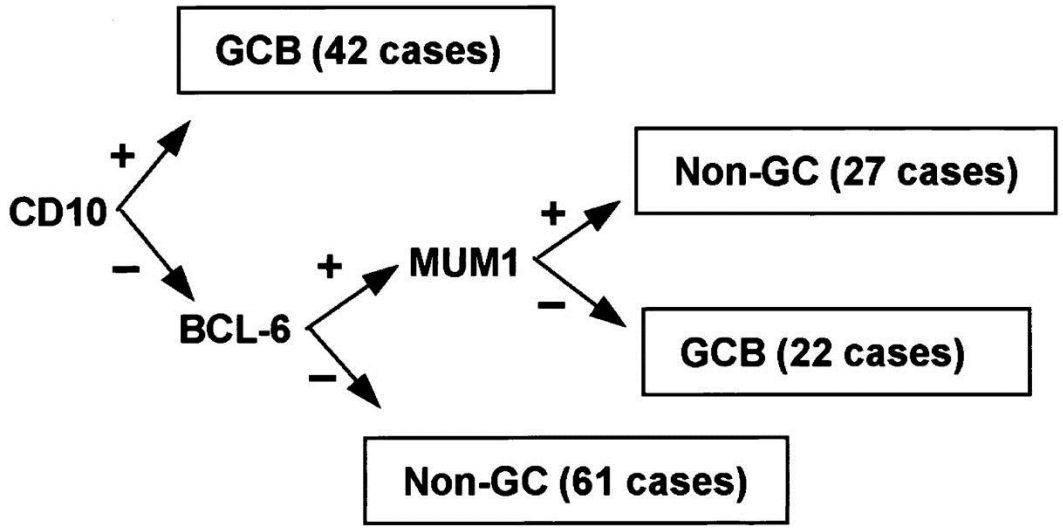

Figure (1): Hans' algorithm. GCB, Germinal center B-cell-like diffuse large B cell lymphoma; Non-GC, Non-germinal center B-cell-like diffuse large B cell lymphoma (Hans et al. 2004).

1.1.3. ABC-DLBCL:

ABC-DLBCL is believed to originate from the plasmablastic stage of B cell development; and their gene expression profile resembles the activated blood memory B cells. The hallmark of the ABC-like DLBCL is the constitutive NF-κB signalling pathway activation, which promotes cell proliferation and survival by inhibiting apoptosis. NF-κB activation in ABC-DLBCL is mainly mediated through the constitutive formation of a protein complex composed of CARMA1, BCL10 and MALT1, also called CBM complex (Thome et al. 2010). Constitutive CBM complex formation may be caused by activating mutations in CARMA1 (about 10% of cases) (Lenz et al. 2008) or chronic active B cell receptor signalling caused by CD79A or CD79B mutations (about 20% of cases). MYD88 mutations which were found in more

than 30% of cases and other genetic lesions also mediate NF-κB activation (Davis et al. 2010). Moreover, loss of function of the negative NF-κB regulator TNFAIP3 (A20) by mutation or deletion can also cause an increased NF-κB activity in the ABC-DLBCL (Kato et al. 2009).

1.1.4. GC-DLBCL:

GC-DLBCL is thought to originate from the germinal center B cells; and its gene expression profile resembles those of the germinal center B-cells as CD10, LMO2 and BCL6 (Alizadeh et al. 2000; Rosenwald et al. 2002). It represents about 40-50% of the DLBCL cases and shows better survival in respond to R-CHOP therapy that ABC-DLBCL cases. Common genetic mutations and active signalling pathways are listed in figure-2. For example, the GC-DLBCL commonly shows mutations involved in the histone methylation or acetylation (EZH2, CREBBP or EP300), cell cycle activation or apoptosis blocking (MYC and BCL2 translocations) or cell signalling pathways (PI3K/AKT/mTOR or JAK/STAT pathways) (Karube et al. 2017).

1.1.5. Therapeutic targets:

The initial therapy of DLBCL is a combination chemotherapy composed of cyclophosphamide, doxorubicin, vincristine and prednisone together with the antagonistic anti-CD20 antibody rituximab (R-CHOP) for six cycles (Habermann et al. 2006). ABC-DLBCL shows a worse prognosis to the conventional R-CHOP therapy (Lenz et al. 2008). Moreover, most patients show relapse or resistance to R-CHOP therapy are thought to have ABC-DLBCL (Staudt and Dave 2005). New clinical trials to target chronic active BCR signalling in ABC-DLBCL are still in early stages. Among these trials are the use of inhibitors for the Bruton tyrosine kinase (BTK) (Wilson et al. 2012), protein kinase C beta (PKCβ) (Robertson et al. 2007), spleen tyrosine kinase (SYK) (Young et al. 2009) or phosphatidylinositol-3-kinase (PI3K) (Lannutti et al. 2011).

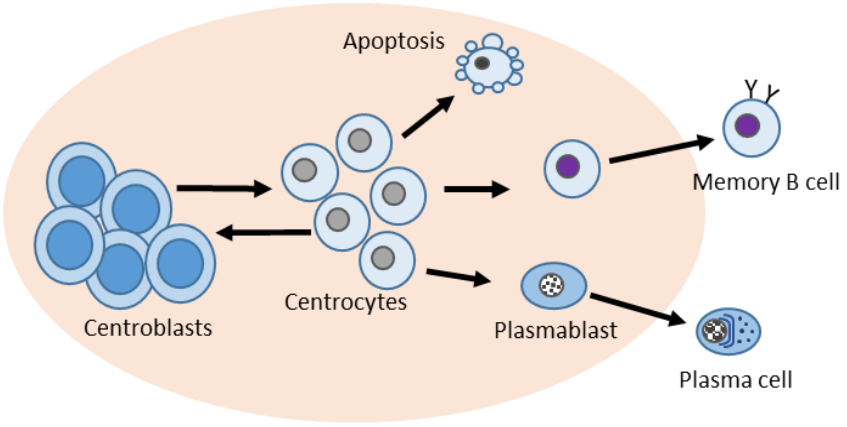

GCB

Histone modification
- EZH2 mutations
- MLL2 mutations
- CREBBP mutations
- EP300 mutations

Blocks to terminal differentiation
- BCL6 expression, EZH2 mutations

Cell cycle activation +/- blocks to apoptosis
- MYC and BCL2 translocations
- (DHIT) and protein over expression.

MTOR pathway activation
Signaling cascades
- PTEN del/loss (PI3K and AKT activation)

ABC

BCR/NF-κB signaling
- CD79A/B, CARD11, MYD88 mutations, TNFAIP3 (A20) deletions

Histone modification
- MLL2 mutations
- CREBBP mutations
- EP300 mutations

Blocks to terminal differentiation
- BCL6 translocations, PRDM1 loss/ mutations.

Cell cycle activation +/- blocks to apoptosis
- MYC translocations, MYC and BCL2 protein over expression

MTOR pathway activation
Signaling cascades
- PI3K and AKT activation.

Cytokine signaling/JAK-STAT pathway activation

Figure (2): Key oncogenic pathways of DLBCL. GCB, Germinal center B-cell-like diffuse large B cell lymphoma; ABC, Activated B-cell-like diffuse large B cell lymphoma; DHIT, double hit lymphoma; del, deletion; BCR, B cell receptor, according to (Sehn and Gascoyne 2015).

1.2 The NF-κB signalling system

The nuclear factor-κB (NF-κB) is a fundamental and tightly regulated family of transcription factors that exist in virtually all mammalian cells. It plays a crucial role in the immune response and inflammation. It mediates the normal development, activation

and proliferation of lymphocytes (Bonizzi and Karin 2004). NF-κB was first discovered in 1986 as a protein binding to the control region of the gene encoding the kappa light chain of the immunoglobulins in B cells, and therefore acquired the abbreviation NF-κB (Sen and Baltimore 1986). Later research data showed the ability of NF-κB transcription factor to control target genes responsible for the regulation of inflammation, cell differentiation, growth, survival and adhesion (Collins et al. 1995; Shishodia and Aggarwal 2002).

1.2.1. The NF-κB family of transcription factors

The NF-κB family of transcription factors in mammalians is composed of five members: RelA (p65), RelB, c-Rel, NF-κB 1 (p50) and NF-κB 2 (p52) (Figure 3A). Those members are capable of forming diverse homo- and heterodimers. These proteins share a Rel homology domain (RHD), which is essential for homo- and heterodimer formation, nuclear translocation, binding to DNA and interaction with inhibitory proteins (May and Ghosh 1997). The NF-κB family members are sequestrated in the cytoplasm of the non-stimulated cells in an inactive form by a structurally and functionally related family of inhibitory proteins called IκB family (Inhibitors of NF-κB). The IκB family consists of the three members IκBα, IκBβ, and IκBε as well as the NF-κB1/p105 and NF-κB2/p100 precursors of p50 and p52, respectively. The main mechanism controlling the activation of the NF-κB signalling pathway is through a site-specific phosphorylation of these inhibitor proteins, followed by their proteasome degradation and the subsequent release of the active NF-κB dimers. The phosphorylation of the IκB is mediated by a multiprotein IκB-kinase complex (IKK complex) composed of the two catalytic subunits IKKα (IKK1) and IKKβ (IKK2) and the non-catalytic regulatory subunit IKKγ (or NEMO for NF-κB essential modifier) (Figure 3C).

Figure 3: Structure of NF-κB, IκB and IKK protein families. RHD, Rel homology domain; Tas, transactivation domains; LZ, leucin-zipper-like motif; ANK, ankyrin; PEST, PEST domain; DD, death domain; CC, coiled-coil domain; ZF, zinc-finger domain; HLH, helix-loop-helix domain; NBD, NEMO-binding domain. The arrows indicate the processing sites in p100 and p105, respectively (Hoeseel and Schmid 2013, CC BY 2.0, https://creativecommons.org/licenses/by/2.0/)

1.2.2. Mechanism of NF-κB activation

The NF-κB signalling can be further subdivided into a canonical and an alternative pathway (Bonizzi and Karin 2004). Activation of these two NF-κB pathways is induced by different sets of agonists, although some of these agonists might activate both NF-κB pathways. For instance, the canonical NF-κB signalling can be activated through ligand binding of the antigen receptors, the T-cell receptor (TCR) or the B-cell receptor (BCR), toll like receptors (TLRs), tumor necrosis factor receptor (TNFR), receptor activator of NF-κB (RANK) or lymphocyte co-receptor such as CD30 or CD40 (Figure 4A) (Ruland and Mak 2003; Bonizzi and Karin 2004). The stimulation through these receptors lead to the activation of the IKK complex, which phosphorylates the IκB proteins, causing an IκB polyubiquitination and proteasomal degradation. Now the NF-κB dimers are free to translocate to the nucleus and mediate gene transcription (Figure 4A).

The alternative pathway, also called non-canonical pathway, is a specialized signalling cascade that is particularly important in mature B cells. This pathway is activated through restricted cell surface receptors, which belong to the TNF receptor superfamily including lymphotoxin β-receptor (LTβR), B-cell activation factor (BAFF-R), CD40 receptor, TNFR2 and Fn14 (Bonizzi and Karin 2004; Sun 2010) (Figure 4B). The engagement of these receptors leads to the activation of the NF-κB inducing kinase (NIK), which acts in concert with IKKα to induce a site-specific phosphorylation of the carboxy-terminus of the p100 precursor. Subsequently, the phosphorylated p100 is processed into the mature p52 protein by proteasome (Xiao et al. 2001). Moreover, the alternative NF-κB signalling is characterized by its independency of NEMO and by a delayed kinetic encompassing several hours in contrast to the canonical NF-κB signalling, which is induced within minutes.

Besides the canonical and alternative pathway, other pathways to activate NF-κB exist, called atypical activation pathways. For example, genotoxic stress activates the IKK complex via the kinase ATM and ubiquitination of NEMO (Huang et al. 2003).

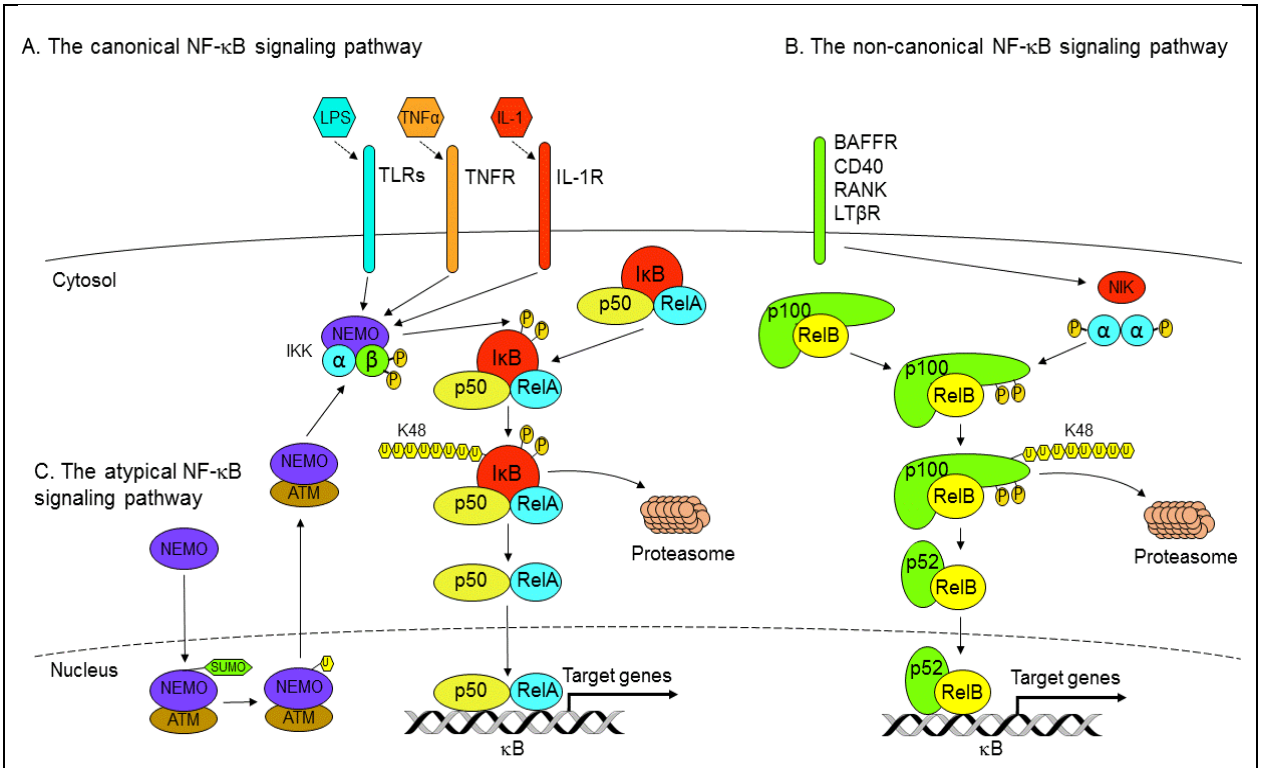

Figure 4: The canonical, non-canonical and atypical NF-κB activation pathways. LPS, Lipopolysaccharides; TNFα, Tumor necrosis factor α; IL-1, Interleukin-1; TLRs, Toll-like receptors; TNFR, Tumor necrosis factor receptor; IL-1R, Interleukin-1 receptor; ATM, Ataxia telangiectasia mutated kinase; IκB, Inhibitors of NF-κB; BAFFR, B-cell activating factor receptor; RANK, Receptor activator of NF-κB; LTβR, Lymphotoxin β-receptor; NIK, NF-κB inducing kinase. Adapted from (Hoeseel and Schmid 2013, CC BY 2.0, https://creativecommons.org/licenses/by/2.0/).

1.2.3. Antigen receptor mediated NF-κB activation

The binding of antigen receptors to their cognate ligands induces the activation of the canonical NF-κB signalling pathway. The identification of a high molecular weight protein complex composed of CARMA1 (also known as CARD11 or BCL10-interacting MAGUK protein 3, BIMP3), BCL10 (B-cell lymphoma/leukaemia 10) and MALT1 (mucosa associated lymphoid tissue lymphoma translocation protein 1), known as CBM complex, is considered a breakthrough in understanding the mechanism underlying the antigen mediated NF-κB activation in B- and T-lymphocytes (Thome 2004). CARMA1 is mainly expressed in hematopoietic cells like spleen, thymus and peripheral blood leukocytes, while BCL10 and MALT1 are expressed in almost all tissues (Blonska and Lin 2011). Moreover, other members of the CARMA family that distribute in different tissues can replace CARMA1 to

form a similar complex with BCL10 and MALT1 and transduce NF-κB signalling from different receptor types (Wegener and Krappmann 2007; Jiang and Lin 2012).

The key role in the activation of this signalling cascade is mediated through PKC-θ and PKC-β in T and B cells, respectively. Upon lymphocyte activation both kinases are translocated to lipid rafts, where PKC-θ in case of T cells or PKC-β in case of B cells phosphorylate CARMA1, triggering conformational changes by loosening the intra-molecular linker CARD interactions. This relieves the auto-inhibition of CARMA1 and allows the recruitment of the pre-assembled MALT1-BCL10 (Sun et al. 2000; Saijo et al. 2002). Functionally, the CBM complex serves as a scaffold for the recruitment of several down-stream effector proteins like the IKK complex in case of NF-κB signalling. Previous studies showed that the CBM complex can recruit NEMO, the regulatory unit of the IKK complex (Stilo et al. 2004). Moreover, MALT1 recruits TRAF6, an E3 ubiquitin ligase, leading to TRAF6 oligomerization and activation, which facilitates polyubiquitination of BCL10, MALT1 and NEMO (Oeckinghaus et al. 2007; Shambharkar et al. 2007). These polyubiquitination events provide a scaffold function for the recruitment of the transforming growth factor beta-activated kinase 1 (TAK1), TAK1 binding protein (TAB) and the IKK complex, thus promoting the IKK/NF-κB activation (Oeckinghaus et al. 2007). However, the exact mechanism by which the CBM complex activates the IKK complex is still not fully elucidated.

IKKβ was shown to be constitutively associated with BCL10-MALT1 (Su et al. 2005). In addition, IKKβ has also a direct impact on CBM complex formation. IKKβ seems to have a dual function on NF-κB: IKKβ is required for the CBM complex formation on one side and phosphorylates BCL10 at its C-terminus and thereby triggering the disengagement of BCL10 and MALT1 on the other side, which serves as a negative feedback mechanism for NF-κB signalling (Wegener et al. 2006). In addition to its scaffold function, MALT1 is a para-caspase and exerts an endoprotease function that is activated upon activation of the antigen receptor.

The MALT1 endoprotease activity increases the duration and the amplitude of NF-κB activation signal through the cleavage of RelB (Marienfeld et al. 2001) and A20. Both are negative regulators of the canonical NF-κB target gene expression, although with different mechanisms (Coornaert et al. 2008). A20 is a ubiquitin editing protein that normally functions as a negative feedback regulator for the tumor necrosis factor receptor (TNFR)

(Wertz et al. 2004) and Toll-like receptor (TLR) mediated for NF-κB activation pathway (Boone et al. 2004) by removing K63-linked ubiquitin chains from NF-κB activators like TRAF6, NEMO and MALT1 (Coornaert et al. 2008). RelB plays an inhibitory role on the NF-κB signalling through different mechanisms including the sequestration of RelA in transcriptionally inactive RelA:RelB complexes (Marienfeld et al. 2003). Other possible mechanisms underlying the repressive effect of RelB include blocking of the NF-κB sites, the sequestration of p50 or p52 in heterodimers (Dobrzanski et al. 1994), an epigenetic silencing of NF-κB target genes or the sequestration of transcription cofactors (Chen et al. 2009).

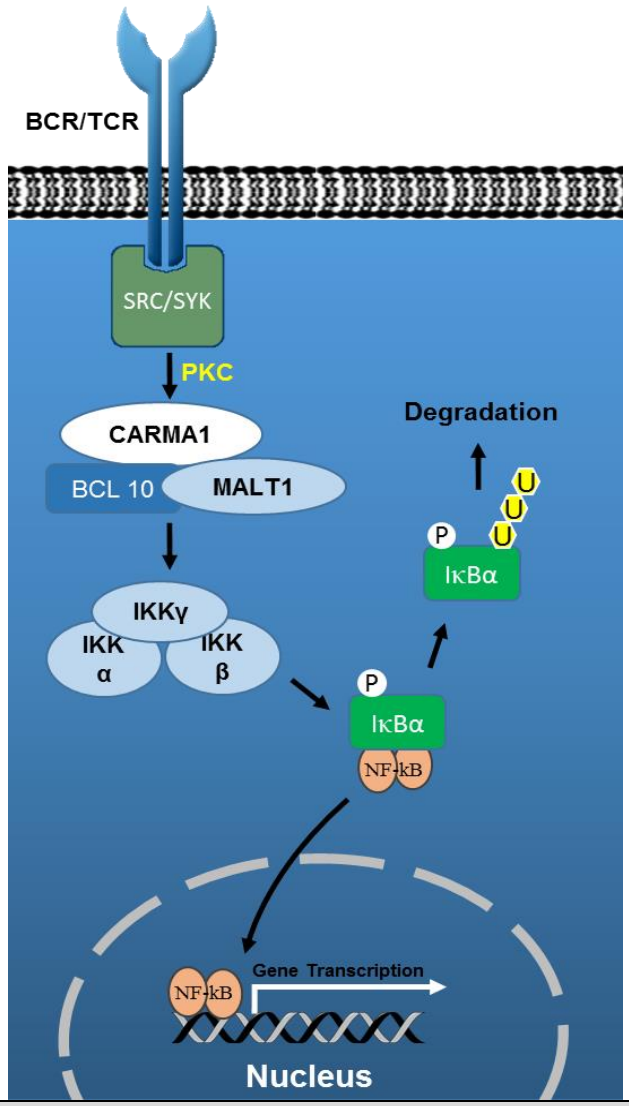

Figure 5: Canonical NF-κB activation through CBM complex. BCR, B-cell receptor; TCR, T-cell receptor; SRC, SRC-kinase; SYK, Spleen tyrosine kinase; PKC, Protein kinase C; IKK, Inhibitors of NF-κB kinase; IκBα, Inhibitors of NF-κB. According to (Thome 2004).

In addition to A20 and RelB, MALT1 endoprotease activity plays a key role in regulating other antigen receptor mediated signalling pathways. For instance, MALT1 is shown to cleave several other substrates, including BCL10 (Rebeaud et al. 2008), CYLD1 (Staal et al. 2011), the linear ubiquitin chain assembly complex (LUBAC) subunit HOIL1 (heme-oxidized IRP2 ubiquitin ligase 1) (Klein et al. 2015), roquin and regnase-1 proteins (Jeltsch et al. 2014).

The constitutive NF-κB activation due to a pathological CBM complex formation is reported in many lymphomas. For example, DLBCL may show a CARMA1 overexpression (Nakamura et al. 2005) or gain of function mutations (Lenz et al. 2008). In addition, MALT lymphoma frequently shows a t(1;14)(p22;q32) and a t(14;18)(q32;q21) chromosomal translocation bringing BCL10 and MALT1 genes to the immunoglobulin heavy chain locus (IGH) resulting in their overexpression and NF-κB activation (Ye et al. 2005). Several studies suggest that the CBM complex might act as a therapeutic target for the treatment of the NF-κB driven lymphomas. For example, silencing CARMA1, BCL10, MALT1 or IKK1 using short hairpin RNA (shRNA) vectors attenuated NF-κB signalling in ABC-DLBCL (Ngo et al. 2006). Moreover, targeting MALT1 endoprotease activity using pharmacological inhibitors represents a potentially important therapeutic target for ABC-DLBCL and MALT lymphoma (Ferch et al. 2009; Fontan et al. 2012).

1.3 The biology of the Glycogen synthase kinase 3β

Glycogen synthase kinase 3β (GSK3β) acquired its name from its ability to phosphorylate and hence deactivate the glycogen synthase enzyme thereby controlling the glycogen synthesis. However, GSK3β is not confined to this particular metabolic role, it plays a crucial role in a wide variety of signalling processes. GSK3 has two highly homologous forms, GSK3α and GSK3β (Woodgett 1990). Although both isoforms are similar in structure and biochemical characters, they cannot totally compensate each other's physiological functions (Lee and Kim 2007). Interestingly, several GSK3β phosphorylation targets need a prior phosphorylation by priming kinases to be phosphorylated by GSK3β (DePaoli-Roach 1984). For example, the phosphorylation of β-catenin by GSK3β requires a prior phosphorylation of β-catenin by a priming kinase called casein kinase Iα (CKIα) and the depletion of CKIα causes an increased Wnt/β-catenin signalling due to the accumulation of β-catenin due to deficient phosphorylation and subsequently degradation (Liu et al. 2002).

Owing to the wide spreading functions of GSK3β, it is tightly regulated by several mechanisms including phosphorylation, subcellular localization or protein complex formation. The most widely studied mechanism for the regulation of the GSK3β function is its site-specific phosphorylation. While the N-terminal phosphorylation of GSK3β at Ser-9 reduces its activity (Plyte et al. 1992), the phosphorylation at Tyr-216 increases its enzymatic activity (Hughes et al. 1993). During basal conditions, GSK3β inhibits glycogen synthesis by inhibitory phosphorylation of Glycogen synthase enzyme (GS). Insulin stimulation activates the PI3K/Akt signalling cascade and subsequent the phosphorylation of GSK3β at Ser-9. This activates the GS and hence the synthesis of glycogen (Eldar-Finkelman 2002). In addition, GSK3β regulates protein synthesis by inhibitory phosphorylation of initiation factor 2B (eIF2B), and insulin stimulation induce protein synthesis in a similar mechanism as GS (Welsh and Proud 1993).

In addition to its metabolic role, GSK3β regulates an impressively large number of transcription factors either directly or indirectly as a sequence of the changes in the activity of GSK3β. Among these transcription factors are NF-κB (Hoeflich et al. 2000), β-catenin (Rubinfeld et al. 1996), AP-1 (Jun) (Boyle et al. 1991), Nuclear factor of activated T cells (NFAT) (Beals et al. 1997), c-Myc (Pulverer et al. 1994) and p53 (Pap and Cooper 1998).

The role of GSK3β for the function of the NF-κB and β-catenin transcription factors will be discussed in detail in the next sections. In the AP-1 pathway, GSK3β is capable of phosphorylating c-Jun at three sites causing a diminished c-Jun activity. The signal-induced activation of protein kinase C, on the other hand, results in a de-phosphorylation of one or more of those c-Jun sites resulting in an increased AP-1 binding activity (Boyle et al. 1991). GSK3β regulates p53 as well which plays a crucial role in cell proliferation and apoptosis. Several studies showed that GSK3β promotes the action of p53 either by facilitating its acetylation or by forming a protein complex with p53 (Watcharasit et al. 2003; Eom and Jope 2009).

1.3.1. The role of GSK3β in the regulation of NF-κB signalling pathway

Previous studies showed a close link between GSK3β and NF-κB signalling. The GSK3β null mice showed an increased sensitivity to TNF-α induced apoptosis and a significant decrease of TNF-α induced NF-κB DNA binding activity (Hoeflich et al. 2000) in a similar way seen in RelA- or IKK2-deficient mice (Beg et al. 1995; Li et al. 1999). Moreover,

GSK3β inhibition by lithium reduced the TNF-α induced NF-κB activation in HEK293T cells (Hoeflich et al. 2000). GSK3β was also suggested to phosphorylate the NF-κB member p65 *in vivo* (Schwabe and Brenner 2002). In contrast to these studies, which suggest a positive role of GSK3β in the NF-κB signalling, other conflicting reports using other cell types suggested an inhibitory influence of GSK3β on the NF-κB signalling. For example, inhibition of GSK3β with lithium or expression of a dominant negative GSK3β variant increases the NF-κB activity and the survival of PC12 cells (Bournat et al. 2000).

A recent study showed that GSK3β is crucial for the signal induced RelB degradation and moreover, a GSK3β-RelB complex was found in unstimulated Jurkat T-cell acute lymphoblastic leukaemia (T-ALL) cells (Neumann et al. 2011). Another study showed that GSK3β together with other β-catenin destruction complex components are recruited to the oncogenic CARMA1 in DLBCL cell lines (Bognar et al. 2016). However, the precise role of GSK3β in modulating the NF-κB signalling pathways is still indistinct.

1.3.2. GSK3β controls the Wnt signalling by inducing the destruction of β-catenin

GSK3β is a member of the β-catenin destruction complex, which is a dynamic multiprotein assembly which plays a fundamental role in regulating the Wnt/β-catenin signalling pathway. This destruction complex is composed of two scaffold proteins, Axin and Adenomatous polyposis coli (APC), as well as two serine/threonine kinases casein kinase 1 (CK1) and glycogen synthase kinase 3 (Figure 6). Noteworthy, both GSK3 isoforms function redundantly in this complex (Doble et al. 2007).

In cell resting state, the β-catenin destruction complex prevents Wnt signalling activation through continuous capturing and phosphorylating of β-catenin by CK1 and GSK3β in a sequential manner. CK1 phosphorylation of β-catenin at Ser45 creates a priming site for further GSK3β phosphorylation at Ser33, Ser37 and Thr41. Next, the β-transducin-repeat-containing protein (β-TRCP) tags β-catenin with ubiquitin, predisposing it for proteasome degradation. This mechanism maintains low cytoplasmic β-catenin levels and prevent its translocation to the nucleus (Fig. 6A). The binding of Wnt to the Frizzled receptor results in a subcellular redistribution of the β-catenin destruction complex and recruitment of Dishevelled (Dvl), allowing the dissociation of GSK3β from Axin. As a result, the β-catenin destruction complex is turned off allowing unphosphorylated β-catenin to accumulate and translocate to the nucleus (Seto and Bellen 2004). Finally, β-catenin binds the transcription

factors TCF (T-cell factor) and/or LEF (lymphocyte-enhancer-binding factor) to induce its target genes (Seidensticker and Behrens 2000) (Fig. 6B).

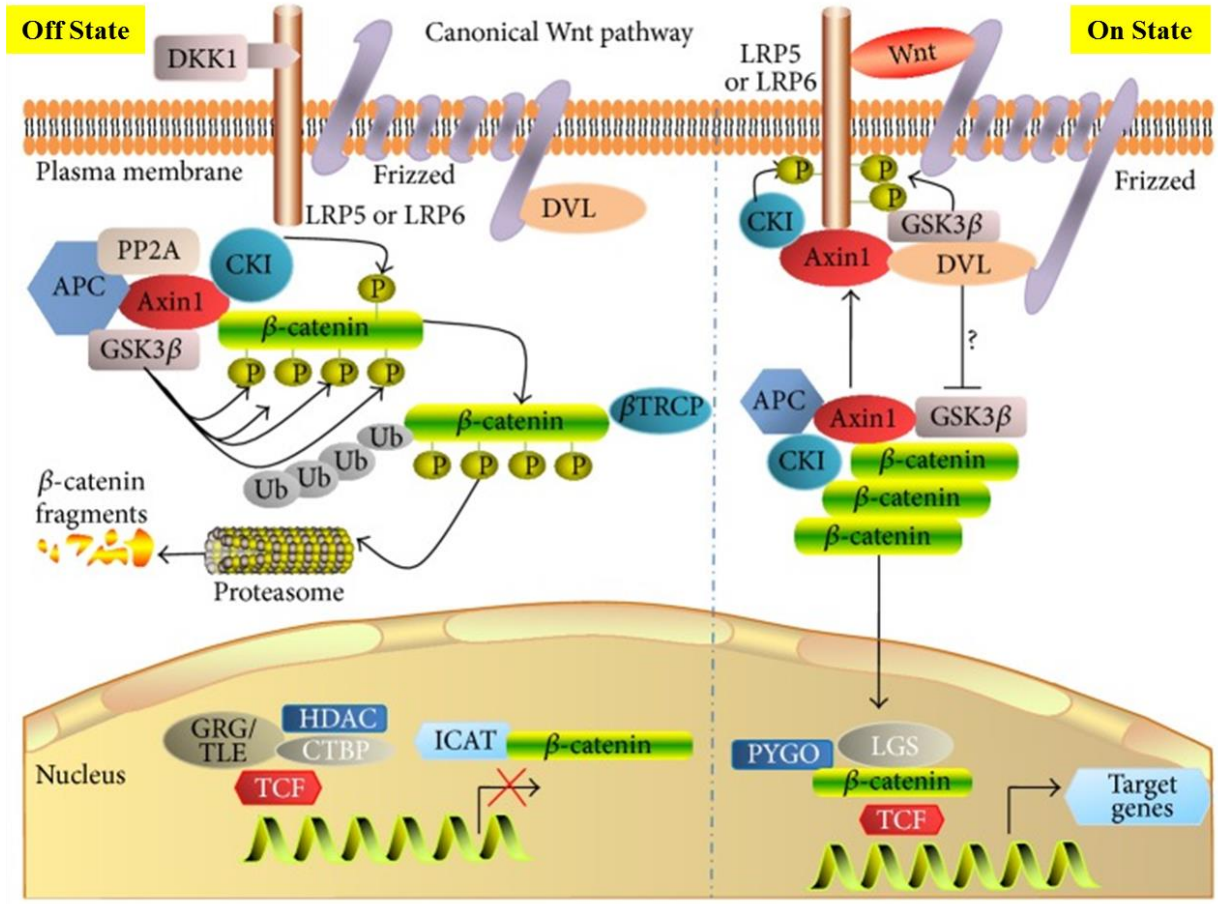

Figure 6: Wnt signalling pathway. Left side: In unstimulated Off state, β-catenin destruction complex; composed of Axin, Adenomatous polyposis coli (APC), Casein kinase 1α (CK1) and Glycogen synthase kinase 3β (GSK3β); phosphorylates β-catenin followed by recognition by β-transducin-repeat-containing protein (β-TRCP) and β-catenin ubiquitination and subsequent proteasome degradation. LCF/TCF family members are kept inactive by suppressors that belong to the GRG (Groucho-related gene) family. DKK1, dickkopf-1; LRP, lipoprotein-related receptor. **Right side:** Binding of Wnt to Frizzled receptor result in GSK3β inactivation through Dishevelled (Dvl). Unphosphorylated β-catenin accumulate and translocate to the nucleus to bind TCF to activate its target genes. The nuclear proteins pygopus homologue (PYGO) and legless homologue (LGS) determine β-catenin transcription activity (Shi et al. 2016, CC BY 4.0, https://creativecommons.org/licenses/by/4.0/).

1.4 Objectives

The previous studies showed that GSK3β modulates NF-κB signalling, probably by various mechanisms, however the exact effect of GSK3β is still obscure due to the conflicting results

obtained from different cell types and models. In T cells and in Jurkat T-ALL cell line, GSK3β was reported to be crucial for the degradation of the NF-κB member RelB. Moreover, in the ABC-type of DLBCL, GSK3β was reported to be recruited to the oncogenic active CARMA1 and is thus related to the CBM complex. As the formation of the CBM complex has been shown to be crucial for the MALT1-mediated cleavage of RelB, the possibility remains that the GSK3β which is bound to the CARMA1 complex might influence RelB degradation (and canonical NF-κB activation) by regulating CBM complex formation and the MALT1 endoprotease activity. Thus, in this study I aim to investigate the role of GSK3β in modulating the NF-κB signalling pathway in lymphocytes in order to understand the possible mechanism by which GSK3β mediate this action. In particular, I aim to focus on the effect of GSK3β inhibition on antigen receptor mediated NF-κB activation. GSK3β inhibition will be achieved by either using GSK3β pharmacological inhibitors SB216763 or SB415286 or by GSK3β gene silencing using either specific small interfering RNA (siRNA) or specific shRNA for a more target specific GSK3β inhibition. Analysis will include the effect of GSK3β inhibition on MALT1 endoprotease activity, cell proliferation, cell survival and NF-κB activation.

For studying the possible mechanism by which GSK3β mediate its action, I intend to perform biochemical and functional analyses of GSK3β interaction with the CBM complex member BCL10 and other NF-κB down streaming signalling members for example the IKK complex.

GSK3β inhibition in ABC- and GC-DLBCL will enable us to study the role of GSK3β in DLBCL proliferation, survival and apoptosis. Moreover, it might reveal the role played by GSK3β in the cross talk between NF-κB, β-catenin and other signalling cascades in DLBCL cell lines. Establishing an immunohistochemistry protocol for GSK3β and other related proteins in ABC- versus GC-DLBCL cell lines and DLBCL patient samples might be a useful tool for improving the ability of IHC to identify ABC- and GC-DLBCL without the need of microarray analysis which is not available for daily diagnostic routine. Finally, this study could present GSK3β as a novel therapeutic target alone or with others for the treatment of ABC-DLBCL.

2- Materials and methods:

2.1 Materials:

2.1.1. Chemicals and reagents:

Reagent	Supplier
Acetic acid	VWR, France
Acrylmide	AppliChem, Germany
Ammonium persulfate (APS)	Roth
Ampuwa	Fresenius Kabi
Anti-FLAG M2 affinity gel	Sigma
Boric acid	Merck
Bovine serum albumin (BSA)	Roth
Bradford reagent	Bio-rad
Calcium chloride (Cacl2)	Merck
CellTiter 96® Aqueous One Solution Cell Proliferation Assay	Promega
Complete Mini (protease inhibitor)	Roche
Cyclohexamide	Sigma
Dimethyle sulfoxide (DMSO)	Sigma
Dithiotreitol (DTT)	Merck
Dulbecco's Modified Eagle Medium (DMEM)	Lonza
Ethanol	Haen
Ethylenediaminetetraacetic acid (EDTA)	AppliChem
Fetal bovine serum (FBS)	Biochrom AG
Ficoll	Pharmacia
L-Glutamine	Gibco
Penicillin	Gibco
Protein G-sepharose	GE Health
Roswell Park Memorial Institute medium (RPMI)	Lonza
Streptomycin	Gibco
SYPER Green	Roche
β-glcerolphosphate	Sigma
β-mercaptoethanol	Sigma

2.1.2. Inducers and inhibitors

Reagent	Catalog	Supplier
Cycloheximid	#C7698	Sigma-Aldrich (St. Louis, MO, USA)
ImmunoCult™ Human CD3/CD28 T Cell Activator	#10971	STEMCELL technologies Inc. (Cologne, Germany)
Ionomycin	#I0634	Sigma-Aldrich (St. Louis, MO, USA)
MI-2	# S7429	Selleckchem
PMA	#524400	Merck (Darmstadt, Germany)
rhTNFα	#11343013	Immunotools (Friesoythe, Germany)
SB216763	#S3442	Sigma-Aldrich (St. Louis, MO, USA)
SB415286	#S3567	Sigma-Aldrich (St. Louis, MO, USA)

2.1.3. Devices

Device	Company
-80°C Fridge	Heraeus
Centrifuge	Eppendorf
Clean-bench	Baker
CO_2 Incubator	Thermo Scientific
Developing machine	AGFA
Multipette	Eppendorf
Fluorescence Microscopy	Zeiss
Fridge	Liebherr
Gel dryer	AlphaMetrix Biotech
Heat block	Eppendorf
Ice machine	Scotsman
Immunohistochemistry Auto-Stainer	Dako
Inverted microscope	Leitz
Magnetic stir	Heidolph
Microcentrifuge	Eppendorf
Microscope	Zeiss
Nucleofector	Lonza
PCR-machine	MWG Biotech AG

pH meter	WTW
Pipettes	Eppendorf
Rotor-Gene Q	Qiagen
Semi-dry blot	Sartorius
Shaker	Hartenstein
UV-spectrophotometer	Epoch
Vortexer	LMS
Weighting machine	Sartorius
Wesern blott gel chamber	C.B.S. Scientific Co.
Western blot scanner	LI-COR

2.1.4. Disposables

0.5, 1.5 and 2 ml reaction tubes	Eppendorf
12/24-well plate	Sarstedt
15 and 50 ml tubes	Sarstedt
6- well plate	Nunc
96-well plate	Nunc
Cell culture flasks	VWR
Cuvettes	Sarstedt
Filter paper	VWL
Glassware	Schott
Gloves	Sempermed
Nitrocellulose membrane	GE Healthcare
Parafilm	American Can Company
Pasteurpipettes	Ratiolab
PCR tubes	Sarstedt
Pipette tips	Biosphere
Steril filter	Whatmann
Syringe	BD
X-ray films	Fujifilm
Petridishes	Nunc

2.1.5. Kits

Nucleofection of Jurkat	Amaxa Nuclofection Kit V (Lonza)
IHC	Dako REAL™ Detection System, Alkaline Phosphatase/RED, Rabbit/Mouse (Dako)
RNA extraction	Rneasy Mini Kit (Qiagen)
Gel extraction	peqGOLD Microspin Gel Extraction Kit (Peqlab)

2.1.6. Cell lines

Cell line	Description	Source
HEK293T	Human embryonic kidney cells	DSMZ (ACC 635)
Jurkat	T cell leukemia	DMSZ (ACC 282)
OCI-LY3	ABC-DLBCL	DMSZ (ACC 761)
OCI-LY10	ABC-DLBCL	Institute for Pathology, Würzburg University, Germany
HBL-1	ABC-DLBCL	ATCC
SUDHL-4	GC-DLBCL	DMSZ (ACC 495)
SUDHL-6	GC-DLBCL	DMSZ (ACC 572)
SUDHL-8	GC-DLBCL	DMSZ (ACC 573)

2.1.7. Buffers and solutions

Buffer	Composition
10X Annealing buffer	200 mM Tris pH 7.6 100 mM MgCl 500 mM NaCl
10X PBS buffer	1.5 M NaCl 27 mM KCl 82.4 mM Na_2HPO_4 20 mM NaH_2PO_4 pH 7.22

10X SDS-running buffer	0.25 M Tris 1.92 M Glycin 1% SDS
10X Transfer buffer	58 g Tris 29 g Glycin 20% SDS ad 1L dH_2O
1X TAE	48.4 g Tris 11.4 ml Acetic acid 3.72 g EDTA ad 1L dH_2O
1X Transfer buffer	100 ml 10X transfer buffer 100 ml Methanol ad 1L dH_2O
20X TBS	48.46 g Tris 105.2 g NaCl pH 7.6 ad 1L dH_2O
2X HEBS	50 mM HEPES 280 mM NaCl 10 mM KCl 1.5 mM Na_2HPO_4 pH 7.06
2X SDS loading buffer (Laemmli buffer)	100 mM Tris pH 6.8 4% SDS 0.2% Bromophenolblue 20% Glycin 0.5% DTT

6X DNA loading dye	80% Glycin 100 mM EDTA 0.025% Bromophenalblue 0.025% Xylenxyanol F
Buffer A^{++} (hypotonic) for cytoplasmic extracts	10 mM HEPES pH 7.9 10 mM KCl 0.1 mM EDTA 0.1 mM EGTA 1 Tablet/20 ml buffer EASYpack phosphatase inhibitor cocktail (Roche) 1 Tablet/20 ml buffer EASYpack protease inhibitor cocktail (Roche) 1 mM DTT
Buffer B^{++} (hypertonic) for nuclear extracts	20 mM HEPES pH 7.9 0.4 M KCl 1 mM EDTA 1 mM EGTA 1 Tablet /20 ml buffer EASYpack phosphatase inhibitor cocktail (Roche) 1 Tablet /20 ml buffer EASYpack protease inhibitor cocktail (Roche) 1 mM DTT
Citrate buffer	10 mM Citric acid pH 6.0
Dignam C buffer	20 mM HEPES pH 7.9 25% Glycin 0.42 M NaCl 1.5 mM $MgCl_2$

	0.2 M EDTA
Dignam C^{++} buffer	20 mM HEPES pH 7.9 25% Glycin 0.42 M NaCl 1.5 mM $MgCl_2$ 0.2 M EDTA 1 Tablet/20 ml buffer EASYpack phosphatase inhibitor cocktail (Roche) 1 Tablet/20 ml buffer EASYpack protease inhibitor cocktail (Roche) 1 mM DTT
EMSA 10X hybridization buffer	70 mM Tris pH 7.5 70 mM $MgCl_2$ 500 mM NaCl
EMSA 10X TBE buffer	106 g Tris 55 g boric acid 40 ml 0.5 M EDTA (pH 8.0) ad 1L dH_2O
EMSA 3X binding buffer	60 mM HEPES pH 7.9 150 mM KCl 3 mM EDTA 3 mM DTT 12% Ficoll
EMSA STE buffer	20 mM Tris-HCl pH 7.5 100 mM NaCl 10 mM EDTA
Kinase assay buffer	20 mM HEBES pH 7.6

	2 mM EGTA 10 M $MgCl_2$ 1 mM DTT 0.1% Triton X100 20 mM β-Glycerophosphate 5 mM Sodium Floride 0.5 mM Na-ortho-vanadat 1 mM PMSF
LB medium	10 g Bacto-tryptone 5 g yeast extract 10 g NaCl pH to 7.5 with NaOH ad 1L dH_2O
Stripping buffer	0.2 M NaOH 5% SDS
TBS-T	50 ml 20X TBS 0.5 ml Tween 20 ad 1L dH_2O
TNT buffer	20 mM Tris pH 8.0 0.2 M NaCl 1% Triton X100 1 mM DTT
TNT^{++} buffer	20 mM Tris pH 8.0 0.2 M NaCl 1% Triton X100 1 mM DTT 1 Tablet/20 ml buffer EASYpack phosphatase inhibitor cocktail (Roche)

	1 Tablet/20 ml buffer EASYpack protease inhibitor cocktail (Roche) 1 mM DTT
WB Blocking solution	5 g skim milk powder 100 ml 1X TBS-T

2.1.8. Protein molecular weight standards

Color Protein Standard	Biolabs
WesternSure® Chemiluminescent Protein Ladder	LI-COR
DNA ladder	Biolab

2.1.9. Antibodies

Antibody	Clone, Number	Source	Company
BCL10	H-197, sc-5611	Rabbit	Santa Cruz Biotechnology
BCL10	331.3, sc-5273	Mouse	Santa Cruz Biotechnology
BCL10	C-17, sc-9560	Goat	Santa Cruz Biotechnology
GSK3β	27C10, #9315	Rabbit	Cell Signaling
pGSK3β (Tyr 216)	Tyr 216, sc-135653	Rabbit	Cell Signaling
pGSK3β (Ser9)	5B3, #9323	Rabbit	Cell Signaling
GSK3α	#9338	Rabbit	Cell Signaling
IKKα	H-744, sc-7218	Rabbit	Santa Cruz Biotechnology
IKKα/β	H470, sc-6707	Rabbit	Santa Cruz Biotechnology
IKKγ	FL-419, sc-8330	Rabbit	Santa Cruz Biotechnology
MALT1	H-300, sc-28246	Rabbit	Santa Cruz Biotechnology
CARD11	1D12	Rabbit	Cell Signaling
RelB	C1E4, #4922	Rabbit	Cell Signaling
IκBα	#9242	Rabbit	Cell Signaling
Cylindromatosis-1	E-10, sc-74435	Rabbit	Santa Cruz Biotechnology
NF-κB p65	F-6, sc-8008	Mouse	Santa Cruz Biotechnology
β-catenin	#610154	Mouse	BD Biosciences
β-actin	AC-74	Mouse	Sigma-Aldrich

β-tubulin	TUB 2.1	Mouse	Sigma-Aldrich
Anti-Mouse	#3143	Goat	Thermo-Scientific
Anti-Rabbit	#A9169	Goat	Sigma-Aldrich

2.1.10. Oligonucleotides

2.1.10.1 Oligonucleotides for DNA binding studies

NF-κB sense:	5'-GCGGGCCTGGGAAAGTCCCCTCAACT-'3
NF-κB antisense:	5'-GCGGAGTTGAGGGGACTTTCCCAGGC-'3
OCT-1 sense:	5'-GCGGACCTGGGTAATTTGCATTTCTAAAAT-'3
OCT-1 antisense:	5'-GCGGATTTTAGAAATGCAAATTACCCAGGT-'3

2.1.10.2 Oligonucleotides for siRNA-mediated knockdown

GSK3βsiRNA1	5'-GACUAGAGGGCAGAGUAAAU-3'
GSK3βsiRNA2	5'-CCGGGAACAAAUCCGAGAGAU-3'
GSK3αsiRNA	5'-GAAGUGGCUUACACGGACA-3'

2.1.10.3 Oligonucleotides for shRNA-mediated knockdown

hGSK3bsh for	5'-GATCCCCGAGAAATGAACCCAAACTATTCAAGA GATAGTTTGGGTTCATTTCTCTTTTTA-3'
hGSK3bsh rev	5'-AGCTTAAAAAGAGAAATGAACCCAAACTATCTC TTGAATAGTTTGGGTTCATTTCTCGGG-3'

2.1.10.4 Oligonucleotides for RT-PCR

hqBIRC3 for	5'-AGTTCTTTGAGGGGGACAAA-3'
hqBIRC3 rev	5'-ACAACAGGTGCTGCAAAAAG-3'
TRAF1 for	5'-CTCCTTCTGGTTGCCTCAGT-3'
TRAF1 rev	5'-AGTTCTAGGCGCTTTTGCTC-3'
hTNFA for	5'-TCCTTCAGACACCCTCAACC-3'
hTNFA rev	5'-AGGCCCCAGTTTGAATTCTT- 3'
bActin for	5'-TGTGGCATCCACGAAACTAC-3'

bActin rev	5’-GGAGCAATGATCTTGATCTTCA-3’
GAPDH for	5’-GCCAAAAGGGTCATCATCTC-3’
GAPDH rev	5’-TGTGGTCATGAGTCCTTCCA-3’

2.1.11. Plasmids

3XkB Luciferase	(Leidner et al. 2008)
Actin-Renilla	(Leidner et al. 2008)
FLAG-BCL10WT	(Wegener et al. 2006)
FLAG-BCL10S5A	(Wegener et al. 2006)
GSK3βWT	Addgene
GSK3βS9A	Addgene
GSK3βDN	Addgene
EYFP-IKK2	(Palkowitsch et al. 2011)
pSUPER	OligoEngine

2.1.12. Enzymes

Shrimp Alkaline Phosphatase	Fermentas
HinDIII	Biolabs
BglII	Biolabs
mMLV-RT	Invitrogen

2.1.13. Software

Software	Source
Gen5	Biotech
Image studio digits 5.2 software	LI-COR
ImageJ 1.49 v	Wayne Rasband
Office	Microsoft
Windows	Microsoft

2.2 Methods

2.2.1. Cell culture techniques

2.2.1.1 Cultivation and harvesting of mammalian cells

The cell lines were obtained frozen from a liquid nitrogen storage. The frozen cell lines were thawed by incubation in a 37ºC water bath until partially thawed. The cells were suspended in a suitable volume of a fresh medium at room temperature, DMSO was removed after centrifugation, then the cell pellet was re-suspended in fresh full medium and kept in culture.

Cells were kept in culture in a suitable flask in DMEM or RPMI medium with 10% FCS, 1% L-glutamine, penicillin (50 unit/ml) and streptomycin (50 µg/ml) and incubated at 37ºC and 5% CO_2. The cells were split every 3-4 days.

The suspension cell lines were seeded out at a cell density about 0.5-1 x 10^6 cells/ml; the optimal split ratio was about 1:3 to 1:5 every 2-3 days. To split adherent cell lines, the cells were firstly washed once with PBS, then 2 ml trypsin were added and incubated 2 min at 37ºC. Afterwards, 6 ml of fresh medium were added, and the cells were then pelleted by centrifugation for 5 min at 1000 rpm/min. Then the cells were re-suspended in 6 ml fresh medium. Finally, the cells were seeded at 1:10 dilution in fresh medium.

To freeze the cell lines, cells were pelleted in 15 ml tube and re-suspended in a freezing medium (70% medium, 20% FBS and 10% DMSO) and then aliquoted in cryovials. The cells were then stored overnight at -80ºC in a controlled rate freezing apparatus, next day the frozen cells were transferred to liquid nitrogen cylinder.

2.2.1.2 Transfection

2.2.1.2.1. Transfection of HEK293T cell line using the calcium phosphate method

HEK293T cells were seeded in a 6 well plate one day before the transfection to reach a cell density about 30-40% at the day of transfection. Up to 2 µg of DNA per well were diluted in 90 µl water and 10 µl of 2 M $CaCl_2$ were added and mixed well and subsequently were incubated at room temperature for 5 minutes. Next, 100 µl of 2X HEBS buffer were added slowly and mixed well and further incubated at room temperature for another 5 minutes. 200 µl of the mixture were added per well and incubated for 24 hours. Next day, the medium was exchanged to remove the calcium phosphate crystals and the cells were further incubated for another 24 hours before they were harvested.

2.2.1.2.2. Transfection using AMAXA nucleofector kit

The cells were split every 2-3 days before nucleofection to maintain the culture between 0.5-1.5 x 10^6 cells/ml. At the day f transfection, a 12 well plate was pre-incubated with 1ml of full medium for each transfection in a humidified incubator at 37ºC and 5% CO_2. For one sample, 18 µl of supplement solution were added to 82 µl of cell suspension nucleofection solution. An appropriate number of cells were pelleted by centrifugation and re-suspended in nucleofection solution in a final concentration of 1.5 x 10^6 cells/100 µl. Next, the 100 µl of cell suspension were mixed with 1-5 µg DNA or 2 nM - 2µM siRNA and then transferred immediately to an AMAXA certified cuvette and placed in the nucleofection apparatus. The suitable program was run, and the sample was transferred to the prepared 12 well plate. The plate was then incubated in a humidified incubator at 37ºC and 5% CO_2 for 72 hours.

2.2.1.3 Induction of the cells

2.2.1.3.1. PMA-Ionomycin induction

PMA was used at a final concentration of 50 ng/ml and ionomycin at 0.5 µM for the required time periods.

2.2.1.3.2. TNF-α induction

TNF-α was used at a final concentration of 20 ng/ml for the required time periods.

2.2.1.3.3. CD3/CD28 induction

For activation of cells using CD3/CD28 antibodies, cell suspension of 1 x10^6 cells/ml were activated using 25 µl/ml of ImmunoCult™ Human CD3/CD28 T Cell Activator. Next, the cells were incubated at 37ºC for the required time periods.

2.2.2. Bacterial culture techniques

2.2.2.1 Transformation of competent bacterial cells

The competent cells were first thawed gently on ice. 1-50 ng of required DNA was mixed with 100 µl of competent cells and incubated on ice for 30 minutes. The cells were heat shocked at 42ºC for 45 seconds and then cells were placed back on ice for 2 minutes. 900 µl of LB medium with no antibiotics were added and the cells were incubated at 37ºC for 1 hour with shaking. Afterwards, the cells were either used for inoculation of 200 ml LB medium with ampicillin in case of midi-prep or were placed into LB/ampicillin plates and incubated overnight at 37ºC to pick up clones.

2.2.2.2 Plasmid isolation from transformed bacteria

For mini- or midi-prep of plasmids, Qiagen Plasmid Mini or Midi Kits were used according to the manufacturer instructions.

2.2.3. Protein extraction from cells

2.2.3.1 Whole cell extract (TNT extract)

For adherent cells, they were firstly washed with 1 ml of ice cold PBS. Next, they were pelleted and re-suspended according to the pellet size in 100-200 µl TNT^{++} buffer and incubated on ice for 10 minutes. For suspension cells, an appropriate number of cells were centrifuged at 1200 rpm, 4^{o}C for 5 minutes. Next, the pellet was washed with 1 ml of ice cold PBS. According to its size, the pellet was resuspended in 100-200 µl TNT^{++} buffer and incubated on ice for 10 minutes. Afterwards the samples were centrifuged at 13000 rpm, 4^{o}C for 10-15 min. The supernatants were transferred to new collection tubes. Next the protein concentrations were measured then the extracts were further processed or stored at -80^{o}C.

2.2.3.2 Dignam C extract

For adherent cells, they were firstly washed with 1 ml of ice cold PBS. Next, they were pelleted and re-suspended according to the pellet size in 100-200 µl Dignam C^{++} buffer and incubated on ice for 20-30 minutes. For suspension cells, an appropriate number of cells were centrifuged at 1200 rpm, 4^{o}C for 5 minutes. Next, the pellet was washed with 1 ml of ice cold PBS. According to its size, the pellet was resuspended in 100-200 µl Dignam C^{++} buffer and incubated on ice for 20-30 minutes. Afterwards, a mechanical stress (scrubbing) was performed to the samples then the reaction tube was frozen shortly in liquid nitrogen and left to thawed back on ice. The freeze-thaw cycle was repeated twice. Finally, the lysate was centrifuged at 13000 rpm, 4^{o}C for 15 min. the supernatants were transferred to new collection tubes. The protein concentrations were measured then the extracts were further processed or stored at -80^{o}C.

2.2.3.3 Nuclear and cytoplasmic extracts preparation

For adherent cells seeded in one of 12 well plate, they were firstly washed with 1 ml of ice cold PBS. Next, they were pelleted and re-suspended in 200 µl of ice cold buffer A^{++} and incubated on ice for 15-20 minutes. For suspension cells, an appropriate number of cells (1-

5 x 10^6 cells) were centrifuged at 1200 rpm, 4^{o}C for 5 minutes. Next, the pellet was washed with 1 ml of ice cold PBS. According to its size, the pellet was resuspended in 200 µl of ice cold buffer A^{++} and incubated on ice for 15-20 minutes. Afterwards, 10 µl of NP40 (1%) solution was added to the cells and mixed. The samples were further incubated for 3-5 minutes at room temperature. The reaction tube was next vortexed for 15 seconds and centrifuged at 8000 rpm, 4^{o}C for 2 minutes. The supernatants (cytoplasmic protein extracts) were transferred to new collection tubes. The pellet was washed with 100 µl Buffer A^{++}, then re-suspended in 50 µl ice cold buffer C^{++} and left on a shaker for 30-45 minutes at 4^{o}C. The cytoplasmic protein extracts and the buffer C^{++} mixed pellets were centrifuged at 13000 rpm, 4^{o}C for 15 minutes. The supernatants of cytoplasmic and nuclear protein extracts were transferred to new collection tubes. Finally, the protein concentrations were measured. The extracts were further processed or stored at -80^{o}C for later use.

2.2.3.4 Bradford assay

To determine the concentration of proteins in a given solution, 2 µl of known control protein concentrations (1, 2.5, 5 or 10 µg/µl of BSA) or 2 µl of sample are added to 1ml of diluted Bradford solution (1:5 with Ampuwa) and incubated for 5 minutes at room temperature. The absorption spectrum of the reaction mix is measured at wave length of 595 nm using UV-spectrophotometer (Epoch). The protein concentrations were automatically calculated using Gen5 program.

2.2.4. Immunoblot analysis

2.2.4.1 SDS-polyacrylamide gel preparation

The prepared SDS-polyacrylamide gel is composed of an 8-14% running gel and a 4.5% stacking gel. The running gel was prepared as follow:

Running gel	8% (µl)	10% (µl)	11% (µl)	12% (µl)	14% (µl)
40% Acrylamide	2270	2824	3140	3403	3970
ddH_2O	2860	2306	2070	1729	1162
Tris-HCl 0.75M pH8.8	5640	5640	5640	5640	5640
APS (10mg/ml)	280	280	280	280	280
10% SDS	224	224	224	224	224
TEMED	20	20	20	20	20

The mixture was casted between two glass plates and the gel was covered with a layer of 100% ethanol to ensure a strait and smooth gel line. After the gel polymerize in about 20 minutes the stacking gel was prepared as follow:

Staking gel	4.5% (µl)
40% Acrylamide	564
ddH_2O	1716
Tris-HCl 0.75M pH8.8	2500
APS (10mg/ml)	125
10% SDS	50
TEMED	10

Immediately after casting the stacking gel mixture, a comb is placed between the two glass plates into the upper stacking gel to form pockets for loading the protein samples. After polymerisation of the stacking gel, the glass plates were clamped into a gel chamber. The gel chamber was filled with 1XSDS running buffer and the comb was removed so that the gel was in contact with the buffer, then air bubbles were removed.

2.2.4.2 SDS-polyacrylamide gel electrophoresis

10-40 µg of protein extracts were mixed with an appropriate amount of 6X SDS loading dye and the samples were boiled for 5-10 minutes at 95^{o}C to denature and negatively charge the proteins. The first pocket of the gel was loaded with 5 µl of a protein molecular weight standard marker and the samples were loaded into the other pockets separately. Then an electric current of about 120 volts was applied to the gel chamber allowing the proteins to migrate through the gel matrix toward the negative charge and separate according to their molecular weight.

2.2.4.3 Semi-dry transfer and blocking

After gel electrophoresis the proteins were elctrophoretically transferred to a nitrocellulose membrane using semi-dry blot. Eight filter papers and a nitrocellulose membrane were cutted to an appropriate size. The nitrocellulose membrane was activated with distilled water before use. Next, the nitrocellulose membrane was equilibrated together with the filter papers in 1X transfer buffer. Four layers of pre-soaked filter papers were placed in the blotter and the nitrocellulose membrane on top. Then the gel was placed on the nitrocellulose

membrane and covered with another four layers of pre-soaked filter papers. The air bubbles between all the layers were removed gently. The blotter lid was placed on the chamber and an electric current (60 mA per gel) was applied for 1.5 hours to the chamber. The negatively charged proteins migrate from the gel to the nitrocellulose membrane. After the transfer was completed, the membrane was blocked with a blocking solution (5% milk powder in TBS + Tween 20) for one hour at room temperature.

2.2.4.4 Protein detection and quantification

After blocking, the membrane was incubated overnight at 4^{o}C on a shaker with the diluted primary antibody at 1:1000 concentration in TBS-Tween or according to the manufacturer instructions. Next day the membrane was washed with TBS-Tween 3 times (5 minutes each). Next, it was incubated one hour at room temperature with the appropriate peroxidase-conjugated secondary antibody in 1:5000 concentration in TBS-Tween or according to the manufacturer instructions. Then the membrane was washed again with TBS-Tween 3 times (5 minutes each). The detection was performed either using ECL substrates when exposed to X-ray film, or using WesternSure®Premium Chemiluminescent Substrate from LI-COR when using C-Digit blot scanner from LI-COR. The quantifications were performed using ImageJ 1.49 v or Image studio digits 5.2 software.

2.2.5. Electrophoretic mobility shift assay

2.2.5.1 Hybridization of the oligonucleotides

The single stranded oligonucleotides were dissolved in distilled water at a concentration of 100pmol/l. The hybridization reaction mix was prepared as follow:

2.5 µg sense oligonucleotide
2.5 µg anti-sense oligonucleotide
10 µl 10X Annealing buffer
Up to 100 µl distilled water

The reaction mix was incubated for 10 minutes at 100^{o}C then it was cooled down gradually over several hours at room temperature (1^{o}C per minute).

2.2.5.2 Radioactive labelling of oligonucleotides

The NF-κB and OCT specific probes were labelled by radioactivity using Klenow reaction. Klenow polymerase fills up the annealed oligonucleotides with supplied radioactive ^{32}P-nucleotides (^{32}P-dCTPs). The Klenow reaction was prepared as follow:

1-2 µl Annealed oligonucleotides (κB or OCT)

5 µl 10X Klenow buffer

2.5 µl 0.5mM dNTP mix (without dCTP)

1 µl Klenow enzyme (5U/µl)

Up to 50 µl distilled water

The reaction mix was incubated for 1 hour at room temperature then 20 µl of STE buffer were added to stop the reaction. The free radioactive labelled nucleotides were removed by purifying the reaction mix with SigmaSpin™ Sequencing Reaction Clean-Up (Sigma) according to the manufacturer instructions.

2.2.5.3 Native polyacrylamide gel preparation

A 6% native polyacrylamide gel was prepared as follow:

Native PA gel	6%
40% Acrylamide	18ml
ddH_2O	96ml
10X TBE	4.8ml
APS (10%)	700 µl
TEMED	70 µl

The mixture was casted between two horizontal glass plates assembly avoiding air bubbles formation. Next, the well forming comb was inserted immediately and the gel was left to polymerize. After polymerisation of the gel, the glass plates were clamped into a vertical electrophoresis chamber. The upper and lower buffer reservoir was filled with 0.4X TBE buffer and the comb was removed so that the gel was in contact with the buffer. 2 µl of DNA dye was added to the first well and an electric current of about 200 volts was applied to the electrophoresis chamber before adding the samples for 2 hours (pre-run).

2.2.5.4 Samples preparation

The reaction mixture of samples was prepared in a total volume of 10 µl as follow:

1-10 µg nuclear protein extract

2 µl 5X Binding-Buffer

0.5 µl poly[pdI:dc] (2 µg/µl)

0.5-1 µl ^{32}P-kB/OCT

Up to 10 µl distilled water

The reaction mix was incubated for 15 minutes on ice. Then the samples were loaded to the native polyacrylamide gel and 2 µl of DNA dye was loaded to the first well.

2.2.5.5 Gel electrophoresis and detection

After loading the samples, an electric current about 220 Volts was applied to the gel chamber for about 2 hours until the DNA dye reached the middle of the gel. The gel was placed on an appropriate size two filter paper and was covered with plastic foil. Afterwards, the gel was dried using a vacuum gel dryer at 80^{o}C for 1-2 hours. The dried membrane was placed in an exposure cassette. An X-ray film was placed on the dried gel and exposed at first for an overnight exposure at -80^{o}C. Next day, the X-ray film was developed. Longer exposures were performed when necessary.

2.2.6. Immunoprecipitation

For immunoprecipitation whole cell extracts were prepared using TNT^{++} buffer. 1 µg of the target protein antibody was added to 250-500 µg of protein extracts in a total volume of 250-500 µl TNT^{++} buffer and incubated for overnight with rotation at 4^{o}C. Next day, 10 µl Protein G-Agarose beads were washed two times with cold PBS and one time with lysis buffer. The beads were finally resuspended in 100 µl TNT^{++} lysis buffer and added to the samples. Next samples were incubated for 1 hour with rotation at 4^{o}C. Then the beads were washed two times with TNT^{++} and one time with PBS buffer. The resulting immunopurified proteins were subjected to immunoblot analysis.

2.2.7. Phosphorylation studies techniques

2.2.7.1 *In vivo* phospho-labelling

2 x 10^7 Jurkat T cells were incubated in a phosphate free medium with 5% dialyzed FCS for 18 hours. Next day, 2 mCi/ml ^{32}P orthophosphate were added to the cells and the cells were subsequently incubated for 6 hours. A whole cell extract of the cells was used for a BCL10 immunoprecipitation. The precipitated proteins were then separated by SDS-PAGE, transferred to nitrocellulose membrane and finally subjected to autoradiography as well as immunoblot analysis.

For *in vivo* labelling using HEK293T cells, the cells were incubated in a phosphate free medium with 5% dialyzed FCS for one hour. Next, 2 mCi/ml ^{32}P orthophosphate were added to the cells and the cells were incubated for additional 2 hours. A whole cell extract using TNT^{++} buffer was done followed by a BCL10 immunoprecipitation. The precipitated proteins were separated by SDS-PAGE, transferred to a nitrocellulose membrane and finally subjected to autoradiography and immunoblot analysis.

2.2.7.2 *In vitro* kinase assay

For *in vitro* kinase assay using Jurkat cells, the cells were treated as indicated prior to TNT^{++} whole cell lysis. An anti-NEMO antibody or an anti-IKK1/2 antibody immunoprecipitation was performed overnight. The resulting immunocomplexes were washed extensively and the reaction was performed at 30ºC for 30 min after adding 10µCi (γ-^{32}P) ATP and 0.5 µg bacterial expressed GST-IκBα in a kinase assay buffer. The beads were then washed extensively with TNT^{++} buffer and PBS prior to separation using SDS-PAGE. The separated proteins were transferred to nitrocellulose membrane and subjected to autoradiography and immunoblot analysis.

For *in vitro* kinase assay with proteins ectopically expressed in HEK293T cells, the indicated FLAG tagged protein were expressed individually or in combination in HEK293T cells followed by FLAG immunoprecipitation. The beads were washed extensively, and the reaction was performed at 30ºC for 30 min after adding 10µCi (γ-^{32}P) ATP and 0.5 µg bacterial expressed GST-IκBα in a kinase assay buffer. The beads were then washed extensively with TNT^{++} buffer and PBS prior to separation using SDS-PAGE. The separated proteins were transferred to nitrocellulose membrane and subjected to autoradiography and immunoblot analysis.

2.2.7.3 *In vitro* dephosphorylation assay

For the verification of the BCL10 phosphorylation, a FLAG-BCL10 protein ectopically expressed in HEK293T cells was used. 48 hours after transfection, whole cell extracts from HEK293T cells were prepared followed by FLAG-immunoprecipitation using about 500 µg protein/sample. Each sample was split, one part was left untreated and the other was treated with 2 units of Shrimp Alkaline Phosphatase (SAP) in 40µl total reaction mixture. Reaction was performed at 37°C for 60 minutes and terminated by incubation at 95°C for 5 minutes. Subsequently, the samples were loaded onto a standard SDS-polyacrylamide gel and subjected to immunoblot analysis.

2.2.8. Luciferase reporter assay

A Jurkat T cell line which was stably transfected with a luciferase reporter construct controlled by a 3xκB site (Jur4 cells) was used. Jur4 cells were pre-treated as indicated for 6 hours then luciferase activity was estimated after TNT++ lysis. For luciferase activity, 20 µl lysate were added to 40 µl luciferase buffer and luciferase activity was measured by luminometer. Then 30 µl of Stop & Glo® buffer were added, and luciferase activity was measured again. Values were obtained in relative light units (RLU) and normalized against control values. The experiments were done in duplicates and were repeated three times with similar results.

2.2.9. Cell proliferation assay

In a 96-well plate, 5X103 cells per well in 100 µl medium were treated for the appropriate time accordingly. Each sample was repeated 6 times in 6 wells. Next, 20 µl of the CellTiter 96® AQueous One Solution Reagent are pipetted into each sample containing well. Another triplicate set of wells (without cells) containing the same volumes of culture medium and CellTiter 96® AQueous One Solution Reagent were also set as a control. The plate was incubated at 37°C for 1 hour in a humidified, 5% CO2 atmosphere. The absorbance of samples at 490nm was recorded using a 96-well plate reader. A reference wavelength of 700 nm was also measured to subtract the non-specific absorbance. The average 490 nm absorbance of the control wells with no cells was subtracted from the sample absorbance.

The mean and standard deviation of the six corrected absorption values of each sample was used for calculations.

2.2.10. Quantitative real time PCR

2.2.10.1 RNA isolation from eukaryotic cells

The isolation of RNA was performed using RNeasy Kit (Qiagen) according to the manufacturer's protocol. An appropriate number of cells were pelleted by centrifugation at room temperature for 5 minutes at 4000 rpm. Next, the pellet was washed with PBS buffer. The pellet was then resuspended in 350 µl of RLT buffer. To homogenize the lysate, it was pipetted into a QIAshredder spin column placed in a 2 ml collection tube and was centrifuged at room temperature for 2 minutes at full speed. An equal volume of 70% ethanol (350 µl) was added to the homogenized lysate and mix well by pipetting. The mixture was afterwards transferred to RNeasy spin column placed in a 2ml collection tube, centrifuged for 30 s at ≥10000 rpm and the flow-through was discarded. The spin column membrane was then washed once with 700 µl RW1 buffer and centrifugation for 30 s at ≥10000 rpm and twice with 500 µl RPE buffer and centrifugation for 30 s at ≥10000 rpm.

The RNeasy spin column was transferred to a new 2 ml collection tube and centrifuged at full speed for 1 min to dry the column. Finally, RNA was eluded by adding 30-50 µl RNase-free water directly to the spin column membrane and incubate 2 min then it was centrifuged for 1 min at ≥10,000 rpm. The RNA concentration was measured using a UV-spectrophotometer and was used directly or was stored at -80^{o}C.

2.2.10.2 cDNA synthesis

For cDNA synthesis, a 20µL reaction volume was used for 1µg of total RNA using Moloney Murine Leukemia Virus Reverse Transcriptase (M-MLV RT) as follows:

1 µl Poly-dT (Random primer)

1 µg RNA

1 µl dNTP (10 mM)

Up to 12 µl RNAse-free water

Samples were then incubated at 65^{o}C for 5 minutes and then were incubated back on ice.

4 µl first strand Buffer (5x)

2 µl DTT (0.1 M)

1 µl RNase out

Samples were then incubated at 37°C for 2 minutes and then were incubated back on ice. Finally, 1 µl of M-MLV RT was added to the reaction mix. The PCR reaction was carried out as follow:

25°C for 10 minutes

37°C for 50 minutes

70°C for 15 minutes

After synthesis, the cDNA samples were used for qRT-PCR or stored at -20°C.

2.2.10.3 qRT-PCR

The qRT-PCR reaction mix was performed in triplicates in an end volume of 10 µl per reaction as follow:

1 µl of diluted cDNA (1:10)

0.4 µl of 10 µM primer mix (Final concentration of 0.4 µM)

3.6 µl ddH_2O

5 µl SYBR Green Master (ROX)

Actin and GAPDH were used as reference genes. An additional negative control sample was used with no cDNA. The following qRT-PCR program was used:

Incubation	95°C for 5 minutes
Cycle (40 times)	95°C for 30 seconds
	58°C for 45 seconds
	72°C for 15 seconds
Melt	From 55°C to 95°C (each step 0.5°C)

2.2.10.4 qRT-PCR data analysis

The Ct values of both target and reference genes were determined automatically using Rotor-Gene Q software version 2.1.0. These Ct values were normalized to the Ct values of the two reference genes of the corresponding sample (ΔCt value). Mean and standard deviation of the ΔCt values of the triplicate was calculated. Fold change of target gene was calculated by normalizing the mean ΔCt value of treated sample to the mean ΔCt value of untreated/control sample (ΔΔCt value). Standard deviation of ΔΔCt value was calculated by dividing the

standard deviation of the of mean ΔCt value of each sample with the mean ΔCt value of control sample.

2.2.11. Cloning methods

2.2.11.1 PCR amplification of DNA for cloning

PCR amplification of DNA was performed using a high-fidelity enzyme – Platinum™ *Pfx* DNA polymerase (Invitrogen). PCR reaction was performed in a total reaction of 50 µl as follows:

Component	Volume for 50 µl reaction	Final concentration
10X *Pfx* amplification buffer	5 µl	1X
10 mM dNTP mixture	1.5 µl	0.3 mM each
50 mM $MgSO_4$	1 µl	1 mM
Primer mix (10 µM each)	1.5 µl	0.3 µM
Template DNA	≥1 µl	10 pg to200 ng
Platinium™ *Pfx* DNA polymerase	0.4 µl	1 U
Nuclease free water	Up to 50 µl	-

The template was denatured for 2–5 minutes at 94°C followed by 25–35 cycles of PCR amplification as follow:

Denature	94°C for 15 seconds
Anneal	55°C for 30 seconds
Extend	68°C for 1 minute per kb

The samples were stored at -20°C until use or were analysed immediately for the products by agarose gel electrophoresis.

2.2.11.2 Isolation of DNA on agarose gel

DNA was isolated and visualized using 1% agarose gel. The gel was prepared with 0.5-gram agarose in 50 ml 1X TAE buffer, heated for few minutes and then left to cool down to about 50°C followed by adding ethidium bromide (EtBr) to a final concentration of approximately 0.2-0.5 µg/ml. The agarose was then poured into a gel tray with the well comb in place and was left until it has completely solidified (20-30 minutes at room temperature). The samples were mixed with DNA dye and loaded to the gel and a protein ladder was loaded in a separate

well. The gel was placed in electrophoresis set and was run at 80-150 volts until the dye line is approximately 75-80% of the way down the gel. The gel was placed on a UV-transilluminator and the desired DNA band was excised.

2.2.11.3 DNA purification/gel extraction

For extraction of the DNA from the agarose gel slice a peqGOLD Microspin Gel Extraction Kit (Peqlab) was used according to the manufacturer instructions. In brief, the approximate volume of the gel slice was determined and 500 µl of GP-buffer was added for gel slice ≤150 mg. The mixture was next incubated at 50-65^{o}C for 10 minutes or until the gel has melt completely. 250 µl of MPC buffer was added to the mixture. Next it was transferred to a MicroSpin DNA column/collection tube assembly and was centrifuged for 1 minute at 10.000 X g. The column was washed with 700 µl of CG-wash buffer diluted with ethanol and was centrifuged again for 1 minute at 10.000 X g. The flow through was discarded and the column was dried by centrifugation for 1 minute at 10.000 X g. DNA was finally eluted from the column with 10-20 µl of elusion buffer and was centrifuged for 1 minute at 10.000 X g. DNA can be stored at -20^{o}C.

2.2.11.4 DNA digestion by restriction enzymes

For digestion of DNA by restriction enzymes, the following reaction was performed at total volume of 20 µl as follow:

0.1-0.4 µg	DNA template
2 µl	10X digestion buffer
1-5 U/ µg DNA	Appropriate enzyme
Up to 20 µl	Nuclease free water

The reaction was incubated at 37^{o}C for 1 hour. 2-5 µl of the digested sample was loaded to an agarose gel to check the result.

2.2.11.5 DNA ligation

The ligation was performed at total volume of 20 µl on ice as follows:

2 µl	10X T4 DNA ligase buffer
50 ng	Vector DNA
50 ng	Insert DNA
Up to 20 µl	Nuclease free water
1 µl	T4 DNA ligase

The mixture was incubated at room temperature for 10 minutes for cohesive ends. 1-5 µl of the reaction was transformed into 50 µl competent cells.

2.2.12. Immunohistochemical staining of FFPE slides (Immunohistochemistry)

For immunohistochemistry, formalin–fixed and paraffin–embedded materials (FFPE) were used (3-4 µm thick sections) for both the DLBCL cell lines and cohort. For the DLBCL cohort samples, the prior approval of the ethics committee of the University of Ulm were obtained (Number: 394/17).

2.2.12.1 Deparaffinization and Rehydration

The slides were incubated 3 times, 5 minutes each in Xylol followed by 5 minutes incubation in each of gradually decreasing concentrations of ethanol (100%, 90% and 70%). Finally, slides were washed in distilled water for 3 times.

2.2.12.2 Antigen retrieval

Antigen retrieval was performed according to the antibody used either with a steamer, a microwave or a pressure cooker. The protocol for each antibody was used as follows or according to the manufacturer instruction.

For the steamer method, slides were incubated in the steamer in preheated EDTA buffer pH 9.0 for 20 minutes. After incubation, the vessel was removed, and cold water was run into for 10 minutes.

For the microwave method, the slides were placed in a microwavable vessel filled with 10 mM citrate buffer pH 6.0. The microwave was set to full power until the solution comes to boil. Samples were boiled for 20 minutes from this point. The vessel was removed from the microwave and cold tap water was run into for 10 minutes.

For the pressure cooker method, 10 mM citrate buffer pH 6.0 were added to the pressure cooker and preheated on a hotplate without securing the lid. Once boiling has reached, the slides where transferred to the pressure cooker and the lid was secured. As soon as the cooker has reached full pressure, temperature was set to 150°C and incubated for 20 minutes. Afterwards, the hotplate was turned off and the pressure cooker was placed in an empty sink

and the pressure valve was released. Once de-pressurized, cold water was run over the cooker for 10 minutes.

2.2.12.3 Staining

For staining, Dako REAL™ Detection System, Alkaline Phosphatase/RED, Rabbit/Mouse was used according to the manufacturer instruction. The protocol for each used antibody was performed as follows:

Antibody	Clone	Source	Dilution	Treatment	Company
β-catenin	14/Beta-catenin	Mouse	1:200	Pressure cooker	BD Bioscience
c-Myc	EP121	Rabbit	1:100	Steamer	Epiotomics
p53	DO-7	Mouse	1:500	Microwave	Dako
RelA (p65)	F-6	Mouse	1:1000	Pressure cooker	Santa Cruz
GSK3β	27C10	Rabbit	1:100	Microwave	Cell Signaling
p-GSK3β (S9)	5B3	Rabbit	1:100	Microwave	Cell Signaling

A negative and positive control were also included for each antibody.

2.2.12.4 Evaluation

The evaluation of IHC staining were evaluated by a certified pathologist. The scoring of IHC staining was performed as follow:

-	No staining
+	Less than 30% of cells are positive
++	30-70% of cells are positive
+++	More than 70% of cells are positive

3- Results:

3.1 GSK3β is required for signal induced MALT1 endoprotease activity

A previous study identified a crucial role of GSK3β in signal induced RelB degradation and showed that GSK3β form a complex with RelB in unstimulated T lymphocytes, but the exact mechanism(s) by which GSK3β modulate NF-κB is still obscure (Neumann et al. 2011). On the other hand, another study showed that oncogenic CARMA1 recruits GSK3β, as a part of β-catenin destruction complex, in ABC-type DLBCL (Bognar et al. 2016), suggesting an additional link between GSK3β and NF-κB in this kind of tumor. To confirm the effect of GSK3β on RelB and explore if also other MALT1 target proteins might be affected by GSK3β, Jurkat T-ALL cells were left untreated or treated with the GSK3β pharmacological inhibitor SB216763 (SB21) prior to the stimulation with PMA+Ionomycin (P/I) for different time intervals, then the MALT1 substrates RelB and Cylindromatosis-1 (CYLD1) were monitored by immunoblot analysis. β-catenin was monitored as an indicator for efficiency of GSK3β inhibition (Figure 7A).

As expected, P/I stimulation led to marked RelB degradation which was attenuated with pre-treatment with SB21 (Figure 7, compare lanes 1-4 to 5-8). Moreover, upon P/I stimulation CYLD1 showed pronounced proteolysis, as evidenced by the appearance of a ≈70 kDa CYLD1 signal representing C-terminal cleavage product of CYLD1 (ΔCYLD1) in addition to the ≈120 kDa full length CYLD1 signal (Figure 7A, lanes 1-4). Upon inhibition of GSK3β with SB21, the level of CYLD1 cleavage product was diminished (Figure 7A, compare lanes 1-4 to 5-8).

Subsequently, this effect of GSK3β was also studied using the more physiological stimulation by agonistic anti-CD3/CD28 antibodies. Again, GSK3β inhibition interfered with the degradation of RelB as well as with the proteolysis of CYLD1 (Figure 7B).

A

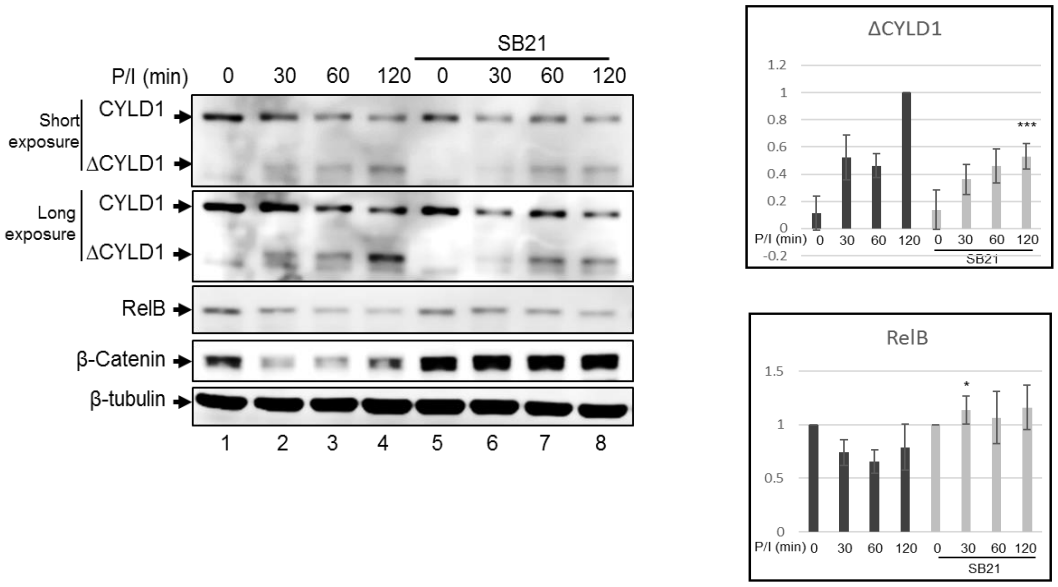

B

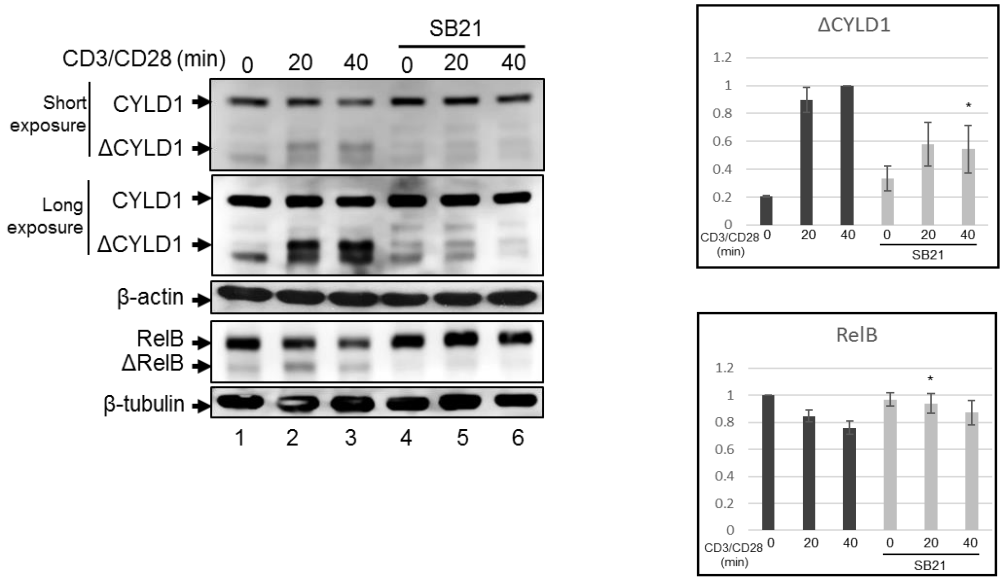

Figure (7): Inhibition of GSK3β attenuates the activity of the MALT1 paracaspase. *A,* Immunoblot analysis of CYLD1, RelB, β-catenin and β-tubulin Jurkat T-ALL cells pre-treated with SB21 before P/I stimulation for the indicated times. The right panel shows the quantifications of ΔCYLD1 and RelB protein analysis of at least three independent experiments. *B,* Immunoblot analysis of CYLD1, β-actin, RelB and β-tubulin using whole cell extracts from Jurkat T-ALL cells pre-treated with SB21 before CD3/CD28 stimulation for the indicated times. The right panel shows the quantifications of ΔCYLD1 and RelB protein analysis of at least three independent experiments (NS $p>0.05$, * $p \leq 0.05$, ** $p \leq 0.01$, *** $p \leq 0.001$).

Moreover, a similar effect of GSK3β inhibition on MALT1 endoprotease activity was observed in HSB2 cells (another T-ALL cell line) which were left untreated or were pre-treated with SB21 prior to P/I stimulation followed by immunoblot analysis (Figure 8).

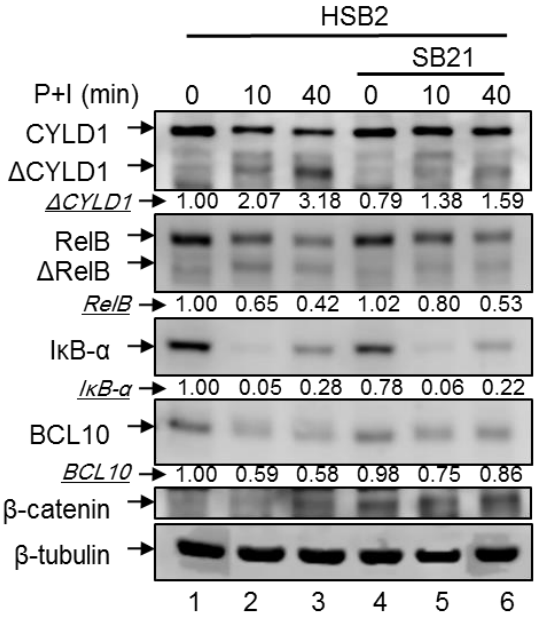

Figure (8): Effects of GSK3β inhibition by SB21 in HSB2 T-ALL cells. Immunoblot analyses for the indicated proteins using whole cell extracts from HSB2 T-ALL cells either with or without SB21 pre-treatment prior to a stimulation with P/I for the indicated time intervals.

This effect of GSK3β inhibition was similar to the effect produced by inhibition of MALT1 endoprotease activity using the MALT1 pharmacological inhibitor (MI-2) which caused attenuated CYLD1 cleavage and RelB degradation (Figure 9). Taken together, these data suggest that GSK3β is required for MALT1 endoprotease activity.

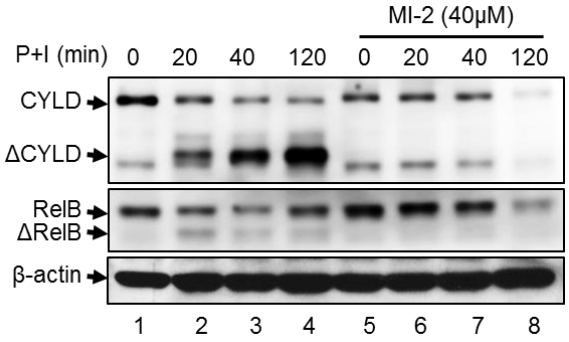

Figure (9): Inhibition of MALT1 endoprotease activity by MALT1 inhibitor. Immunoblot analysis of CYLD1, RelB and β-actin in Jurkat T-ALL cells stimulated with P/I for indicated time intervals after pre-treatment with the specific MALT1 inhibitor MI-2.

To further extend this study, Jurkat T-ALL cell clones were established either transfected with control sh-RNA (Jurkat sh-Control cells) or specific GSK3β specific sh-RNA (Jurkat sh-GSK3β cells) and the efficiency of GSK3β suppression were monitored by immunoblot analysis. Indeed, the GSK3β expression level in Jurkat sh-GSK3β cells was distinctive decreased in comparison to the sh-Control cell line. Moreover, GSK3β activity was also decreased in Jurkat sh-GSK3β cells as evidenced by the increase of β-catenin levels (Figure 10A). In addition, the CBM complex components protein expression were determined by immunoblot analysis. While CARD11 expression in Jurkat sh-GSK3β cells seemed to be slightly increased, no considerable changes were found upon quantification of the other CBM complex components in both cell lines (Figure 10B).

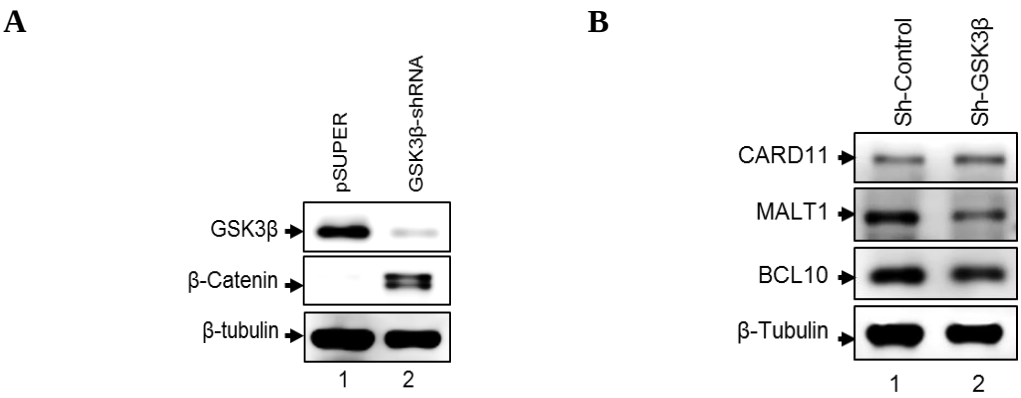

Figure (10): Establishing Jurkat sh-Control and Jurkat sh-GSK3β cell lines. *A,* Immunoblot analysis of GSK3β, β-catenin and β-tubulin in the stable sh-Control (pSUPER) and sh-GSK3β Jurkat T-ALL (GSK3β-shRNA) cell lines. *B,* Expression levels of distinct CBM signalling components in Jurkat sh-Control and Jurkat sh-GSK3β cells.

The MALT1 endoprotease activity was next studied in both established cell lines after P/I stimulation. For this, CYLD1 and RelB protein levels were examined by immunoblot analysis. As expected, RelB degradation in Jurkat sh-GSK3β was reduced in compare to Jurkat sh-Control (Figure 11, compare lanes 1-4 and lanes 5-8). Moreover, the basal level of RelB expression in Jurkat sh-GSK3β was found to be elevated (Figure 11, compare lanes 1,5). In line with our findings, the levels of the CYLD1 cleavage product upon stimulation were attenuated in Jurkat sh-GSK3β cells as compared to the Jurkat sh-Control cells (Figure 11, compare lanes 1-4 and lanes 5-8).

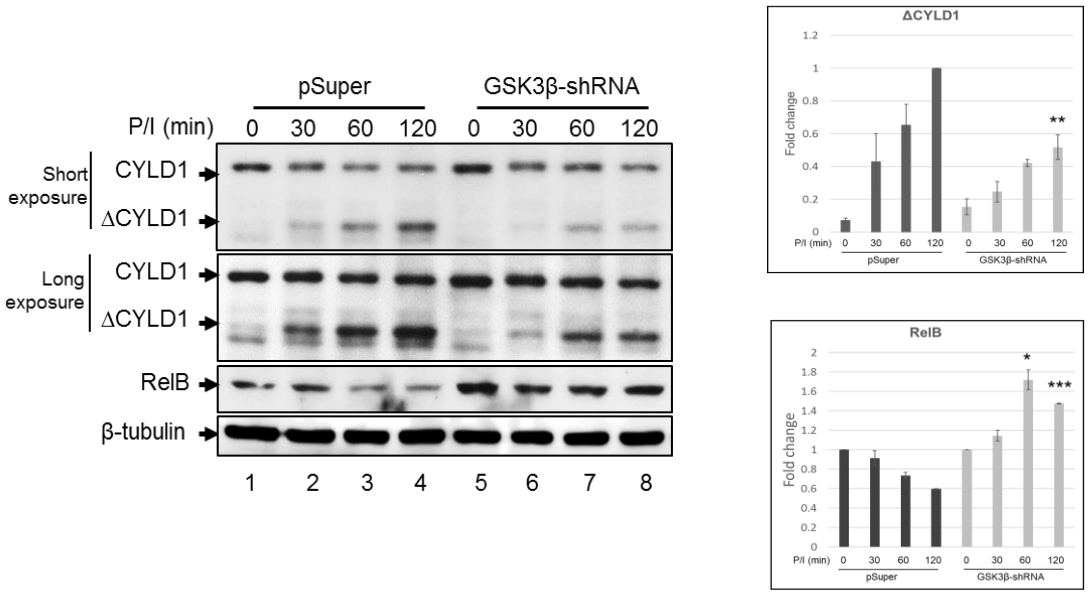

Figure (11): Inhibition of GSK3β with specific shRNA attenuates MALT1 activity. Immunoblot analysis of CYLD1, RelB and β-tubulin in Jurkat sh-Control (pSUPER) and sh-GSK3β T-ALL (GSK3β-shRNA) cells stimulated with P/I for indicated time intervals. Right panel shows the quantifications of ΔCYLD1 and RelB protein analysis of at least three independent experiments (NS $p>0.05$, * $p \leq 0.05$, ** $p \leq 0.01$, *** $p \leq 0.001$).

To exclude that the effect of GSK3β inhibition on the MALT1 activity is caused by an impact on protein neo-synthesis rather than protein degradation, cleavage and stability, Jurkat T-ALL cells were pre-treated with the translation inhibitor cycloheximide (CHX) alone or in combination with SB21 prior to P/I stimulation. Again, CYLD1, RelB and IκBα were monitored by immunoblot analysis (Figure 12). Whereas CHX pre-treatment alone had no effect on basal CYLD1 expression or P/I induced CYLD1 cleavage (Figure 12, compare lanes 1-4), SB21 pre-treatment either alone or with CHX showed distinct inhibition of CYLD1 cleavage (Figure 12, lanes 5-8). Furthermore, CHX pre-treatment had no effect on SB21 mediated RelB stabilization (Figure 12). In addition, CHX pre-treatment totally blocked IκBα neo-synthesis after P/I stimulation (Figure 12, compare lanes 2,4), whereas SB21 pre-treatment attenuated IκBα degradation (Figure 12, lanes 5-8). These data denote that these protein changes are not influenced by an impact of GSK3β on protein neo-synthesis. Taken together, these data suggest that GSK3β is required for signal induced MALT1 endoprotease activity.

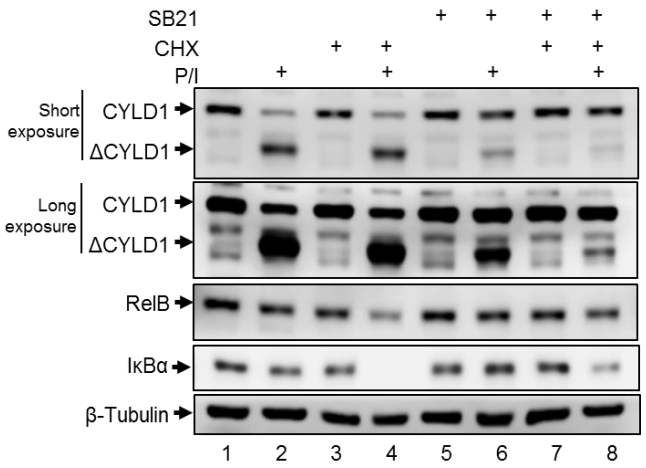

Figure (12): The effect of GSK3β inhibition on MALT1 is not affected by neo-synthesis. Immunoblot analysis of CYLD1, RelB, IκBα and β-actin in Jurkat T-ALL cells stimulated with P/I for indicated times after pre-treatment with CHX and or SB21.

3.2 GSK3β modulates the canonical NF-κB signalling pathway

The data presented point so far toward an impact of GSK3β on signal induced MALT1 endoprotease activity. MALT1 activity is controlled by the signal-induced CBM complex formation. Moreover, CBM complex formation is a crucial step for the antigen receptor-induced canonical NF-κB activity. Therefore, the effect of GSK3β inhibition on this particular canonical NF-κB signalling pathway was dissected. For this, Jurkat sh-Control or Jurkat sh-GSK3β cells were either left unstimulated or were stimulated with P/I for different time intervals, then IκBα and BCL10 protein levels were monitored by immunoblot analysis (Figure 13A). As expected, P/I stimulation led to marked IκBα degradation in Jurkat sh-Control cells (Figure 13A, lanes 1-3). By contrast, IκBα degradation was attenuated in Jurkat sh-GSK3β cells, which in addition showed an increased basal IκBα expression (Figure 13A, lanes 4-6). Similarly, P/I mediated BCL10 decrease was attenuated in Jurkat sh-GSK3β cells in comparison to Jurkat sh-Control cells (Figure 13A). In line with the previous findings, IκBα degradation and BCL10 decrease were likewise diminished upon GSK3β inhibition in Jurkat T-ALL cells by SB21 prior to anti-CD3/CD28 antibody stimulation compared to cells without GSK3β inhibition (Figure 13B).

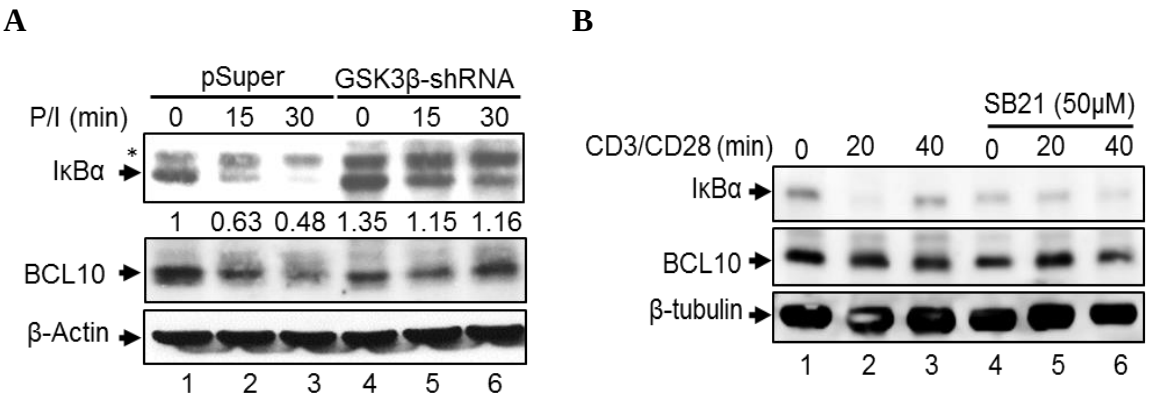

Figure (13): GSK3β inhibition interferes with the degradation of the canonical NF-κB signalling pathway members. *A,* Immunoblot analysis of IκBα, BCL10 and β-actin in Jurkat sh-Control (pSUPER) or Jurkat sh-GSK3β (GSK3β-shRNA) cells stimulated with P/I. The numbers below indicate the quantifications of IκBα proteins analysis normalized to β-actin protein. *B,* Immunoblot analysis of IκBα, BCL10 and β-tubulin in in Jurkat T-ALL cells stimulated with anti-CD3/CD28 antibodies after pre-treatment with SB21.

To extend the analysis of the effect of GSK3β on the canonical NF-κB signalling pathway, the effect of GSK3β inhibition on NF-κB activity was determined by luciferase reporter assays using a Jurkat T-ALL cell line stably transfected with a luciferase reporter construct controlled by 3XκB sites (Jur4 cells). The Jur4 cells were either left untreated or were pre-treated with increasing concentrations of GSK3β inhibitors SB21 or SB41, or with 30 μM of the pharmacological MALT1 inhibitor MI-2 prior to stimulation with P/I for 6 hours. Subsequently, the NF-κB-dependent luciferase activity was measured. As shown in figure 14A, P/I stimulation increased NF-κB activity about 70-fold. However, the inhibition of GSK3β using either SB21 or SB41 led to a dose-dependent decrease of the P/I induced NF-κB activation, although SB21 seemed to be a better inhibitor than SB41 (Figure 14A). In addition, MALT1 inhibition using MI-2 led to a complete loss of NF-κB activation. Similarly, P/I-induced NF-κB reporter gene activity was distinctively lower in Jurkat sh-GSK3β cells than in Jurkat sh-Control cells after transient transfection of a 3XκB luciferase reporter construct (Figure 14B).

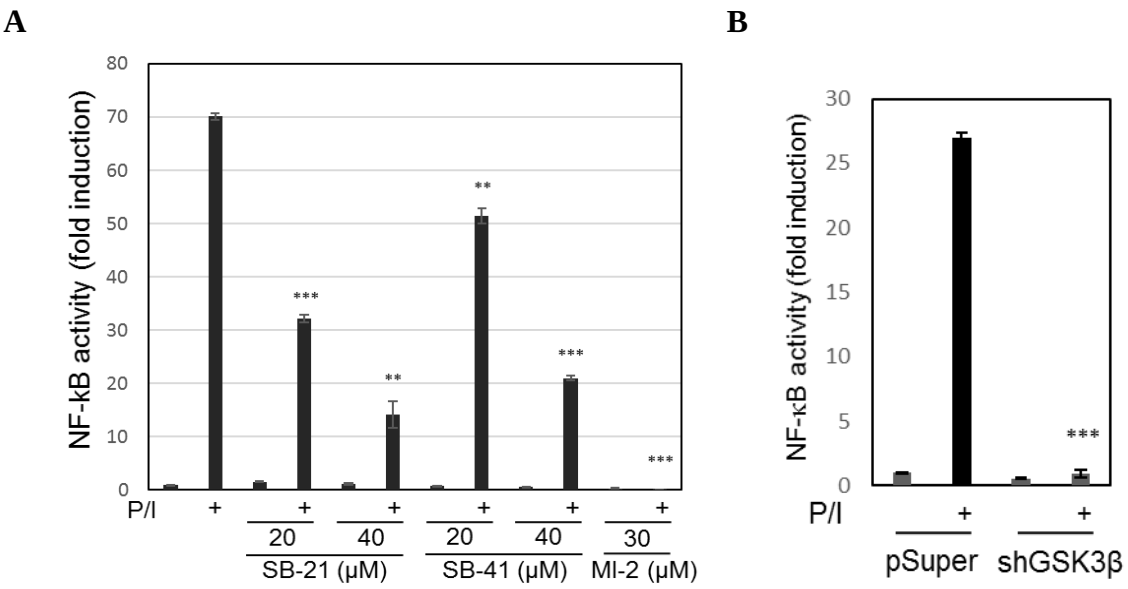

Figure (14): GSK3β inhibition attenuates activation of NF-κB signalling. *A,* Luciferase reporter assay of Jur4 cells pre-treated with indicated concentrations of SB21, SB41 or MI-2 prior to stimulation with P/I for 6 hours. *B,* Luciferase reporter assay of Jurkat sh-Control (pSUPER) or Jurkat sh-GSK3β (GSK3β-shRNA) cells transiently transfected with 3xκB reporter construct prior to P/I stimulation (NS $p>0.05$, * $p \leq 0.05$, ** $p \leq 0.01$, *** $p \leq 0.001$).

Next, the P/I induced DNA-binding activity of NF-κB upon GSK3β inhibition in Jurkat T-ALL cells was assessed using an Electrophoretic Mobility Shift Assay (EMSA). The inhibition of GSK3β by GSK3β specific sh-RNA (Figure 15) impaired the P/I induced DNA-binding activity of NF-κB. Likewise, the inhibition of MALT1 using MI-2 attenuated the P/I induced NF-κB DNA binding activity as measured by EMSA analysis (Figure 16).

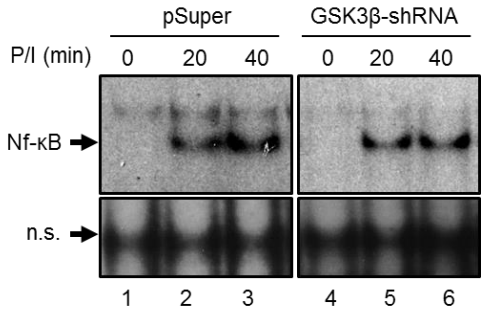

Figure (15): Inhibition of GSK3β attenuates NF-κB DNA binding. EMSA study of NF-κB DNA binding activity of Jurkat sh-Control (pSUPER) or Jurkat sh-GSK3β (GSK3β-shRNA) cells stimulated with P/I for indicated times. n.s.= non-specific binding.

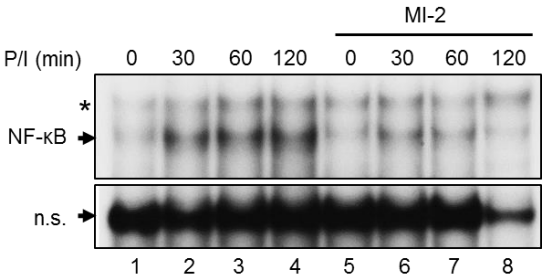

Figure (16): Inhibition of MALT1 activity attenuates NF-κB DNA binding. EMSA study of NF-κB DNA binding activity of Jurkat T-ALL cells treated with MI-2 prior to P/I stimulation. n.s.= non-specific binding.

In line with previous findings, the induction of NF-κB the target genes BIRC3, TNFA and TRAF1 upon P/I stimulation was impaired by GSK3β inhibition using either SB21 or SB41 as measured by quantitative RT-PCR analysis (Figure 17).

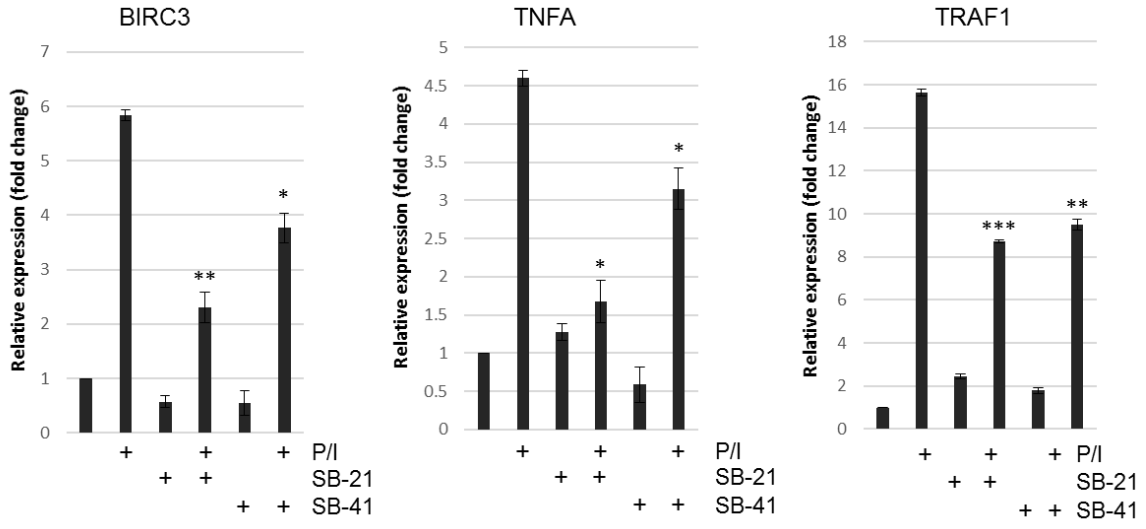

Figure (17): Quantitative real time PCR analysis of mRNA level of BIRC3, TNFA and TRAF1. Jurkat T-ALL cells were left untreated or pre-treated with either SB21 or SB41 prior to stimulation with P/I for 16 hours (NS $p>0.05$, * $p \leq 0.05$, ** $p \leq 0.01$, *** $p \leq 0.001$).

A similar significant effect on the P/I induced expression of NF-κB the target genes BIRC3 and TNFA was observed in Jurkat sh-GSK3β cells compared to Jurkat sh-Control cells. However, for the NF-κB target gene TRAF1 only a tendency to be less expressed in Jurkat sh-GSK3β compared to Jurkat sh-Control cells was seen (Figure 18).

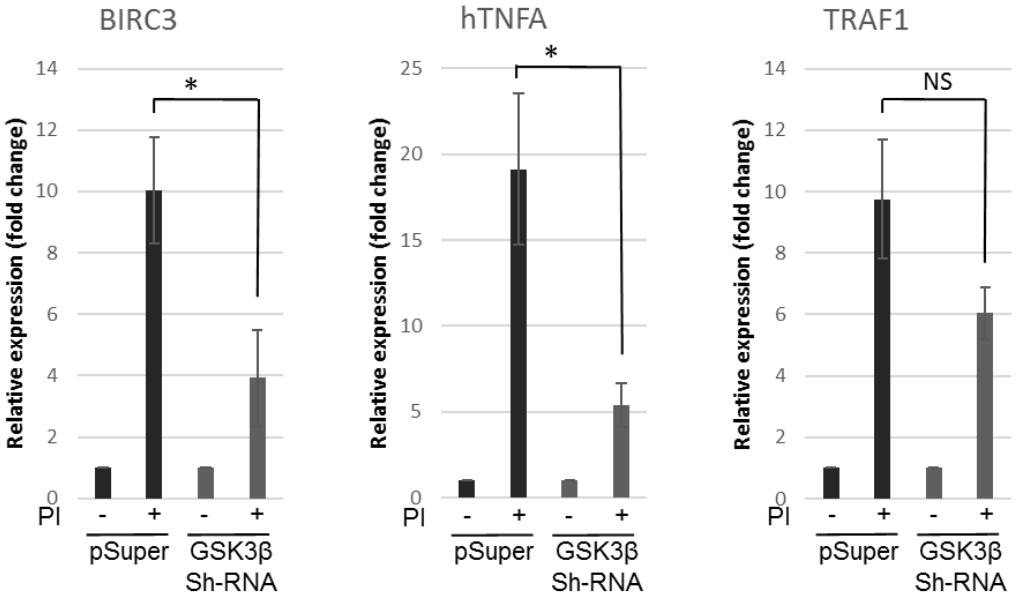

Figure (18): Quantitative real time PCR analysis of mRNA level of BIRC3, TNFA and TRAF1 in Jurkat sh-Control and Jurkat sh-GSK3β. Jurkat sh-Control (pSUPER) or Jurkat sh-GSK3β (GSK3β-shRNA) cells left unstimulated or prior to stimulation with P/I for 16 hours prior to mRNA extraction and analysis with fold change expression in relation to unstimulated cells (NS $p>0.05$, * $p \leq 0.05$, ** $p \leq 0.01$, *** $p \leq 0.001$).

Taken together, these data suggest a role of GSK3β in the P/I or anti-CD3/CD28 induced canonical NF-κB signalling pathway.

3.3 GSK3β modulates CBM complex formation

The CBM complex plays a pivotal role in the antigen receptor mediated NF-κB activation in B and T lymphocytes as well as in the pathogenesis of ABC-DLBCL (Thome et al. 2010). Previous data suggested that GSK3β is essential for antigen receptor mediated MALT1 endoprotease activity and canonical NF-κB activation. Accordingly, co-immunoprecipitation experiments were performed in order to investigate if GSK3β mediates RelB degradation and NF-κB activation through interfering with the CBM complex

formation. Jurkat sh-Control or sh-GSK3β cells were stimulated with P/I for 20 minutes followed by a BCL10 immunoprecipitation coupled with CARMA1 and MALT1 immunoblot analysis. P/I stimulation of Jurkat sh-Control cells led to BCL10-CARMA1 interaction as evidenced by appearance of a CARMA1 signal (Figure 19A, lane 2). While the CBM complex formation, as monitored by BCL10-CARMA1 interaction, was readily seen after 20 minutes of P/I stimulation of sh-Control cells, it was hardly visible in Jurkat sh-GSK3β cells (Figure 19A, compare lanes 2 and 4). Similarly, the inhibition of GSK3β using the specific GSK3β-siRNA attenuated the BCL10-CARMA1 interaction as compared to the control-siRNA transfected Jurkat T-ALL cells (Figure 19B). These results imply that GSK3β mediates MALT1 endoprotease activity and canonical NF-κB activation via modulating CBM complex formation.

A

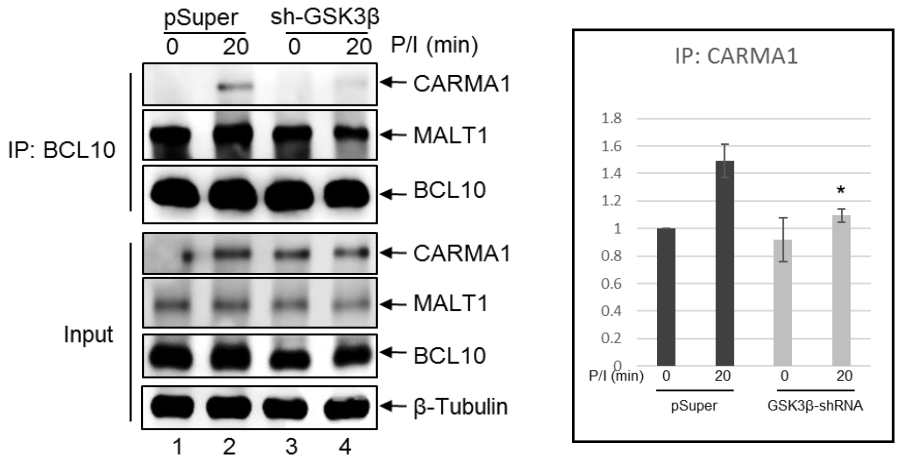

B

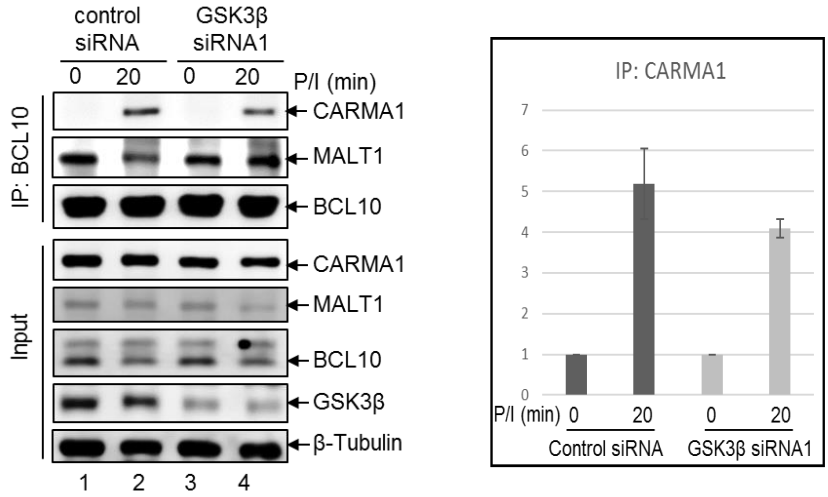

Figure (19): Diminished P/I induced CBM complex formation upon GSK3β inhibition. *A,* Anti-BCL10 immunoprecipitation analysis of whole cell extracts of unstimulated or P/I stimulated Jurkat sh-Control (pSUPER) or Jurkat sh-GSK3β (GSK3β-shRNA) (upper part). Additional immunoblot analysis of the same whole cell extracts were used to control protein expression levels (lower part, input). The chart shows the quantifications the analysis of immunoprecipitated CARMA1 protein of at least three independent experiments are shown below. *B,* Anti-BCL10 immunoprecipitation analysis of whole cell extracts of unstimulated or P/I stimulated Jurkat T-ALL cells transfected with either control small interfering RNA (control siRNA) or GSK3β specific small interfering RNA (GSK3β-siRNA1) (upper part). Additional immunoblot analysis of the same whole cell extracts were used to control protein expression levels (lower part, input). The chart shows the quantifications the analysis of immunoprecipitated CARMA1 protein of at least three independent experiments are shown below (NS $p>0.05$, * $p \leq 0.05$, ** $p \leq 0.01$, *** $p \leq 0.001$).

3.4 GSK3β is a BCL10 kinase

The data so far implied a role of GSK3β in CBM complex formation, MALT1 endoprotease activity, and subsequent canonical NF-κB activation. To unravel the mechanism by which GSK3β interferes with CBM complex formation, BCL10 protein levels in Jurkat sh-Control and Jurkat sh-GSK3β cells were monitored. As shown in (Figure 13A), P/I stimulation led to the formation of slower migrating BCL10 isoforms, which might represent phospho-BCL10 isoforms which were less pronounced in Jurkat sh-GSK3β cells (Figure 13A, lanes 5,6). The appearance of slower migrating BCL10 isoforms induced by P/I stimulation of Jurkat T-ALL is largely assumed to result from stimulation induced BCL10 phosphorylation (Wegener et al. 2006). The attenuated BCL10 phosphorylation upon GSK3β inhibition suggests that GSK3β might regulate BCL10 phosphorylation, directly or indirectly. To study this, BCL10 was ectopically expressed in HEK293T cells either alone or together with GSK3β or IKK2, followed by immunoblot analysis of BCL10 to monitor its phosphorylation status. In addition to a rapidly migrating BCL10 signal, several slowly migrating BCL10 variants were detected denoting possible different BCL10 phosphorylation isoforms (Figure 20A, lane 1). Co-expression of either IKK2 or GSK3β augmented the slowly migrating BCL10 signals (Figure 20A, lane 3 and 4 respectively). However, the BCL10 patterns obtained by either IKK2 or GSK3β co-expression were different. In addition, IKK2 co-expression caused diminished levels of the fastest migrating BCL10 signal, which might highlight a role of IKK2 in the regulation of BCL10 proteolysis (Figure 20A, lane 3).

To further confirm that those slowly migrating BCL10 signals represent BCL10 phosphorylation isoforms, whole cell extracts from HEK293T cells ectopically expressing FLAG-BCL10 alone or in combination with IKK2 or GSK3β were used to immune-purify BCL10, which was subsequently either left untreated or was treated with Shrimp alkaline phosphatase (SAP) for 60 Minutes prior to immunoblot analysis. As shown in (Figure 20B), untreated samples showed three different BCL10 isoforms, while SAP pre-treatment strongly diminished the level of the slowly migrating BCL10 signals, supporting the notion that these slowly migrating bands represent BCL10 phosphorylation isoforms.

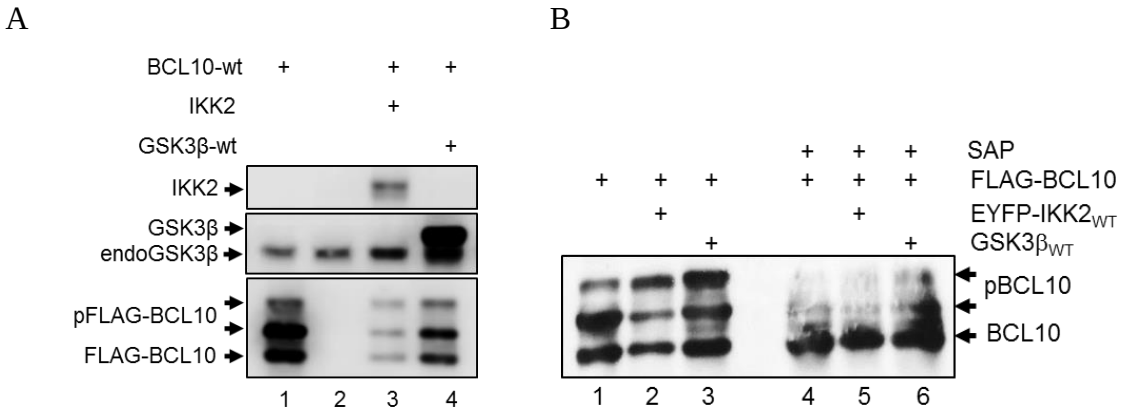

Figure (20): GSK3β regulates BCL10 phosphorylation. *A,* Immunoblot analysis of ectopically expressed FLAG-BCL10$_{WT}$ either alone or together with IKK2 or GSK3β$_{WT}$ in HEK293T cells. *B,* Immunoblot analysis of ectopically expressed FLAG-BCL10$_{WT}$ either alone or together with IKK2 or GSK3β$_{WT}$ in HEK293T cells. FLAG-BCL10 proteins were immunopurified and left untreated (lane 1-3) or treated with shrimp alkaline phosphatase (SAP) (lane 4-6) prior to analysis.

In line with these previous findings is the result obtained from the *in vivo* labelling experiment of Jurkat T-ALL cells. Since both GSK3β and IKK2 appear to take part in the regulation of BCL10 phosphorylation, the activity of both kinases was blocked, either individually or in combination. In particular, GSK3β was inhibited with SB21 and IKK2 with specific sh-RNA (Figure 21). As expected, increased BCL10 phosphorylation was observed upon P/I stimulation of Jurkat sh-Control cells (Figure 21, lane 3). Moreover, a reduction of BCL10 phosphorylation was observed upon inhibition of GSK3β or IKK2 (Figure 21, lanes 4 and 7 respectively). Moreover, a more pronounced reduction of BCL10 phosphorylation was observed upon inhibition of both GSK3β and IKK2 (Figure 21, lane 8). Taken together, these data suggest that GSK3β, like IKK2, is a BCL10 kinase.

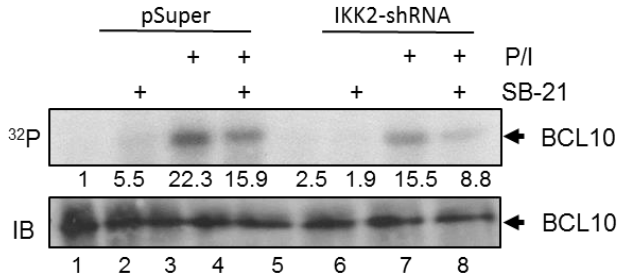

Figure (21): Analysis of GSK3β and IKK2 mediated BCL10 phosphorylation in Jurkat T-ALL *in vivo*. *In vivo* phosphorylation of BCL10 in Jurkat sh-control (pSuper) or Jurkat sh-IKK2 (IKK2-shRNA) cells. The cells were metabolically labeled using ^{32}P orthophosphate and BCL10 proteins were immunopurified and separated with SDS-PAGE.

Previously published studies showed that IKK2 is able to phosphorylate BCL10 at least at five specific serine residues (Ser134, Ser136, Ser138, Ser141, and Ser144) (Wegener et al. 2006). A BCL10 mutant with substitution of those five serine residues with alanine is called $BCL10_{S5A}$ (Figure 22A). To further unravel the proposed GSK3β phosphorylation sites in BCL10, and to determine if the already mapped IKK2 target sites are also used by GSK3β, HEK293T cells were transfected with an expression vector for either $BCL10_{WT}$ or $BCL10_{S5A}$ alone, or together with IKK2 and/or GSK3β encoding vectors. Subsequently, the phosphorylation status of BCL10 was monitored by immunoblot analysis of the resulting whole cell extracts. Again, co-expression of $BCL10_{WT}$ with either IKK2 or GSK3β augmented the slowly migrating BCL10 phosphorylation isoforms with different patterns (Figure 22B, lanes 2-4). Interestingly, also the co-expression of $BCL10_{S5A}$ with either IKK2 or GSK3β alone led to the augmentation of the slowly migrating BCL10 signals (Figure 22B, lanes 5-7). Moreover, the co-expression of both IKK2 and GSK3β together with either $BCL10_{WT}$ or $BCL10_{S5A}$ augmented the slowly migrating BCL10 signals more effectively than either one of those kinases alone suggesting a potential priming effect of IKK2 for BCL10 phosphorylation mediated by GSK3β (Figure 22B, lanes 10-11). Together, these data suggest that IKK2 and GSK3β might use overlapping serine residues in BCL10 and both kinases possibly phosphorylate BCL10 at additional sites other than previously reported ones.

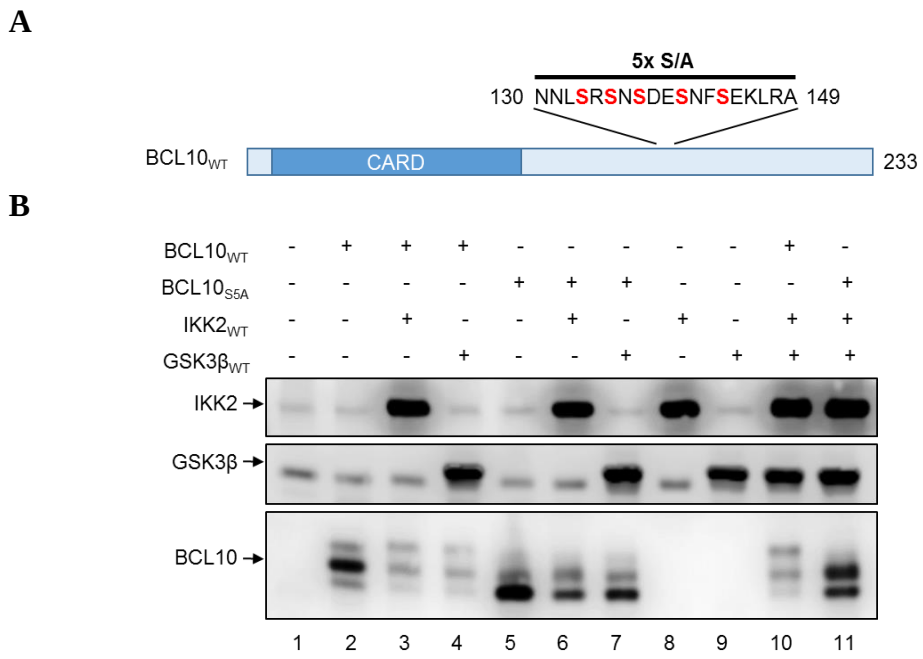

Figure (22): GSK3β can phosphorylate BCL10 at additional sites. *A*, schematic structure of $BCL10_{S5A}$ mutant showing the substitution of five serine residues with alanine *B*, Immunoblot analysis of HEK293T cells ectopically expressed with FLAG-$BCL10_{WT}$ or FLAG-$BCL10_{S5A}$ either alone or together with IKK2 and/or $GSK3\beta_{WT}$.

The notion that IKK2 and GSK3β target overlapping serine residues including still unknown sites was supported by *in vivo* labelling study with HEK293T cells ectopically expressing either FLAG-$BCL10_{WT}$ or FLAG-$BCL10_{S5A}$ alone or together with IKK2 or GSK3β. The phosphorylation status of BCL10 was monitored by immuno-purification of BCL10. As expected, $BCL10_{WT}$ showed a strong basal phosphorylation whereas, $BCL10_{S5A}$ was found largely unphosphorylated (Figure 23, lanes 2,4 respectively). The co-expression of $BCL10_{WT}$ with either $IKK2_{WT}$ or $GSK3\beta_{WT}$ had no impact on the overall $BCL10_{WT}$ phosphorylation but increased the slowly migrating BCL10 isoforms (signal 1) (Figure 23, lanes 2,6-7). In case of $BCL10_{S5A}$, the addition of either $IKK2_{WT}$ or $GSK3\beta_{WT}$ strongly increased the overall $BCL10_{S5A}$ phosphorylation in addition to increasing the slowly migrating BCL10 isoforms. However, the BCL10 phosphorylation patterns caused by IKK2 or GSK3β co-expression differs distinctively (Figure 23, lanes 8-9). Together these data underscore the notion that IKK2 and GSK3β can phosphorylate BCL10 at sites additional to previously reported serine residues.

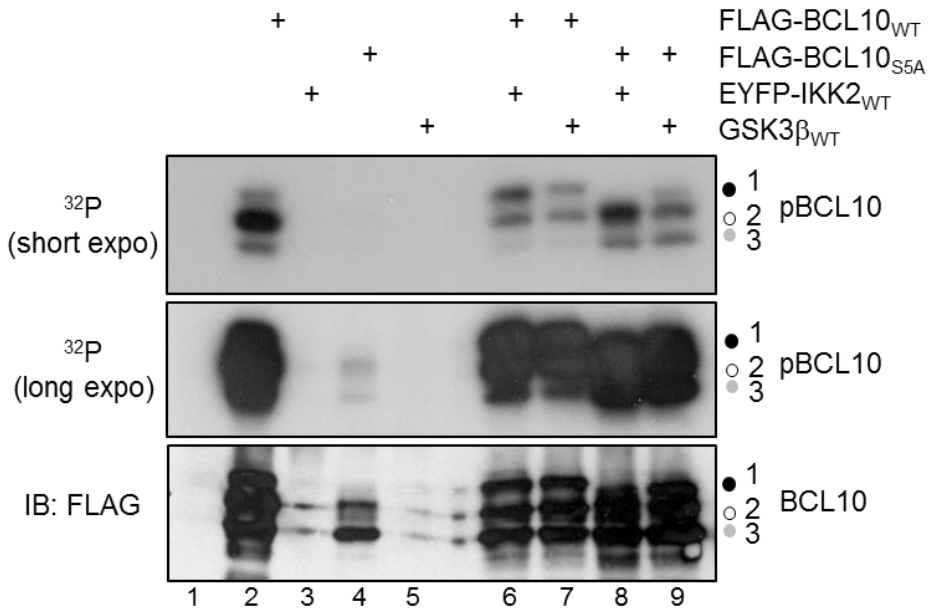

Figure (23): Analysis of GSK3β and IKK2 mediated BCL10 phosphorylation in HEK293T. In vivo phosphorylation of FLAG-BCL10$_{WT}$ or FLAG-BCL10$_{S5A}$ ectopically expressed either alone or together with IKK2$_{WT}$ or GSK3β$_{WT}$ in HEK293T cells. The cells were metabolically labelled using ^{32}P orthophosphate and BCL10 proteins were immunopurified and separated with SDS-PAGE. FLAG-BCL10 phosphorylation was analyzed by autoradiography (upper and middle panel). The expression of FLAG-BCL10$_{WT}$ and FLAG-BCL10$_{S5A}$ was monitored by anti-FLAG immunoblot staining (lower panel).

3.5 GSK3β modulates the activity of the IKK complex

The data shown above demonstrated that GSK3β augments BCL10 phosphorylation, CBM complex formation, MALT1 activity, NF-κB DNA-binding activity and canonical NF-κB activation. This led to the question of whether GSK3β interferes with the structure or the activity of the IKK complex. To answer this question, an *in vitro* kinase assay was performed using GST-IκBα (1-53) as substrate and immunopurified IKK complex from Jurkat T-ALL cells pre-treated with either SB21 or SB41 prior to P/I stimulation (Figure 24A). P/I stimulation of Jurkat T-ALL cells led to a pronounced IKK complex activity as evident by increased IκBα phosphorylation (Figure 24A, lane 1-2). Inhibition of GSK3β either by SB21 or by SB41 reduced the activity of the IKK complex monitored by the IκBα phosphorylation (Figure 24A, lane 4,6). Moreover, unstimulated SB21 and SB41 pre-treated samples caused a decreased basal activity of the IKK complex (Figure 24A, lane 3,5). Similarly, the immunopurified IKK complex from unstimulated or P/I stimulated Jurkat sh-GSK3β cells

displayed a weaker activity as compared to the IKK complex purified from Jurkat sh-Control cells (Figure 24B).

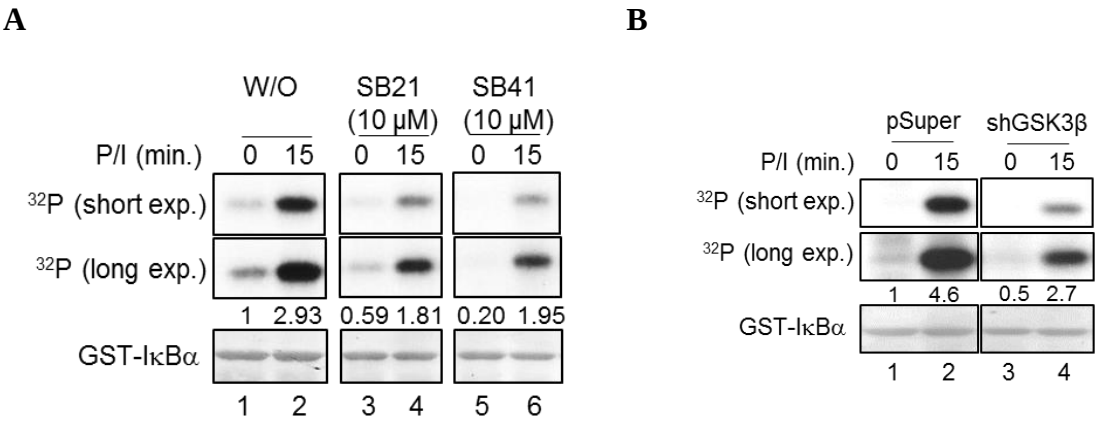

Figure (24): GSK3β inhibition modulate IKK complex activity. *A, In vitro* kinase assay using immunopurified IKK2 from unstimulated or stimulated Jurkat T-ALL cells which were untreated or pre-treated with either SB21 or SB41. Phosphorylation of GST-IκBα (1-53) was monitored by autoradiography (upper and middle panel). The numbers below show the densitometric intensities of the phospho-IκBα signals equalized to the GST-IκBα protein Ponceau S staining values (lower panel). *B, In vitro* kinase assay using immunopurified IKK2 from unstimulated or stimulated Jurkat sh-Control or Jurkat-shGSK3β cells. Phosphorylation of GST-IκBα (1-53) was monitored by autoradiography (upper and middle panel). The numbers below show the densitometric intensities of the phospho-IκBα signals equalized to the GST-IκBα protein Ponceau S staining values (lower panel).

To exclude that the effect of GSK3β inhibition on the activity of IKK complex is due to a direct impact of GSK3β on IKK2 activity, FLAG-IKK2 was ectopically expressed in HEK293T cells either alone or together with $GSK3\beta_{WT}$, $GSK3\beta_{S9A}$ or $GSK3\beta_{K85A}$. The FLAG-IKK2 was immunopurified using anti-FLAG antibody coupled beads followed by an *in vitro* kinase assay using GST-IκBα (1-35) as a substrate. One additional sample was treated with SB21 to test the effect of inhibition of endogenous GSK3β on IKK2 activity (Figure 25A). The activity of the immunopurified FLAG-IKK2 was not affected with either co-expression of the different GSK3β subtypes or by SB21 pre-treatment suggesting that the negative effect of GSK3β inhibition on the IKK activity is rather indirect. Consistently, GSK3β inhibition by a specific siRNA had no impact on IKK complex formation as shown by an anti-NEMO co-immunoprecipitation analysis (Figure 25B).

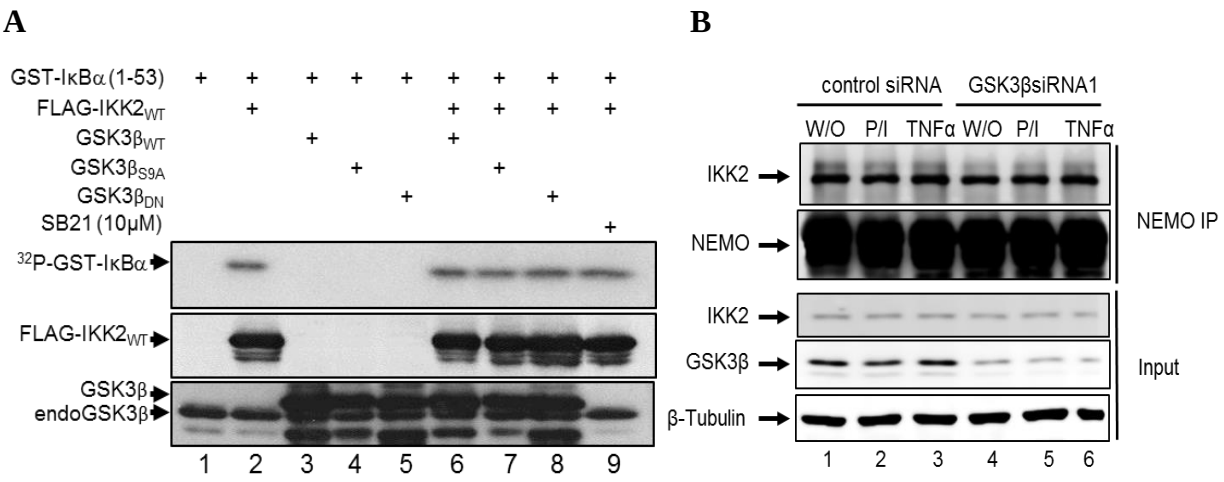

Figure (25): GSK3β show no direct impact on IKK2 activity or IKK complex structure. *A*, *In vitro* kinase assay using ectopically expressed FLAG-IKK2 immunopurified from HEK293T transiently transfected as indicated. Cells were left untreated (lane 1-8) or were pre-treated with SB21 (lane 9). Phosphorylation of GST-IκBα (1-53) was monitored by autoradiography (upper panel). The expression of IKK2 and GSK3β were analysed by immunoblot (middle and lower panel). *B,* IKK complexes were immunopurified form Jurkat T-ALL cells transiently transfected with a control small interfering RNA (control-siRNA) or GSK3β specific small interfering RNA (GSK3βsiRNA1) using an anti-NEMO antibody. IKK2 and NEMO protein levels were subsequently determined by immunoblot analysis (upper part, NEMO IP). The expression of IKK2 and GSK3β in the input was determined by control immunoblot analyses (lower part, Input).

Taken together, these data show no direct impact of GSK3β on IKK complex structure or activity suggesting that GSK3β exert its effects on the antigen receptor induced canonical NF-κB signalling at a more upstream level.

3.6 GSK3β inhibition depresses ABC-DLBCL survival and proliferation

One hallmark of ABC-DLBCL is the constitutive activation of the canonical NF-κB signalling, which promotes its survival and proliferation. This constitutively activated canonical NF-κB signalling is largely depending on the pathologically permanent CBM formation. Accordingly, the role of GSK3β on ABC-DLBCL cells was studied next. First, the expression of GSK3β, pGSK3β (Tyr 216) and pGSK3β (S9) in ABC- and GC-DLBCL cell lines was analyzed by immunoblot experiments (Figure 26). No significant pattern difference between ABC- and GC-DLBCL cell lines could be detected, However GSK3β was slightly more expressed in GC-DLBCL cell lines.

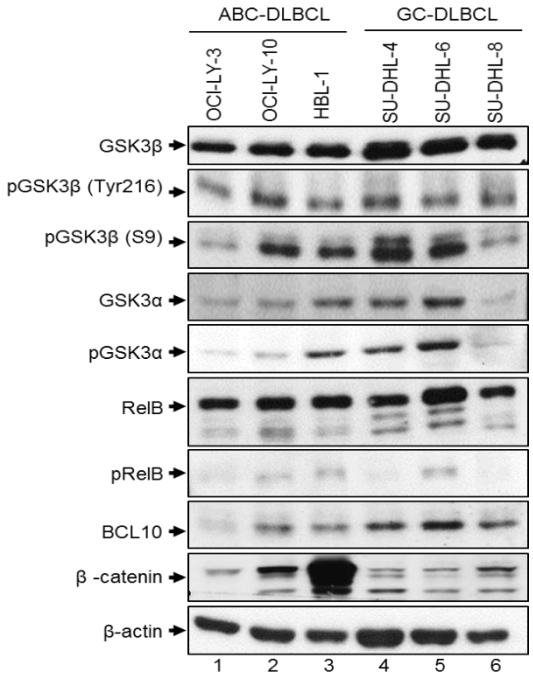

Figure (26): Different protein expression in DLBCL cell lines. Immunoblot analysis of the indicated proteins in three ABC-DLBCL cell lines (OCI-LY-3, OCI-LY-10 and HBL-1) and three GC-DLBCL cell lines (SU-DHL-4, SU-DHL-6 and SU-SHL-8).

Next, cell proliferation assays were performed to assess the proliferation of three ABC-DLBCL cell lines (OCI-LY-3, OCI-LY-10 and HBL-1) and three GC-DLBCL cell lines (SU-DHL-4, SU-DHL-6 and SU-DHL-8) which were treated with 10μM of SB21 or equal volume of DMSO for 3 days (Figure 27). In ABC-DLBCL cell lines, GSK3β inhibition supressed the proliferation of all cell lines significantly. Whereas the proliferation of GC-DLBCL cell lines were either depressed (SU-DHL-4) or promoted upon the inhibition of GSK3β (Figure 27).

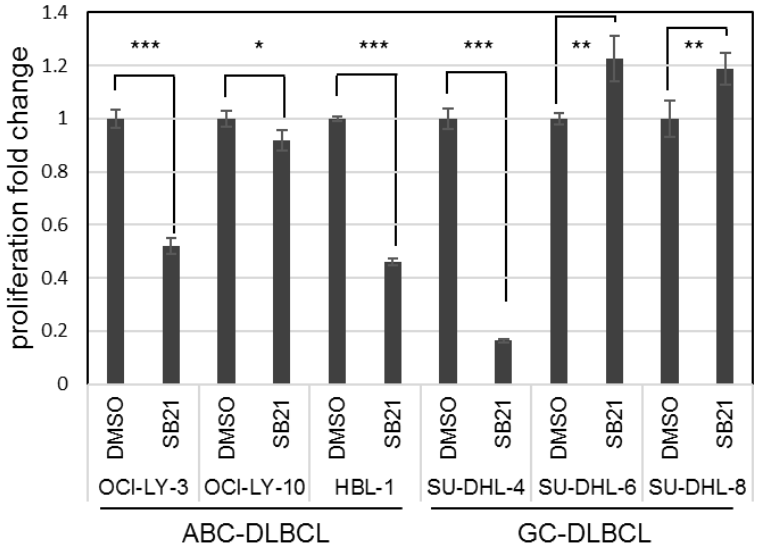

Figure (27): GSK3β inhibition suppress ABC-DLBCL cell proliferation. Cell proliferation assay of three ABC-DLBCL cell lines (OCI-LY-3, OCI-LY-10 and HBL-1) and three GC-DLBCL cell lines (SU-DHL-4, SU-DHL-6 and SU-DHL-8) treated with 10µM of SB21 or equal volume of DMSO for 3 days (NS $p>0.05$, * $p \leq 0.05$, ** $p \leq 0.01$, *** $p \leq 0.001$).

3.7 GSK3β inhibition attenuates MALT1 endoprotease activity in ABC-DLBCL:

Although MALT1 was not found to be mutated or translocated in DLBCL (Dierlamm et al. 2008), previous studies showed that ABC-DLBCL cell lines depend on the catalytic activity of MALT1 (Ferch et al. 2009), since MALT1 inhibitors kill ABC-DLBCL *in vivo* and *in vitro* (Fontan et al. 2012). As our results demonstrate that GSK3β inhibition attenuates MALT1 endoprotease activity in T-ALL cell lines (Figure 8 and 10) and depress ABC-DLBCL proliferation (Figure 28), the effect of GSK3β inhibition on MALT1 activity in DLBCL was studied next. For this, GSK3β activity was blocked in ABC- as well as GC-DLBCL cell lines by SB21 treatment for 16 hours and MALT1 activity was monitored by immunoblot for CYLD1 (Figure 28). As expected, the cleavage product of CYDL1 was more pronounced in untreated ABC-DLBCL cell lines in comparison to untreated GC-DLBCL (Figure 28, compare lanes 1,3,5 with 7,9,11). Inhibition of GSK3β with SB21 slightly attenuated the appearance of CYLD1 cleavage products in DLBCL cell lines. However, the SB21 treated samples showed in addition a decreased overall CYLD expression (Figure 28).

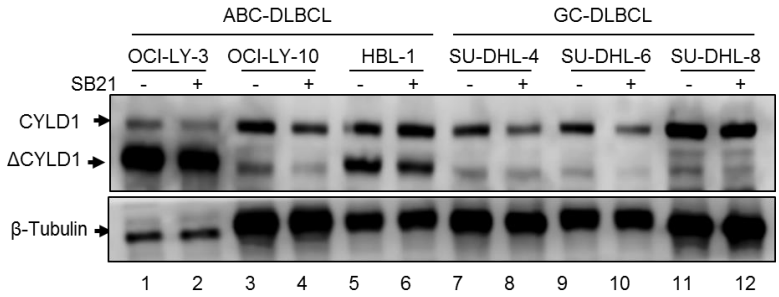

Figure (28): Inhibition of GSK3β reduces CYLD1 proteins in DLBCL cell lines. Immunoblot analysis of CYLD1and β-tubulin in three ABC-DLBCL cell lines (OCI-LY-3, OCI-LY-10 and HBL-1) and three GC-DLBCL (SU-DHL-4, SU-DHL-6 and SU-SHL-8) which are left untreated or treated with SB21 for 16 hours.

3.8 GSK3β modulates CBM complex formation and NF-κB signalling in ABC-DLBCL

As the data so far suggest a role of GSK3β in BCL10 phosphorylation and CBM complex formation, the effect of GSK3β inhibition on CBM complex formation in DLBCL cell lines was tested. For this, OCI-LY-10, HBL-1, SU-DHL-4 and SU-DHL-6 cell lines were treated with SB21 for 16 hours followed by BCL10 immunoprecipitation coupled with CARMA1 and MALT1 immunoblot. The BCL10-CARMA1 interaction was found in untreated ABC-DLBCL as evidenced by appearance of CARMA1 signal. In addition, the GC-DLBCL cell lines showed a minimal basal BCL10-CARMA1 interaction. As shown in (Figure 29), inhibition of GSK3β with SB21 attenuates BCL10-CARMA1 interaction in ABC-DLBCL cell lines OCI-LY-10 and HBL-1. Of note, SB21-mediated GSK3β-inhibition also attenuated the basal CBM complex formation in GC-DLBCL cell lines, although to a lesser extend (Figure 29).

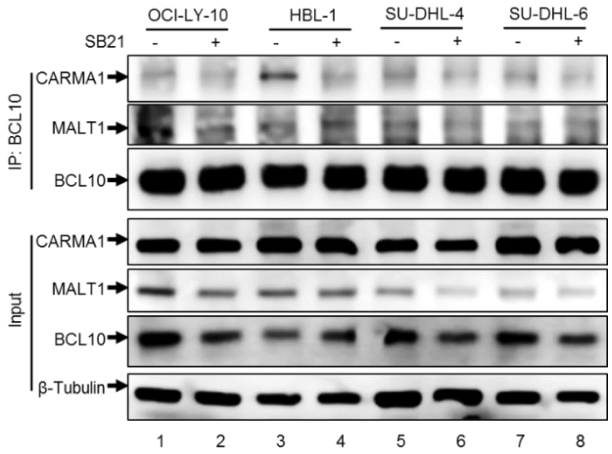

Figure (29): Diminished CBM complex formation in DLBCL cell lines upon GSK3β inhibition. Anti-BCL10 immunoprecipitation analysis of whole cell extracts of two ABC-DLBCL cell lines (OCI-LY-10 and HBL-1) and two GC-DLBCL (SU-DHL-4 and SU-DHL-6), which were left untreated or treated with SB21 for 16 hours (upper part, IP: BCL10). Additional immunoblot analysis of the same whole cell extracts were used to control protein expression levels (lower part, input).

In line with our previous findings, inhibition of GSK3β using SB21 supresses the activation of the NF-κB target gene BIRC3 expression in ABC-DLBCL cell lines, whereas it has no significant effect on BIRC3 expression in tested GC-DLBCL cell lines (Figure 30).

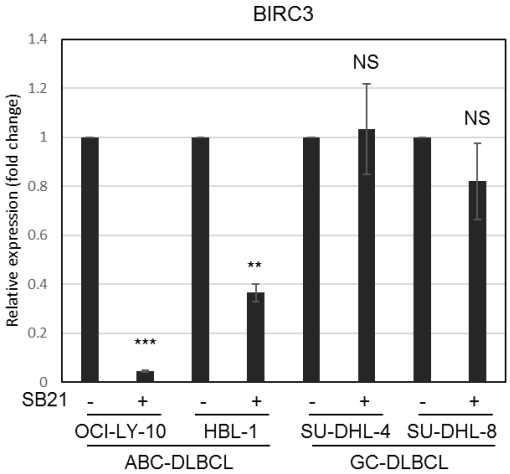

Figure (30): Quantitative real time PCR analysis of the mRNA levels of BIRC3 in DLBCL cell lines. Two ABC-DLBCL cell lines (OCI-LY-10 and HBL-1) and two GC-DLBCL (SU-DHL-4 and SU-DHL-6) were either left untreated or were treated with SB21 (NS $p>0.05$, * $p \leq 0.05$, ** $p \leq 0.01$, *** $p \leq 0.001$).

3.9 GSK3β modulates the Wnt/β-catenin pathway in DLBCL:

Although inhibition of GSK3β using 10 μM of SB21 suppresses the proliferation of ABC-DLBCL cell lines, it promotes GC-DLBCL cell lines proliferation suggesting that GSK3β interferes with other signalling pathways including the Wnt/β-catenin signalling pathway (Figure 27). To study the effect of GSK3β inhibition on the Wnt/β-catenin signalling pathway, three ABC-DLBCL cell lines (OCI-LY-3, OCI-LY-10 and HBL-1) and three GC-DLBCL cell lines (SU-DHL-4, SU-DHL-6 and SU-DHL-8) were treated with SB21 for 16 hours and the expression of β-catenin was monitored by immunoblot analysis (Figure 31A). Inhibition of GSK3β increased the expression of β-catenin in all tested DLBCL cell lines (Figure 31A). Similar results were observed using SB41 for different time intervals. Moreover, β-catenin expression increased with longer GSK3β inhibition (Figure 31B).

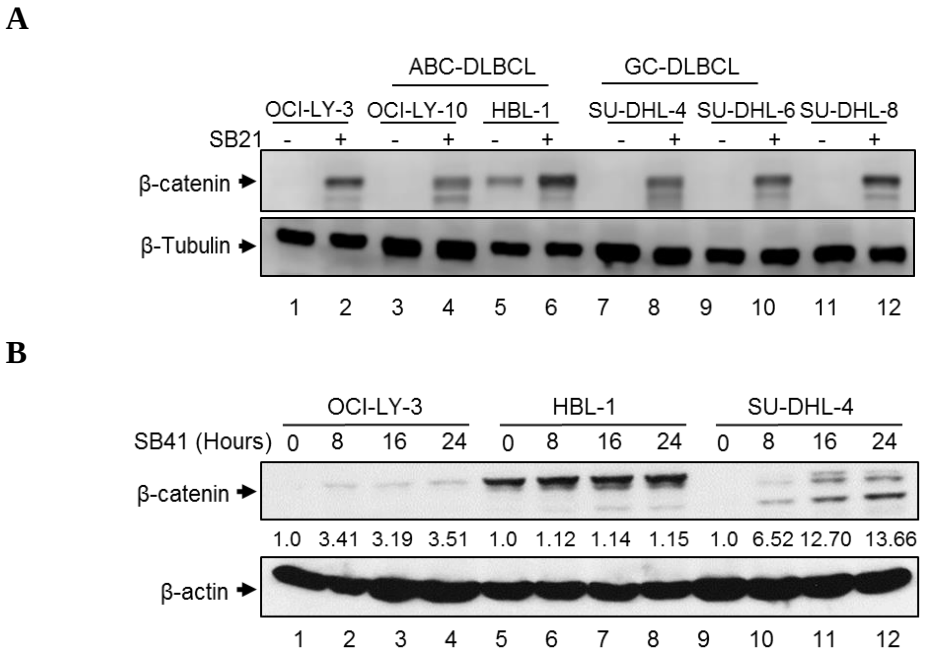

Figure (31): GSK3β inhibition increase β-catenin expression in DLBCL. *A,* Immunoblot analysis of β-catenin and β-tubulin proteins in three ABC-DLBCL cell lines (OCI-LY-3, OCI-LY-10 and HBL-1) and three GC-DLBCL (SU-DHL-4, SU-DHL-6 and SU-SHL-8) which were either left untreated or were treated with 10μM of SB21 for 16 hours. *B,* Immunoblot analysis of β-catenin and β-actin protein in two ABC-DLBCL cell lines (OCI-LY-3 and HBL-1) and one GC-DLBCL (SU-DHL-4) which were either left untreated or were treated with SB21 for the indicated time intervals. The numbers below the upper panel indicate the quantifications of β-catenin proteins analysis normalized to β-actin.

3.10 Immunohistochemistry expression of GSK3β and other related proteins in DLBCL

To investigate the multifaceted role played by GSK3β in DLBCL in modulating the canonical NF-κB and other signalling cascades, the expression of GSK3β, the NF-κB member RelA as well as other GSK3β related proteins were evaluated by immunohistochemistry. RelA sequestration is one of the mechanisms by which RelB exerts an inhibitory effect on NF-κB (Marienfeld et al. 2003). In addition, the immunohistochemical detection of nuclear RelA/p65 expression has been used as a surrogate marker for the canonical NF-κB signalling activation (Espinosa et al. 2008) and the RelA nuclear over-expression was found to correlate with poor survival in early stage DLBCL patients (Zhang et al. 2016). β-catenin is a crucial indicator for GSK3β activity in Wnt/β-catenin signalling pathway and it was reported to be expressed in the nucleus in some DLBCL cases (Ge et al. 2011). Another important factor which determine the fate of the tumour cells including DLBCL is the transcriptional and functional crosstalk between the anti-apoptotic NF-κB and the proapoptotic p53 (an important tumour suppressor) (Ak and Levine 2010). Previous studies showed that p53 can bind to GSK3β directly increasing the activity of GSK3β and the activated GSK3β contributes to the transcription activity of p53 (Bijur and Jope 2001). The over expression of p53 detected by IHC is an independent factor denoting a poorer prognosis in DLBCL patients (Xie et al. 2014). Moreover, the over-expression of p53 adds an additional negative prognostic effect of c-Myc in DLBCL patients (Wang et al. 2017). Another study reported that GSK3β is capable of phosphorylating c-Myc at Thr58 which targets c-Myc for ubiquitination and subsequent proteolysis (Sears et al. 2000).

The IHC expression of GSK3β and other related protein were first investigated in three ABC-DLBCL cell lines (OCI-LY-3, OCI-LY-10 and HBL-1) and three GC-DLBCL cell lines (SU-DHL-4, SU-DHL-6 and SU-DHL-8) using IHC stainings for GSK3β, β-catenin, RelA, p53 and c-Myc. The evaluations are shown in table-2.

Table (2): IHC of DLBCL cell lines. C= cytoplasmic staining; N= nuclear staining; +++ >70% positive cells; ++ 30-70% positive cells; + <30% positive cells; - no positive cells; ( ) weak staining.

Cell line	Type	GSK3β	RelA		β-catenin	p53	c-Myc
		C	C	N	N	N	N
OCI-LY-3	ABC	+++	+++	-	-	++	-
OCI-LY-10	ABC	+++	++	-	-	+++	(+)
HBL-1	ABC	++	+++	-	-	+++	+
SU-DHL-4	GC	+++	++	-	-	+++	+
SU-DHL-6	GC	+++	++	-	-	+++	+
SU-DHL-8	GC	+++	++	-	-	+++	-

GSK3β and RelA was found to be almost equally expressed in the cytoplasm of all immunohistochemically stained DLBCL cell lines, however, RelA was found to be higher expressed in OCI-LY-3 and HBL-1 cell lines. The nuclear expression of RelA was undetectable by IHC in our DLBCL cell lines. All stained cell lines were β-catenin negative and p53 positive in the nucleus with variable intensity (Table-2). The expression of c-Myc showed a variable nuclear expression from negative, weak positive to positive in the stained cell lines, however, no specific correlation could be detected comparing ABC- and GC-DLBCL cell lines (Table-2 and figure 32).

Subsequently, 37 cases of DLBCL (19 men and 18 women), were collected from the archive of the Institute of Pathology, Ulm University. The cases were diagnosed between the years 2002-2016 with a median age of 66 years (rang 40-90) and were classified according to Hans' algorithm into two groups non-GC and GC-DLBCL using the three IHC markers CD10, BCL-6 and MUM-1 (Hans et al., 2004). 62.16% of the collected cases were in the non-GC group (23 cases), while 37.84% were in the GC-DLBCL group (14 cases). Next, the expression of β-catenin and c-Myc in the DLBCL cohort cases were evaluated using IHC technique (Table-3).

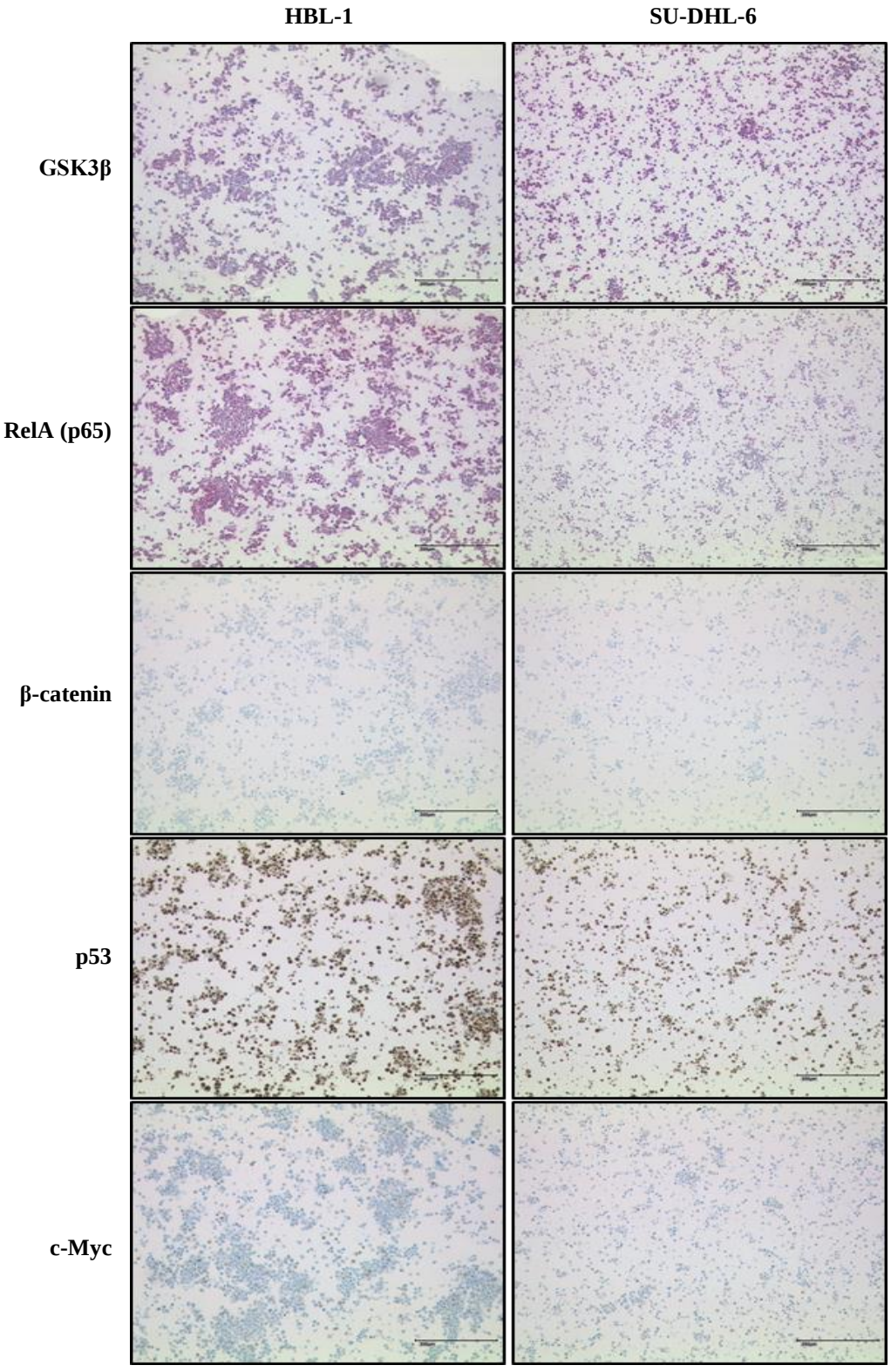

Figure (32): IHC stainings of the DLBCL cell lines HBL-1 and SU-DHL-6. Scale bar = 200 µm.

Table (3): Immunohistochemical protein analysis of 37 patients with DLBCL. +++ >70% positive cells; ++ 30-70% positive cells; + <30% positive cells; - no positive cells; ( ) weak staining; C= cytoplasmic staining; N= nuclear staining.

Case #	Gender	Age (Years)	Type	β-catenin	c-Myc
				N	N
1	M	63	Non-GC	-	(+)
2	M	65	Non-GC	-	(+)
3	F	90	Non-GC	-	+++
4	F	66	Non-GC	-	(+)
5	M	73	Non-GC	-	(+)
6	F	70	Non-GC	-	(+)
7	M	68	Non-GC	-	-
8	F	66	Non-GC	-	+
9	F	72	Non-GC	-	++/(+)
10	M	82	Non-GC	-	(+)
11	F	62	Non-GC	-	+
12	M	73	Non-GC	-	(+)
13	F	81	Non-GC	-	(+)
14	M	87	Non-GC	-	++
15	F	74	Non-GC	-	+
16	F	76	Non-GC	-	+
17	F	71	Non-GC	-	+
18	M	55	Non-GC	-	+
19	M	66	Non-GC	-	++
20	M	47	Non-GC	-	-
21	M	71	Non-GC	-	+
22	F	64	Non-GC	-	-
23	M	40	Non-GC	-	(+)
24	M	58	GC	-	(+)
25	F	61	GC	-	(+)
26	M	54	GC	-	-
27	M	68	GC	-	+
28	M	66	GC	-	+
29	F	69	GC	-	(+)
30	M	67	GC	-	(+)
31	F	67	GC	-	+

32	M	62	GC	-	-
33	F	62	GC	-	-
34	F	53	GC	-	++
35	F	62	GC	-	+
36	M	64	GC	-	+
37	F	50	GC	-	-

All tested DLBCL cohort cases were β-catenin negative. However, c-Myc expression in the nucleus was variable from negative to strong positive (Table 3 and Figure 33). 86.96% of non-GC group and 71.43% of the GC group were c-Myc positive (total 80% of all cases). However, 17.4% of non-GC group showed a high c-Myc expression (≥40% positive cells). Meanwhile, only 7.14% of GC-DLBCL showed a high c-Myc expression (Figure 33). Mann-Whitney test was used to compare the c-Myc expression between the none-GC- and GC-DLBCL groups or between male and female groups. The p-value between GC- and non-GC-DLBCL cases equals 0.14. No significant correlation could be determined between males and females and p-value was 0.32.

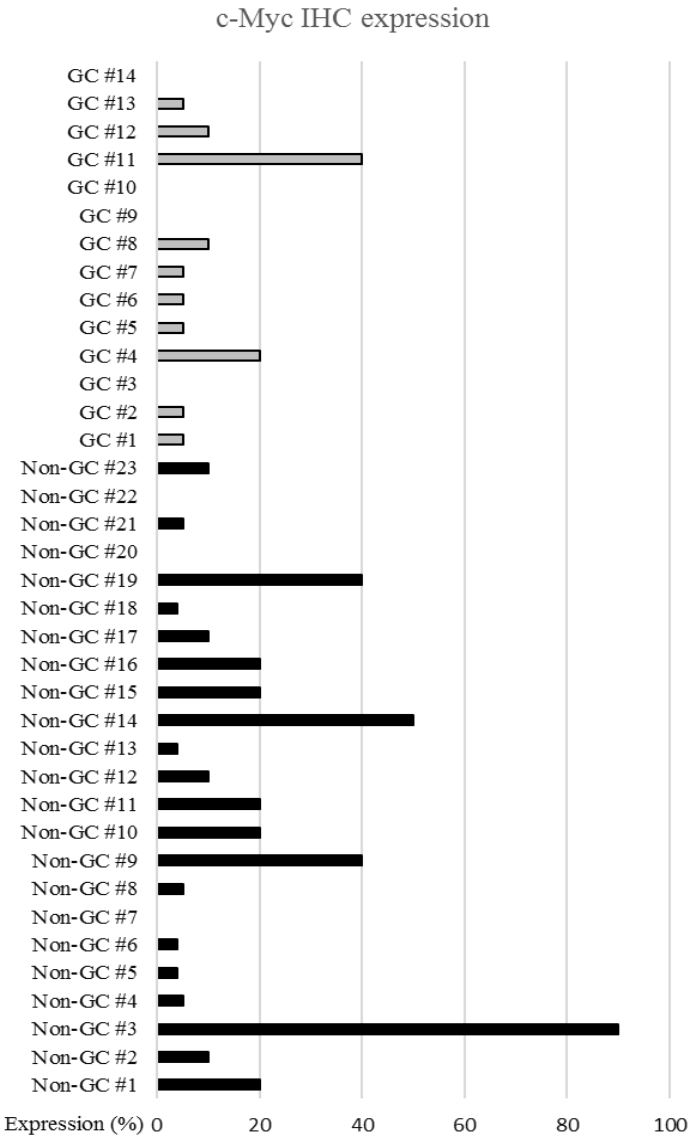

Figure (33): Diagram of immunohistochemistry (IHC) staining evaluation of c-Myc expression in DLBCL cohort cases.

4- Discussion

4.1 GSK3β is required for the endoprotease activity of MALT1 and the degradation of RelB

The hallmark of the pathogenesis of the ABC-DLBCL is the constitutive NF-κB activation due to the constitutive formation of a protein complex composed of CARMA1, BCL10 and MALT1 (CBM complex) (Thome et al. 2010). The CBM complex formation is a key event in the antigen receptor mediated activation of the canonical NF-κB signalling pathway which is highly similar in both B and T lymphocytes (Thome 2004). The CBM complex formation is tightly regulated by a variety of phosphorylation events primary occurring in CARMA1 leading to an intramolecular conformational change of this protein. This relieves the auto-inhibition of CARMA1 allowing the recruitment of BCL10 and MALT1(Saijo et al. 2002; Sun et al. 2004). Following the formation of the CBM complex, MALT1 mediates the antigen receptor mediated NF-κB signalling pathway activation either through its scaffolding function as a member of the CBM complex or through its endoprotease activity. As a scaffolding protein, MALT1 mediates the recruitment of different downstream effector proteins required for the NF-κB signalling activation (Sun et al. 2004).

MALT1 is the only member of the CBM complex which possesses a proteolytic activity. In addition to its scaffolding functions to activate the downstream NF-κB signalling cascade, MALT1 proteolytic activity enhances the duration and the amplitude of the NF-κB signal by regulating the negative feedback pathways. For example, MALT1 cleaves the NF-κB inhibitory proteins RelB (Marienfeld et al. 2001) and A20 (Coornaert et al. 2008). However, RelB and A20 are not the only targets of the MALT1 endoproteolytic activity. Other targets of MALT1 include BCL10, Haem-oxidized IRP2 ubiquitin ligase 1 (HOIL-1) (Klein et al. 2015) and Cylindromatosis-1 (CYLD1), whose cleavage is required for c-Jun N terminal kinase (JNK) pathway activation (Staal et al. 2011).

A20 negatively regulates the NF-κB transcription factor in the tumor necrosis factor (TNFR) (Wertz et al. 2004) and Toll-like receptor (TLR) mediated pathway (Boone et al. 2004). However, RelB plays its inhibitory role on NF-κB signalling through different mechanisms. For example, RelB sequestrates the NF-κB member RelA in transcriptionally inactive complexes (Marienfeld et al. 2003). An additional mechanism includes a direct interaction of RelB with the histone H3 lysine 9 methyltransferase G9a to induce facultative heterochromatin formation and transcriptional silencing (Chen et al. 2009) Thus, the

degradation of RelB upon the activation of the antigen receptor might be a crucial mechanism by which the NF-κB target genes are released from the RelB mediated epigenetic blockage allowing the NF-κB signal to activate its target genes. Previous studies showed that the constitutive NF-κB dependent ABC-DLBCL cell lines show a constitutive RelB degradation and a constitutive MALT1 activity as well. In those cells, MALT1 initiate the degradation of RelB through mediating its cleavage. This degradation results in enhanced RelA and cRel dependent DNA binding in those cells (Hailfinger et al. 2011).

Another study reported that RelB degradation is regulated in Jurkat cells by a GSK3β-mediated phosphorylation of a serine residue at the position 552. Furthermore, a physical interaction between GSK3β and RelB was founded in resting cells (Neumann et al. 2011). In this study, the authors showed that inhibition of GSK3β by either pharmacological inhibitors or specific siRNA suppression diminished RelB degradation assuming a direct link between GSK3β-mediated RelB phosphorylation and RelB proteolysis. Furthermore, a recent study reported that an oncogenic CARMA1 mutant identified in DLBCL cell lines recruits GSK3β to a specific high molecular weight protein complex which includes also the CBM complex (Bognar et al. 2016). Based on these previously published findings, the ability of GSK3β to modulate CBM complex, MALT1 endoprotease activity and the canonical NF-κB signalling cascade were investigated in a Jurkat T-ALL model system, as the molecular mechanisms involved in the activation of the antigen receptors in B and T lymphocytes are highly similar.

The data presented in this thesis imply that GSK3β is required to induce the MALT1 endoprotease activity and RelB degradation upon antigen receptor engagement. This notion is supported by the observation that inhibition of GSK3β either by pharmacological inhibitor SB21 (Figure 7A) or GSK3β-specific shRNA (Figure 11) attenuated the P/I induced proteolysis of RelB as well as the MALT1 target substrates CYLD1 and BCL10. Similar results were also observed in HSB2 cells (another T-ALL cell line) upon GSK3β inhibition prior to P/I stimulation (Figure 8). Moreover, a distinct attenuation of RelB degradation and MALT1 activity were also observed upon inhibition of GSK3β followed by activation with the more physiological stimulation using agonistic anti-CD3/CD28 antibodies, which directly bind to the CD3 part of the TCR and the CD28 co-receptor, thus activating the down-stream signalling cascades (Figure 7B). These results are comparable to the results obtained by inhibition of MALT1 activity using the MALT1 specific pharmacological inhibitor MI-

2 (Figure 9). Previous data imply together that GSK3β is required for signal induced MALT1 endoprotease activity in T-ALL cell lines.

4.2 GSK3β modulates the CBM complex formation and the canonical NF-κB signalling pathway

The activation of MALT1 endoprotease activity needs the prior assembly of the CARMA1-BCL10-MALT1 complex (Rebeaud et al. 2008). The observed attenuation of the antigen receptor mediated MALT1 endoprotease activity upon the inhibition of GSK3β could be explained by an effect of GSK3β inhibition on the CBM complex formation. This notion is supported by the observations that GSK3β inhibition either by specific shRNA (Figure 19A) or siRNA (Figure 19B) attenuates the P/I induced CBM formation in Jurkat cells. As the CBM complex formation is a crucial event in the antigen receptor mediated activation of the canonical NF-κB signalling pathway in lymphocytes as well as ABC-DLBCL, the impact of GSK3β inhibition on the canonical NF-κB signalling pathway was further investigated.

The previous studies reported conflicting effects of GSK3β on NF-κB signalling depending on the tested cell type. For instance, GSK3β inhibition with lithium or expression of a dominant negative GSK3β increased NF-κB activity and survival of PC12 cell line (a cell line derived from a pheochromocytoma of the rat adrenal medulla) (Bournat et al. 2000). By contrast, the inhibition of both GSK3α and GSK3β in pancreatic cancer cell lines blocked the IKK and the NF-κB activity (Wilson and Baldwin 2008). Additional studies suggested that GSK3β directly affects the NF-κB signalling by phosphorylating RelA in primary rat hepatocytes (Schwabe and Brenner 2002) or modulating the IKK complex subunit NEMO (Medunjanin et al. 2016). In the Jurkat T-ALL model system, which was used in this thesis, GSK3β inhibition either by pharmacological inhibitors or by specific shRNA interfered with the proteolysis of IκBα and BCL10 (Figure 13A+B), which play an essential role in the regulation of the canonical NF-κB signalling in activated lymphocytes. Moreover, GSK3β inhibition attenuated the NF-κB activity determined by specific luciferase reporter assays (Figure 14A+B), the activity of IKK complex (Figure 24) and P/I induced NF-κB DNA binding activity (Figure 15A). In addition, quantitative RT-PCR analysis of the NF-κB target genes BIRC3, TNFA and TRAF1 revealed a diminished expression upon inhibition of GSK3β (Figure 17+18). As the CBM complex formation occurs independent of MALT1 para-caspase activity, which is rather a consequence of the CBM formation, a higher upstream mechanism regulating CBM complex formation must be affected by GSK3β.

Taken together, this study presents the CBM complex formation as a novel mechanism by which GSK3β mediates the NF-κB signalling pathway.

4.3 GSK3β modulate CBM complex formation through a site-specific phosphorylation of BCL10

As mentioned earlier, the CBM complex formation is controlled by a set of distinct phosphorylation events, of which the majority occurs on CARMA1. However, also BCL10 is known to be phosphorylated upon antigen receptor stimulation and some of these BCL10 phosphorylations have been shown to be crucial for the CBM complex formation. The IKK2 mediated BCL10 phosphorylation, for instance, is required for the initiation of CBM complex formation. However, it also interferes with the BCL10-MALT1 association at a later phase of lymphocyte activation and is thus representing a negative regulatory feedback for the CBM complex formation and the NF-κB activation (Wegener et al. 2006). Taken together, IKK2 mediated BCL10 phosphorylation possesses both –negative and positive-effects on the CBM complex formation and the NF-κB activation. The data presented in this thesis suggest that the GSK3β mediated phosphorylation of BCL10 is a mechanism by which GSK3β controls the CBM complex formation and subsequent the NF-κB activation. For instance, the co-expression of BCL10 and GSK3β in HEK293T cells augmented the appearance of BCL10 phosphorylation isoforms in a similar way to the co-expression of BCL10 and IKK2, however the patterns obtained in both cases were not identical (Figure 20A). These BCL10 phosphorylation isoforms were more pronounced with co-expression of BCL10 together with both GSK3β and IKK2 (Figure 22). In addition, the BCL10 phosphorylation estimated with *in vivo* phosphorylation studies was reduced upon the inhibition of either GSK3β or IKK2. This reduction was even more pronounced upon a combined inhibition of both GSK3β and IKK2 (Figure 21, lane 8). The phosphorylation studies using the $BCL10_{S5A}$ mutant harbouring serine to alanine substitutions in all five previously mapped IKK2 target sites in BCL10 showed that both IKK2 and GSK3β are capable of phosphorylating BCL10 in additional sites more than the previously reported five serine residues (Figure 22+23). Many of the GSK3β phosphorylation targets require a prior phosphorylation by a priming kinase to be phosphorylated by GSK3β (DePaoli-Roach 1984). In this case, IKK2 might serve as a priming kinase for GSK3β mediated phosphorylation of BCL10 or they form together a redundant system to ensure BCL10 phosphorylation. Alternatively, IKK2 and GSK3β might phosphorylate BCL10 at overlapping sites attempting to tune the multifaceted functions of BCL10. However, the

complete set of the exact phosphorylation sites targeted by GSK3β and their function are still to be determined. Although BCL10 has not been reported to bind to the CARMA1:β-catenin destruction complex, it is feasible to speculate that BCL10 can be recruited to this complex due to its interaction with CARMA1, at least temporary. Alternatively, GSK3β can also be recruited to the CBM complex as a part of RelB:GSK3β complex as RelB cleavage is mediated by MALT1. Therefore, the results of the *in vivo* BCL10 phosphorylation studies suggest that GSK3β is another BCL10 kinase similar to IKK2. Functionally, the GSK3β mediated BCL10 phosphorylation seems to augment the CBM complex formation, MALT1 activation and the NF-κB signalling.

4.4 GSK3β modulates the canonical NF-κB signalling pathway and CBM complex formation in DLBCL

The data observed in the Jurkat model system suggest a role of GSK3β in regulating CBM complex formation, MALT1 endoprotease activity and the canonical NF-κB signalling. These observations are tentatively applicable in the ABC-DLBCL cell lines, as the antigen receptor mediated NF-κB activation is highly similar in T and B lymphocytes. As mentioned before, the hallmark of ABC-DLBCL is the constitutive activation of the NF-κB signalling cascade owing to the constitutive formation of CBM complex (Thome et al. 2010). The previous studies on targeting the constitutive NF-κB signalling cascade or MALT1 endoproteolytic activity in ABC-DLBCL showed a selective toxicity of MALT1 pharmacological inhibitors to the MALT1-dependent ABC-DLBCL cells highlighting the crucial role of MALT1 endoprotease activity in those cells (Nagel et al. 2012). The reduced proliferation of the NF-κB dependent ABC-DLBCL cell lines observed upon the inhibition of GSK3β by pharmacological inhibitors (Figure 27) are in line with the previous findings, as GSK3β inhibition attenuates the MALT1 endoprotease activity in Jurkat cells (Figure 7A+11). The analysis of the activity of MALT1 in DLBCL cell lines by detecting the expression of the cleavage products of its target protein CYLD1 by immunoblot analysis suggested that MALT1 endoprotease activity seemed to be more active in ABC-DLBCL cell lines (Figure 28). However, in line with our findings MALT1 endoprotease activity was attenuated in DLBCL upon GSK3β inhibition (Figure 28). Interestingly, the ABC-DLBCL cell lines OCI-LY-3 and HBL-1 that showed a higher MALT1 activity showed also a lower proliferation upon GSK3β inhibition than the other ABC-DLBCL cell line (Figure 28 and 27 respectively). Moreover, the constitutive CBM complex formation (Figure 29) and the relative expression of NF-κB target gene BIRC3 (Figure 30) were attenuated in ABC-

DLBCL cell lines upon GSK3β inhibition. On the other hand, BIRC3 expression show no significant change upon GSK3β inhibition in GC-DLBCL cell lines (Figure 30). In contrast to the observations in the ABC-DLBCL cell lines, the proliferation of the GC-DLBCL cell lines SU-DHL-6 and SU-DHL-8 was not inhibited but was even promoted by the inhibition of GSK3β compared to the ABC-DLBCL cell lines (Figure 27). However, the attenuated proliferation of the GC-DLBCL cell line SU-DHL-4 upon GSK3β inhibition suggests that GSK3β regulates the proliferation in the GC-DLBCL cell lines, probably by other mechanisms or signalling pathways.

4.5 GSK3β inhibition promotes the Wnt/β-catenin signalling pathway in DLBCL

In addition to the NF-κB signalling, GSK3β participate in the regulation of a wide variety of signalling processes including the Wnt/β-catenin signalling pathway. Analysis of the effect of GSK3β inhibition upon Wnt/β-catenin signalling revealed increase β-catenin expression in all tested ABC- and GC-DLBCL cell lines upon inhibition of GSK3β (Figure 31), this effect might explain the promotion of proliferation of some GC-DLBCL cell lines upon the inhibition of GSK3β (Figure 27). Moreover, the attenuated proliferation of ABC-DLBCL cell lines upon GSK3β inhibition (Figure 27) despite of the increase β-catenin expression emphasizes the crucial role of NF-κB signalling pathway in the survival of the ABC-DLBCL cells. Targeting GSK3β either alone or in combination with other targets might be helpful to treat ABC-DLBCL. Taken together, the data shown in this thesis imply a role of GSK3β in the pathogenesis of the DLBCL cell lines by mediating the CBM complex formation, the MALT1 endoprotease activity, the expression of NF-κB target gene BIRC3 and the Wnt/β-catenin signalling pathway.

4.6 The complex role of GSK3β in the pathogenesis of DLBCL

GSK3β plays a multifaceted role in the pathogenesis of DLBCL. Previous data suggested that GSK3β is involved in the CBM complex formation, MALT1 endoprotease activity, NF-κB signalling and the Wnt/β-catenin signalling pathway in DLBCL cell lines. This effect was seen in both the NF-κB dependent ABC-DLBCL as well as the GC-DLBCL. However, recent studies reported that NF-κB expression is not exclusively limited to ABC-DLBCL but also can occur in GC-DLBCL (Espinosa et al. 2008; Odqvist et al. 2014; Ok et al. 2015) and thus GSK3β inhibition might explain the suppression of the GC-DLBCL cell line SU-DHL-4 (Figure 27), however the role of other signalling cascades cannot be ruled out. The

Wnt/β-catenin signalling pathway is another important pathway controlled by GSK3β and β-catenin was reported to be expressed in all DLBCL cell lines at different levels. Moreover, the use of β-catenin inhibitors ICG-001 and PAM-1 reduced the viability of ABC- and GC-DLBCL significantly, regardless of the DLBCL subtype (Fachel et al. 2016). The tumor suppressor protein p53, which shows a functional and transcriptional cross talk with NF-κB, can directly bind GSK3β in the nucleus increasing the activity of both of them (Bijur and Jope 2001). Moreover, c-Myc, which is a negative prognostic factor in DLBCL, is reported to be a GSK3β phosphorylation target (Sears et al. 2000). However, the mechanisms by which GSK3β regulate all these factors and how can GSK3β coordinates between these functions is still not fully understood.

To dissect the complex role of GSK3β in the pathogenesis of DLBCL, immunohistochemistry stainings of GSK3β, RelA, β-catenin, p53 and c-Myc were done in the DLBCL cell line (OCI-LY-3, OCI-LY-10, HBL-1, SU-DHL-4, SU-DHL-6 and SU-DHL-8) (Table 2). While the IHC staining of GSK3β in the DLBCL cell lines gives a crude idea about the overall expression of GSK3β in DLBCL, the protein interaction profile of GSK3β, leading to the existence of different GSK3β-containing protein complexes, is difficult to be recognized using the IHC techniques only. The nuclear expression of RelA alone by IHC, which is used as a surrogate marker for NF-κB activation, was unable to distinguish ABC- from GC-DLBCL cell lines (Table 2) or DLBCL cohort (data not shown). However, the cytoplasmic expression of RelA by IHC represents the cytoplasmic inactive RelA containing dimers (Table 2 and Figure 32). p53 was highly expressed in the nucleus in all tested DLBCL cell lines. However, a high c-Myc expression (≥40% positive cells), which could not be seen in DLBCL cell lines, was observed more frequently in the GC-DLBCL cohort group.

Based on the previous data presented in this thesis, the ability of the immunohistochemistry to differentiate between the ABC- and the GC-DLBCL samples might be improved using a specific anti-phospho-BCL10 antibody targeting specifically the GSK3β mediated BCL10 phosphorylation sites. Alternatively, investigating the appearance of the BCR-induced cytoplasmic structures that are enriched in BCL10 which are called POLKADOTS (punctate and oligomeric killing or activating domains transducing signals) (Schaefer et al. 2004) might differentiate between the ABC and GC-DLBCL cells.

In conclusion, this study provides an evidence that GSK3β modulates the canonical NF-κB signalling pathway, MALT1 endoprotease activity and CBM complex formation in activated T cells and in the pathogenesis of DLBCL.

5- Summary

Activated B cell like type of Diffuse Large B cell lymphoma (ABC-DLBCL) is one of the most aggressive types of Non-Hodgkin's lymphoma and shows a bad prognosis even with treatment using the R-CHOP protocol. The hallmark of this type of DLBCL is the constitutive formation of a protein complex called the CBM complex, which is composed of CARMA1, BCL10 and MALT1. Moreover, the constitutive CBM complex formation has been shown to be responsible for the uncontrolled and stimulus independent activation of NF-κB signalling pathway. Glycogen synthase kinase 3β (GSK3β) is a protein kinase which was identified recently to be required for RelB degradation in T lymphocytes. Moreover, GSK3β was shown to be recruited to oncogenic CARMA1 in DLBCL cell lines. However, the role of GSK3β in CBM complex formation and the pathogenesis of ABC-DLBCL remains unravelled. The data presented in this thesis demonstrate that inhibition of GSK3β in Jurkat model system attenuated antigen receptor mediated MALT1 endoprotease activity evidenced by reduced cleavage of CYLD1 protein and RelB degradation. Moreover, GSK3β inhibition attenuated the antigen receptor induced canonical NF-κB activation as demonstrated by the reduction of stimulus induced IκBα degradation, the IKK complex activity, the NF-κB DNA binding activity and the expression of NF-κB target genes. This effect appears to be due to an attenuated CBM complex formation observed upon GSK3β inhibition. Moreover, GSK3β found to be a BCL10 kinase as it is capable of phosphorylating BCL10 at additional sites to the previously reported IKK2 mediated serine residues. The constitutive CBM complex dependent ABC-DLBCL cell lines showed also an attenuated proliferation upon the inhibition of GSK3β. However, the effect of GSK3β inhibition on GC-DLBCL cell proliferation was either attenuation or augmentation probably due to the activation of Wnt/β-catenin signalling pathway. In addition, MALT1 endoprotease activity and constitutive CBM complex formation in DLBCL cell lines were attenuated upon inhibition of GSK3β. Besides, the expression of NF-κB target gene BIRC3 was decreased in ABC- but not GC-DLBCL cells upon GSK3β inhibition. However, GSK3β plays a multi-faceted role in the pathogenesis of DLBCL not confined to NF-κB signalling pathway. The establishment of new immunohistochemistry protocols using antibodies specific for the GSK3β-mediated BCL10 phosphorylation sites might improve the ability of this technique

to differentiate between ABC- and GC-DLBCL without the need of microarray analysis which is not available for daily diagnostic routine. Taken together, this study presented BCL10 phosphorylation as a novel regulatory mechanism by which GSK3β mediates the MALT1 endoprotease activity, CBM complex formation and the NF-κB signalling in activated T cells as well as the pathogenesis of DLBCL.

6- References:

1) Ak P and Levine A J (2010). "p53 and NF-kappaB: different strategies for responding to stress lead to a functional antagonism." FASEB J **24**: 3643-3652.
2) Alizadeh A A, Eisen M B, Davis R E, Ma C, Lossos I S, Rosenwald A, Boldrick J C, Sabet H, Tran T, Yu X, Powell J I, Yang L, Marti G E, Moore T, Hudson J, Jr., Lu L, Lewis D B, Tibshirani R, Sherlock G, Chan W C, Greiner T C, Weisenburger D D, Armitage J O, Warnke R, Levy R, Wilson W, Grever M R, Byrd J C, Botstein D, Brown P O and Staudt L M (2000). "Distinct types of diffuse large B-cell lymphoma identified by gene expression profiling." Nature **403**: 503-511.
3) Beals C R, Sheridan C M, Turck C W, Gardner P and Crabtree G R (1997). "Nuclear export of NF-ATc enhanced by glycogen synthase kinase-3." Science **275**: 1930-1934.
4) Beg A A, Sha W C, Bronson R T, Ghosh S and Baltimore D (1995). "Embryonic lethality and liver degeneration in mice lacking the RelA component of NF-kappa B." Nature **376**: 167-170.
5) Bijur G N and Jope R S (2001). "Proapoptotic stimuli induce nuclear accumulation of glycogen synthase kinase-3 beta." J Biol Chem **276**: 37436-37442.
6) Blonska M and Lin X (2011). "NF-kappaB signaling pathways regulated by CARMA family of scaffold proteins." Cell Res **21**: 55-70.
7) Bognar M K, Vincendeau M, Erdmann T, Seeholzer T, Grau M, Linnemann J R, Ruland J, Scheel C H, Lenz P, Ott G, Lenz G, Hauck S M and Krappmann D (2016). "Oncogenic CARMA1 couples NF-kappaB and beta-catenin signaling in diffuse large B-cell lymphomas." Oncogene **35**: 4269-4281.
8) Bonizzi G and Karin M (2004). "The two NF-kappaB activation pathways and their role in innate and adaptive immunity." Trends Immunol **25**: 280-288.
9) Boone D L, Turer E E, Lee E G, Ahmad R C, Wheeler M T, Tsui C, Hurley P, Chien M, Chai S, Hitotsumatsu O, McNally E, Pickart C and Ma A (2004). "The ubiquitin-modifying enzyme A20 is required for termination of Toll-like receptor responses." Nat Immunol **5**: 1052-1060.
10) Bournat J C, Brown A M and Soler A P (2000). "Wnt-1 dependent activation of the survival factor NF-kappaB in PC12 cells." J Neurosci Res **61**: 21-32.

11) Boyle W J, Smeal T, Defize L H, Angel P, Woodgett J R, Karin M and Hunter T (1991). "Activation of protein kinase C decreases phosphorylation of c-Jun at sites that negatively regulate its DNA-binding activity." Cell **64**: 573-584.
12) Chen X, El Gazzar M, Yoza B K and McCall C E (2009). "The NF-kappaB factor RelB and histone H3 lysine methyltransferase G9a directly interact to generate epigenetic silencing in endotoxin tolerance." J Biol Chem **284**: 27857-27865.
13) Chen X, Yoza B K, El Gazzar M, Hu J Y, Cousart S L and McCall C E (2009). "RelB sustains IkappaBalpha expression during endotoxin tolerance." Clin Vaccine Immunol **16**: 104-110.
14) Choi W W, Weisenburger D D, Greiner T C, Piris M A, Banham A H, Delabie J, Braziel R M, Geng H, Iqbal J, Lenz G, Vose J M, Hans C P, Fu K, Smith L M, Li M, Liu Z, Gascoyne R D, Rosenwald A, Ott G, Rimsza L M, Campo E, Jaffe E S, Jaye D L, Staudt L M and Chan W C (2009). "A new immunostain algorithm classifies diffuse large B-cell lymphoma into molecular subtypes with high accuracy." Clin Cancer Res **15**: 5494-5502.
15) Collins T, Read M A, Neish A S, Whitley M Z, Thanos D and Maniatis T (1995). "Transcriptional regulation of endothelial cell adhesion molecules: NF-kappa B and cytokine-inducible enhancers." Faseb J **9**: 899-909.
16) Coornaert B, Baens M, Heyninck K, Bekaert T, Haegman M, Staal J, Sun L, Chen Z J, Marynen P and Beyaert R (2008). "T cell antigen receptor stimulation induces MALT1 paracaspase-mediated cleavage of the NF-kappaB inhibitor A20." Nat Immunol **9**: 263-271.
17) Davis R E, Ngo V N, Lenz G, Tolar P, Young R M, Romesser P B, Kohlhammer H, Lamy L, Zhao H, Yang Y, Xu W, Shaffer A L, Wright G, Xiao W, Powell J, Jiang J K, Thomas C J, Rosenwald A, Ott G, Muller-Hermelink H K, Gascoyne R D, Connors J M, Johnson N A, Rimsza L M, Campo E, Jaffe E S, Wilson W H, Delabie J, Smeland E B, Fisher R I, Braziel R M, Tubbs R R, Cook J R, Weisenburger D D, Chan W C, Pierce S K and Staudt L M (2010). "Chronic active B-cell-receptor signalling in diffuse large B-cell lymphoma." Nature **463**: 88-92.
18) De Paepe P and De Wolf-Peeters C (2007). "Diffuse large B-cell lymphoma: a heterogeneous group of non-Hodgkin lymphomas comprising several distinct clinicopathological entities." Leukemia **21**: 37-43.

19) DePaoli-Roach A A (1984). "Synergistic phosphorylation and activation of ATP-Mg-dependent phosphoprotein phosphatase by F A/GSK-3 and casein kinase II (PC0.7)." J Biol Chem **259**: 12144-12152.

20) Dierlamm J, Murga Penas E M, Bentink S, Wessendorf S, Berger H, Hummel M, Klapper W, Lenze D, Rosenwald A, Haralambieva E, Ott G, Cogliatti S B, Moller P, Schwaenen C, Stein H, Loffler M, Spang R, Trumper L and Siebert R (2008). "Gain of chromosome region 18q21 including the MALT1 gene is associated with the activated B-cell-like gene expression subtype and increased BCL2 gene dosage and protein expression in diffuse large B-cell lymphoma." Haematologica **93**: 688-696.

21) Doble B W, Patel S, Wood G A, Kockeritz L K and Woodgett J R (2007). "Functional redundancy of GSK-3alpha and GSK-3beta in Wnt/beta-catenin signaling shown by using an allelic series of embryonic stem cell lines." Dev Cell **12**: 957-971.

22) Dobrzanski P, Ryseck R P and Bravo R (1994). "Differential interactions of Rel-NF-kappa B complexes with I kappa B alpha determine pools of constitutive and inducible NF-kappa B activity." Embo J **13**: 4608-4616.

23) Eldar-Finkelman H (2002). "Glycogen synthase kinase 3: an emerging therapeutic target." Trends Mol Med **8**: 126-132.

24) Eom T Y and Jope R S (2009). "GSK3 beta N-terminus binding to p53 promotes its acetylation." Mol Cancer **8**: 14.

25) Espinosa I, Briones J, Bordes R, Brunet S, Martino R, Sureda A, Sierra J and Prat J (2008). "Activation of the NF-kappaB signalling pathway in diffuse large B-cell lymphoma: clinical implications." Histopathology **53**: 441-449.

26) Fachel A A, Muley S M, Meydan C, Agirre X, Cerchietti L, Melnick A and L. R K (2016). "Targeting ß-Catenin Signaling in DLBCL with ICG-001 and PAM-1 Suppresses Cell Proliferation and Induces Apoptosis." Blood **128**: 5382.

27) Ferch U, Kloo B, Gewies A, Pfander V, Duwel M, Peschel C, Krappmann D and Ruland J (2009). "Inhibition of MALT1 protease activity is selectively toxic for activated B cell-like diffuse large B cell lymphoma cells." J Exp Med **206**: 2313-2320.

28) Fontan L, Yang C, Kabaleeswaran V, Volpon L, Osborne M J, Beltran E, Garcia M, Cerchietti L, Shaknovich R, Yang S N, Fang F, Gascoyne R D,

Martinez-Climent J A, Glickman J F, Borden K, Wu H and Melnick A (2012). "MALT1 small molecule inhibitors specifically suppress ABC-DLBCL in vitro and in vivo." Cancer Cell **22**: 812-824.

29) Ge X, Lv X, Feng L, Liu X and Wang X (2011). "High expression and nuclear localization of beta-catenin in diffuse large B-cell lymphoma." Mol Med Rep **5**: 1433-1437.

30) Gutierrez-Garcia G, Cardesa-Salzmann T, Climent F, Gonzalez-Barca E, Mercadal S, Mate J L, Sancho J M, Arenillas L, Serrano S, Escoda L, Martinez S, Valera A, Martinez A, Jares P, Pinyol M, Garcia-Herrera A, Martinez-Trillos A, Gine E, Villamor N, Campo E, Colomo L and Lopez-Guillermo A (2011). "Gene-expression profiling and not immunophenotypic algorithms predicts prognosis in patients with diffuse large B-cell lymphoma treated with immunochemotherapy." Blood **117**: 4836-4843.

31) Habermann T M, Weller E A, Morrison V A, Gascoyne R D, Cassileth P A, Cohn J B, Dakhil S R, Woda B, Fisher R I, Peterson B A and Horning S J (2006). "Rituximab-CHOP versus CHOP alone or with maintenance rituximab in older patients with diffuse large B-cell lymphoma." J Clin Oncol **24**: 3121-3127.

32) Hailfinger S, Nogai H, Pelzer C, Jaworski M, Cabalzar K, Charton J E, Guzzardi M, Decaillet C, Grau M, Dorken B, Lenz P, Lenz G and Thome M (2011). "Malt1-dependent RelB cleavage promotes canonical NF-kappaB activation in lymphocytes and lymphoma cell lines." Proc Natl Acad Sci U S A **108**: 14596-14601.

33) Hans C P, Weisenburger D D, Greiner T C, Gascoyne R D, Delabie J, Ott G, Muller-Hermelink H K, Campo E, Braziel R M, Jaffe E S, Pan Z, Farinha P, Smith L M, Falini B, Banham A H, Rosenwald A, Staudt L M, Connors J M, Armitage J O and Chan W C (2004). "Confirmation of the molecular classification of diffuse large B-cell lymphoma by immunohistochemistry using a tissue microarray." Blood **103**: 275-282.

34) Harris N L, Jaffe E S, Stein H, Banks P M, Chan J K, Cleary M L, Delsol G, De Wolf-Peeters C, Falini B, Gatter K C and et al. (1994). "A revised European-American classification of lymphoid neoplasms: a proposal from the International Lymphoma Study Group." Blood **84**: 1361-1392.

35) Hoeflich K P, Luo J, Rubie E A, Tsao M S, Jin O and Woodgett J R (2000). "Requirement for glycogen synthase kinase-3beta in cell survival and NF-kappaB activation." Nature **406**: 86-90.

36) Hoesel B and Schmid J A (2013). "The complexity of NF-kappaB signaling in inflammation and cancer." Mol Cancer **12**: 86.

37) Huang T T, Wuerzberger-Davis S M, Wu Z H and Miyamoto S (2003). "Sequential modification of NEMO/IKKgamma by SUMO-1 and ubiquitin mediates NF-kappaB activation by genotoxic stress." Cell **115**: 565-576.

38) Hughes K, Nikolakaki E, Plyte S E, Totty N F and Woodgett J R (1993). "Modulation of the glycogen synthase kinase-3 family by tyrosine phosphorylation." Embo J **12**: 803-808.

39) Jeltsch K M, Hu D, Brenner S, Zoller J, Heinz G A, Nagel D, Vogel K U, Rehage N, Warth S C, Edelmann S L, Gloury R, Martin N, Lohs C, Lech M, Stehklein J E, Geerlof A, Kremmer E, Weber A, Anders H J, Schmitz I, Schmidt-Supprian M, Fu M, Holtmann H, Krappmann D, Ruland J, Kallies A, Heikenwalder M and Heissmeyer V (2014). "Cleavage of roquin and regnase-1 by the paracaspase MALT1 releases their cooperatively repressed targets to promote T(H)17 differentiation." Nat Immunol **15**: 1079-1089.

40) Jiang C and Lin X (2012). "Regulation of NF-kappaB by the CARD proteins." Immunol Rev **246**: 141-153.

41) Karube K, Enjuanes A, Dlouhy I, Jares P, Martin-Garcia D, Nadeu F, Ordonez G R, Rovira J, Clot G, Royo C, Navarro A, Gonzalez-Farre B, Vaghefi A, Castellano G, Rubio-Perez C, Tamborero D, Briones J, Salar A, Sancho J M, Mercadal S, Gonzalez-Barca E, Escoda L, Miyoshi H, Ohshima K, Miyawaki K, Kato K, Akashi K, Mozos A, Colomo L, Alcoceba M, Valera A, Carrio A, Costa D, Lopez-Bigas N, Schmitz R, Staudt L M, Salaverria I, Lopez-Guillermo A and Campo E (2017). "Integrating genomic alterations in diffuse large B-cell lymphoma identifies new relevant pathways and potential therapeutic targets." Leukemia.

42) Kato M, Sanada M, Kato I, Sato Y, Takita J, Takeuchi K, Niwa A, Chen Y, Nakazaki K, Nomoto J, Asakura Y, Muto S, Tamura A, Iio M, Akatsuka Y, Hayashi Y, Mori H, Igarashi T, Kurokawa M, Chiba S, Mori S, Ishikawa Y, Okamoto K, Tobinai K, Nakagama H, Nakahata T, Yoshino T, Kobayashi Y

and Ogawa S (2009). "Frequent inactivation of A20 in B-cell lymphomas." Nature **459**: 712-716.

43) Klein T, Fung S Y, Renner F, Blank M A, Dufour A, Kang S, Bolger-Munro M, Scurll J M, Priatel J J, Schweigler P, Melkko S, Gold M R, Viner R I, Regnier C H, Turvey S E and Overall C M (2015). "The paracaspase MALT1 cleaves HOIL1 reducing linear ubiquitination by LUBAC to dampen lymphocyte NF-kappaB signalling." Nat Commun **6**: 8777.

44) Lannutti B J, Meadows S A, Herman S E, Kashishian A, Steiner B, Johnson A J, Byrd J C, Tyner J W, Loriaux M M, Deininger M, Druker B J, Puri K D, Ulrich R G and Giese N A (2011). "CAL-101, a p110delta selective phosphatidylinositol-3-kinase inhibitor for the treatment of B-cell malignancies, inhibits PI3K signaling and cellular viability." Blood **117**: 591-594.

45) Lee J and Kim M S (2007). "The role of GSK3 in glucose homeostasis and the development of insulin resistance." Diabetes Res Clin Pract **77 Suppl 1**: S49-57.

46) Leidner J, Palkowitsch L, Marienfeld U, Fischer D and Marienfeld R (2008). "Identification of lysine residues critical for the transcriptional activity and polyubiquitination of the NF-kappaB family member RelB." Biochem J **416**: 117-127.

47) Lenz G, Wright G, Dave S S, Xiao W, Powell J, Zhao H, Xu W, Tan B, Goldschmidt N, Iqbal J, Vose J, Bast M, Fu K, Weisenburger D D, Greiner T C, Armitage J O, Kyle A, May L, Gascoyne R D, Connors J M, Troen G, Holte H, Kvaloy S, Dierickx D, Verhoef G, Delabie J, Smeland E B, Jares P, Martinez A, Lopez-Guillermo A, Montserrat E, Campo E, Braziel R M, Miller T P, Rimsza L M, Cook J R, Pohlman B, Sweetenham J, Tubbs R R, Fisher R I, Hartmann E, Rosenwald A, Ott G, Muller-Hermelink H K, Wrench D, Lister T A, Jaffe E S, Wilson W H, Chan W C and Staudt L M (2008). "Stromal gene signatures in large-B-cell lymphomas." N Engl J Med **359**: 2313-2323.

48) Li Q, Van Antwerp D, Mercurio F, Lee K F and Verma I M (1999). "Severe liver degeneration in mice lacking the IkappaB kinase 2 gene." Science **284**: 321-325.

49) Liu C, Li Y, Semenov M, Han C, Baeg G H, Tan Y, Zhang Z, Lin X and He X (2002). "Control of beta-catenin phosphorylation/degradation by a dual-kinase mechanism." Cell **108**: 837-847.

50) Marienfeld R, Berberich-Siebelt F, Berberich I, Denk A, Serfling E and Neumann M (2001). "Signal-specific and phosphorylation-dependent RelB degradation: a potential mechanism of NF-kappaB control." Oncogene **20**: 8142-8147.

51) Marienfeld R, May M J, Berberich I, Serfling E, Ghosh S and Neumann M (2003). "RelB forms transcriptionally inactive complexes with RelA/p65." J Biol Chem **278**: 19852-19860.

52) Martelli M, Ferreri A J, Agostinelli C, Di Rocco A, Pfreundschuh M and Pileri S A (2013). "Diffuse large B-cell lymphoma." Crit Rev Oncol Hematol **87**: 146-171.

53) May M J and Ghosh S (1997). "Rel/NF-kappa B and I kappa B proteins: an overview." Semin Cancer Biol **8**: 63-73.

54) Medunjanin S, Schleithoff L, Fiegehenn C, Weinert S, Zuschratter W and Braun-Dullaeus R C (2016). "GSK-3beta controls NF-kappaB activity via IKKgamma/NEMO." Sci Rep **6**: 38553.

55) Nagel D, Spranger S, Vincendeau M, Grau M, Raffegerst S, Kloo B, Hlahla D, Neuenschwander M, Peter von Kries J, Hadian K, Dorken B, Lenz P, Lenz G, Schendel D J and Krappmann D (2012). "Pharmacologic inhibition of MALT1 protease by phenothiazines as a therapeutic approach for the treatment of aggressive ABC-DLBCL." Cancer Cell **22**: 825-837.

56) Nakamura S, Nakamura S, Matsumoto T, Yada S, Hirahashi M, Suekane H, Yao T, Goda K and Iida M (2005). "Overexpression of caspase recruitment domain (CARD) membrane-associated guanylate kinase 1 (CARMA1) and CARD9 in primary gastric B-cell lymphoma." Cancer **104**: 1885-1893.

57) Neumann M, Klar S, Wilisch-Neumann A, Hollenbach E, Kavuri S, Leverkus M, Kandolf R, Brunner-Weinzierl M C and Klingel K (2011). "Glycogen synthase kinase-3beta is a crucial mediator of signal-induced RelB degradation." Oncogene **30**: 2485-2492.

58) Ngo V N, Davis R E, Lamy L, Yu X, Zhao H, Lenz G, Lam L T, Dave S, Yang L, Powell J and Staudt L M (2006). "A loss-of-function RNA interference screen for molecular targets in cancer." Nature **441**: 106-110.

59) Odqvist L, Montes-Moreno S, Sanchez-Pacheco R E, Young K H, Martin-Sanchez E, Cereceda L, Sanchez-Verde L, Pajares R, Mollejo M, Fresno M F, Mazorra F, Ruiz-Marcellan C, Sanchez-Beato M and Piris M A (2014). "NFkappaB expression is a feature of both activated B-cell-like and germinal center B-cell-like subtypes of diffuse large B-cell lymphoma." Mod Pathol **27**: 1331-1337.

60) Oeckinghaus A, Wegener E, Welteke V, Ferch U, Arslan S C, Ruland J, Scheidereit C and Krappmann D (2007). "Malt1 ubiquitination triggers NF-kappaB signaling upon T-cell activation." Embo J **26**: 4634-4645.

61) Ok C Y, Xu-Monette Z Y, Li L, Manyam G C, Montes-Moreno S, Tzankov A, Visco C, Dybkaer K, Routbort M J, Zhang L, Chiu A, Orazi A, Zu Y, Bhagat G, Richards K L, Hsi E D, Choi W W, van Krieken J H, Huh J, Ponzoni M, Ferreri A J, Parsons B M, Rao H, Moller M B, Winter J N, Piris M A, Wang S A, Medeiros L J and Young K H (2015). "Evaluation of NF-kappaB subunit expression and signaling pathway activation demonstrates that p52 expression confers better outcome in germinal center B-cell-like diffuse large B-cell lymphoma in association with CD30 and BCL2 functions." Mod Pathol **28**: 1202-1213.

62) Palkowitsch L, Marienfeld U, Brunner C, Eitelhuber A, Krappmann D and Marienfeld R B (2011). "The Ca2+-dependent phosphatase calcineurin controls the formation of the Carma1-Bcl10-Malt1 complex during T cell receptor-induced NF-kappaB activation." J Biol Chem **286**: 7522-7534.

63) Pap M and Cooper G M (1998). "Role of glycogen synthase kinase-3 in the phosphatidylinositol 3-Kinase/Akt cell survival pathway." J Biol Chem **273**: 19929-19932.

64) Plyte S E, Hughes K, Nikolakaki E, Pulverer B J and Woodgett J R (1992). "Glycogen synthase kinase-3: functions in oncogenesis and development." Biochim Biophys Acta **1114**: 147-162.

65) Pulverer B J, Fisher C, Vousden K, Littlewood T, Evan G and Woodgett J R (1994). "Site-specific modulation of c-Myc cotransformation by residues phosphorylated in vivo." Oncogene **9**: 59-70.

66) Rebeaud F, Hailfinger S, Posevitz-Fejfar A, Tapernoux M, Moser R, Rueda D, Gaide O, Guzzardi M, Iancu E M, Rufer N, Fasel N and Thome M (2008). "The

proteolytic activity of the paracaspase MALT1 is key in T cell activation." Nat Immunol **9**: 272-281.

67) Robertson M J, Kahl B S, Vose J M, de Vos S, Laughlin M, Flynn P J, Rowland K, Cruz J C, Goldberg S L, Musib L, Darstein C, Enas N, Kutok J L, Aster J C, Neuberg D, Savage K J, LaCasce A, Thornton D, Slapak C A and Shipp M A (2007). "Phase II study of enzastaurin, a protein kinase C beta inhibitor, in patients with relapsed or refractory diffuse large B-cell lymphoma." J Clin Oncol **25**: 1741-1746.

68) Rodriguez-Abreu D, Bordoni A and Zucca E (2007). "Epidemiology of hematological malignancies." Ann Oncol **18 Suppl 1**: i3-i8.

69) Rosenwald A, Wright G, Chan W C, Connors J M, Campo E, Fisher R I, Gascoyne R D, Muller-Hermelink H K, Smeland E B, Giltnane J M, Hurt E M, Zhao H, Averett L, Yang L, Wilson W H, Jaffe E S, Simon R, Klausner R D, Powell J, Duffey P L, Longo D L, Greiner T C, Weisenburger D D, Sanger W G, Dave B J, Lynch J C, Vose J, Armitage J O, Montserrat E, Lopez-Guillermo A, Grogan T M, Miller T P, LeBlanc M, Ott G, Kvaloy S, Delabie J, Holte H, Krajci P, Stokke T and Staudt L M (2002). "The use of molecular profiling to predict survival after chemotherapy for diffuse large-B-cell lymphoma." N Engl J Med **346**: 1937-1947.

70) Rubinfeld B, Albert I, Porfiri E, Fiol C, Munemitsu S and Polakis P (1996). "Binding of GSK3beta to the APC-beta-catenin complex and regulation of complex assembly." Science **272**: 1023-1026.

71) Ruland J and Mak T W (2003). "From antigen to activation: specific signal transduction pathways linking antigen receptors to NF-kappaB." Semin Immunol **15**: 177-183.

72) Saijo K, Mecklenbrauker I, Santana A, Leitger M, Schmedt C and Tarakhovsky A (2002). "Protein kinase C beta controls nuclear factor kappaB activation in B cells through selective regulation of the IkappaB kinase alpha." J Exp Med **195**: 1647-1652.

73) Schaefer B C, Kappler J W, Kupfer A and Marrack P (2004). "Complex and dynamic redistribution of NF-kappaB signaling intermediates in response to T cell receptor stimulation." Proc Natl Acad Sci U S A **101**: 1004-1009.

74) Schwabe R F and Brenner D A (2002). "Role of glycogen synthase kinase-3 in TNF-alpha-induced NF-kappaB activation and apoptosis in hepatocytes." Am J Physiol Gastrointest Liver Physiol **283**: G204-211.

75) Sears R, Nuckolls F, Haura E, Taya Y, Tamai K and Nevins J R (2000). "Multiple Ras-dependent phosphorylation pathways regulate Myc protein stability." Genes Dev **14**: 2501-2514.

76) Sehn L H and Gascoyne R D (2015). "Diffuse large B-cell lymphoma: optimizing outcome in the context of clinical and biologic heterogeneity." Blood **125**: 22-32.

77) Seidensticker M J and Behrens J (2000). "Biochemical interactions in the wnt pathway." Biochim Biophys Acta **1495**: 168-182.

78) Sen R and Baltimore D (1986). "Inducibility of kappa immunoglobulin enhancer-binding protein Nf-kappa B by a posttranslational mechanism." Cell **47**: 921-928.

79) Seto E S and Bellen H J (2004). "The ins and outs of Wingless signaling." Trends Cell Biol **14**: 45-53.

80) Shambharkar P B, Blonska M, Pappu B P, Li H, You Y, Sakurai H, Darnay B G, Hara H, Penninger J and Lin X (2007). "Phosphorylation and ubiquitination of the IkappaB kinase complex by two distinct signaling pathways." Embo J **26**: 1794-1805.

81) Shi J, Chi S, Xue J, Yang J, Li F and Liu X (2016). "Emerging Role and Therapeutic Implication of Wnt Signaling Pathways in Autoimmune Diseases." J Immunol Res **2016**: 9392132.

82) Shishodia S and Aggarwal B B (2002). "Nuclear factor-kappaB activation: a question of life or death." J Biochem Mol Biol **35**: 28-40.

83) Staal J, Driege Y, Bekaert T, Demeyer A, Muyllaert D, Van Damme P, Gevaert K and Beyaert R (2011). "T-cell receptor-induced JNK activation requires proteolytic inactivation of CYLD by MALT1." Embo J **30**: 1742-1752.

84) Staudt L M and Dave S (2005). "The biology of human lymphoid malignancies revealed by gene expression profiling." Adv Immunol **87**: 163-208.

85) Stilo R, Liguoro D, Di Jeso B, Formisano S, Consiglio E, Leonardi A and Vito P (2004). "Physical and functional interaction of CARMA1 and CARMA3 with Ikappa kinase gamma-NFkappaB essential modulator." J Biol Chem **279**: 34323-34331.

86) Su H, Bidere N, Zheng L, Cubre A, Sakai K, Dale J, Salmena L, Hakem R, Straus S and Lenardo M (2005). "Requirement for caspase-8 in NF-kappaB activation by antigen receptor." Science **307**: 1465-1468.

87) Sun L, Deng L, Ea C K, Xia Z P and Chen Z J (2004). "The TRAF6 ubiquitin ligase and TAK1 kinase mediate IKK activation by BCL10 and MALT1 in T lymphocytes." Mol Cell **14**: 289-301.

88) Sun S C (2010). "Non-canonical NF-kappaB signaling pathway." Cell Res **21**: 71-85.

89) Sun Z, Arendt C W, Ellmeier W, Schaeffer E M, Sunshine M J, Gandhi L, Annes J, Petrzilka D, Kupfer A, Schwartzberg P L and Littman D R (2000). "PKC-theta is required for TCR-induced NF-kappaB activation in mature but not immature T lymphocytes." Nature **404**: 402-407.

90) Swerdlow S, Campo E, Harris N, Jaffe E, Pileri S, Stein H, Thiele J and Vardiman J (2008). WHO Classification of Tumours of Haematopoietic and Lymphoid Tissues. Lyon, France, IARC Press.

91) Thome M (2004). "CARMA1, BCL-10 and MALT1 in lymphocyte development and activation." Nat Rev Immunol **4**: 348-359.

92) Thome M, Charton J E, Pelzer C and Hailfinger S (2010). "Antigen receptor signaling to NF-kappaB via CARMA1, BCL10, and MALT1." Cold Spring Harb Perspect Biol **2**: a003004.

93) Wang X J, Medeiros L J, Bueso-Ramos C E, Tang G, Wang S, Oki Y, Desai P, Khoury J D, Miranda R N, Tang Z, Reddy N and Li S (2017). "P53 expression correlates with poorer survival and augments the negative prognostic effect of MYC rearrangement, expression or concurrent MYC/BCL2 expression in diffuse large B-cell lymphoma." Mod Pathol **30**: 194-203.

94) Watcharasit P, Bijur G N, Song L, Zhu J, Chen X and Jope R S (2003). "Glycogen synthase kinase-3beta (GSK3beta) binds to and promotes the actions of p53." J Biol Chem **278**: 48872-48879.

95) Wegener E and Krappmann D (2007). "CARD-Bcl10-Malt1 signalosomes: missing link to NF-kappaB." Sci STKE **2007**: pe21.

96) Wegener E, Oeckinghaus A, Papadopoulou N, Lavitas L, Schmidt-Supprian M, Ferch U, Mak T W, Ruland J, Heissmeyer V and Krappmann D (2006).

"Essential role for IkappaB kinase beta in remodeling Carma1-Bcl10-Malt1 complexes upon T cell activation." Mol Cell **23**: 13-23.

97) Welsh G I and Proud C G (1993). "Glycogen synthase kinase-3 is rapidly inactivated in response to insulin and phosphorylates eukaryotic initiation factor eIF-2B." Biochem J **294 (Pt 3)**: 625-629.

98) Wertz I E, O'Rourke K M, Zhou H, Eby M, Aravind L, Seshagiri S, Wu P, Wiesmann C, Baker R, Boone D L, Ma A, Koonin E V and Dixit V M (2004). "De-ubiquitination and ubiquitin ligase domains of A20 downregulate NF-kappaB signalling." Nature **430**: 694-699.

99) Wilson H, Gerecitano F, Goy A, de Vos S, Kenkre A, Barr P, Blum K, Shustov A, Advani R, Lih J, Williams M, Schmitz R, Yang Y, Pittaluga S, Wright G, Kunkel L, McGreivy J, Balasubramanian S, Cheng M, Moussa D, J. B and Staudt L (2012). "The Bruton's Tyrosine Kinase (BTK) Inhibitor, Ibrutinib (PCI-32765), Has Preferential Activity in the ABC Subtype of Relapsed/Refractory De Novo Diffuse Large B-Cell Lymphoma (DLBCL): Interim Results of a Multicenter, Open-Label, Phase 2 Study." Blood **120**: 686.

100) Wilson W, 3rd and Baldwin A S (2008). "Maintenance of constitutive IkappaB kinase activity by glycogen synthase kinase-3alpha/beta in pancreatic cancer." Cancer Res **68**: 8156-8163.

101) Woodgett J R (1990). "Molecular cloning and expression of glycogen synthase kinase-3/factor A." Embo J **9**: 2431-2438.

102) Xiao G, Harhaj E W and Sun S C (2001). "NF-kappaB-inducing kinase regulates the processing of NF-kappaB2 p100." Mol Cell **7**: 401-409.

103) Xie Y, Bulbul M A, Ji L, Inouye C M, Groshen S G, Tulpule A, O'Malley D P, Wang E and Siddiqi I N (2014). "p53 expression is a strong marker of inferior survival in de novo diffuse large B-cell lymphoma and may have enhanced negative effect with MYC coexpression: a single institutional clinicopathologic study." Am J Clin Pathol **141**: 593-604.

104) Ye H, Gong L, Liu H, Hamoudi R A, Shirali S, Ho L, Chott A, Streubel B, Siebert R, Gesk S, Martin-Subero J I, Radford J A, Banerjee S, Nicholson A G, Ranaldi R, Remstein E D, Gao Z, Zheng J, Isaacson P G, Dogan A and Du M Q (2005). "MALT lymphoma with t(14;18)(q32;q21)/IGH-MALT1 is characterized by strong cytoplasmic MALT1 and BCL10 expression." J Pathol **205**: 293-301.

105) Young R M, Hardy I R, Clarke R L, Lundy N, Pine P, Turner B C, Potter T A and Refaeli Y (2009). "Mouse models of non-Hodgkin lymphoma reveal Syk as an important therapeutic target." Blood **113**: 2508-2516.

106) Zhang M, Xu-Monette Z Y, Li L, Manyam G C, Visco C, Tzankov A, Wang J, Montes-Moreno S, Dybkaer K, Chiu A, Orazi A, Zu Y, Bhagat G, Richards K L, Hsi E D, Choi W W, Han van Krieken J, Huh J, Ponzoni M, Ferreri A J, Moller M B, Parsons B M, Winter J N, Piris M A, Medeiros L J, Pham L V and Young K H (2016). "RelA NF-kappaB subunit activation as a therapeutic target in diffuse large B-cell lymphoma." Aging (Albany NY) **8**: 3321-3340.

Acknowledgements

First of all, I would like to thank **Prof. Dr. med. Peter Möller** for giving me the opportunity to work in the Institute of pathology in Ulm university. I appreciate his persistent support and insightful ideas.

No words can express my deep gratitude and sincere appreciation to **Prof. Dr. Ralf Marienfeld** for his great help, continuous support, meticulous supervision and helpful advices throughout this work. He kindly offered his valuable experience. With him I found my confidence and I learned how to approach new molecular pathology techniques. He saved no time or effort in helping me during this work. His continuous guidance and worthy remarks are beyond words of thanks.

I would like to express my sincere thanks and gratitude to **Prof. med. Dr. Thomas Barth** for his continuous assistance and great help. As a professor of pathology, he saved no effort in improving and evaluating the immunohistochemistry stainings. I really appreciate all the time and effort he spent during this work.

I am grateful to all the present and former members of the molecular pathology lab who provided me the friendly atmosphere which I find indispensable to achieve this work. They were nice, helpful and cooperative. I would like to thank especially Dr. Kevin Mellert. Malena Zahn and Anna Meißner and frankly everybody in the lab.

I also should thank the **Egyptian Ministry of Higher Education** and the **Deutscher Akademischer Austauschdienst (DAAD)** who financially supported this work.

Finally, I would like to acknowledge everyone who has assisted me throughout this work.

Ali Abd-Ellah

Curriculum Vitae

This part was removed due to data protection.

This part was removed due to data protection.